8-2020

N-Acetyltranserase 2 (NAT2) genotype polymorphism in cryopreserved human hepatocytes and Chinese hamster ovary (CHO) cells.

Mariam Refaat Zaky Habil
University of Louisville

N-ACETYLTRANSFERASE 2 (*NAT2*) GENOTYPE POLYMORPHISM IN CRYOPRESERVED HUMAN HEPATOCYTES AND CHINESE HAMSTER OVARY (CHO) CELLS

By

Mariam Refaat Zaky Habil

M.B.B.Ch., Faculty of Medicine, Cairo University, 2009

M.Sc. of Medical Pharmacology, Cairo University, 2016

A Thesis

Submitted to the Faculty of the

School of Medicine of the University of Louisville

in Partial Fulfillment of the Requirements

for the Degree of

Master of Science

in Pharmacology and Toxicology

Department of Pharmacology and Toxicology

University of Louisville

August 2020

N-ACETYLTRANSFERASE 2 (*NAT2*) GENOTYPE POLYMORPHISM IN CRYOPRESERVED HUMAN HEPATOCYTES AND CHINESE HAMSTER OVARY (CHO) CELLS

By

Mariam Refaat Zaky Habil

M.B.B.Ch., Faculty of Medicine, Cairo University, 2009

M.S. of Medical Pharmacology, Cairo University, 2016

A Thesis Approved on

April 27, 2020

by the following Thesis Committee:

_____

Dr. David W. Hein

_____

Dr. La Creis R. Kidd

_____

Dr. Leah J. Siskind

DEDICATION

I dedicate this Master thesis to my husband Mina and my kids, Raphael, and Verena whose prayers and words of encouragement blessed me. I am eternally grateful for their love.

ACKNOWLEDGEMENT

First, I would like to thank **God** Almighty for giving me the strength in my journey towards this degree. I would like to express my deep and sincere gratitude to my mentor, **Dr. David Hein**, for his insightful guidance, support, patience, and belief in my ability to succeed. I am honored to work with such a kind, caring, and great human being. I am also grateful to **Mark Doll** and **Dr. Raul Salazar-Gonzalez** for their help and advice. I would also like to thank my valued committee members **Dr. La Creis R. Kidd** and **Dr. Leah J. Siskind** for their assistance, feedback, and scientific contributions.

Also, I would like to thank **Dr. David Hein** and **Dr. Osama El-Tawil** for their efforts to build an academic partnership between Department of Pharmacology & Toxicology, University of Louisville, and Cairo University, providing me an opportunity to study here. A special thanks to my husband, **Mina Iskander,** for always being there as a husband and a friend. Words cannot express how blessed I am to be your wife. I am forever indebted to my parents, my mother-in law, father-in-law, for all the sacrifices they have made on my behalf. Their continuous prayers sustained me through the way. I would also like to express my overwhelming gratitude to my family, friends, and professors for their continuous love and undying support. *Portions of this thesis have been published (Pharmacogenetics and Genomics 30: 61-65, 2020).*

ABSTRACT

N-ACETYLTRANSFERASE 2 (*NAT2*) GENOTYPE POLYMORPHISM IN CRYOPRESERVED HUMAN HEPATOCYTES AND CHINESE HAMSTER OVARY (CHO) CELLS

Mariam Refaat Zaky Habil

April 27, 2020

Arylamine *N*-acetyltransferases, NAT1 and NAT2, catalyze the detoxification and/or activation of drugs and aromatic amine carcinogens. Single nucleotide polymorphisms or SNPs result in different human NAT2 genotypes thus dividing the population into rapid, intermediate, and slow acetylators. *We hypothesize allelic variants of NAT2 genotype will decrease levels of N-acetylation, cytotoxicity, oxidative stress, DNA adduct formation, and mutagenesis compared to the reference allele NAT2*4.* Cryopreserved human hepatocytes expressing different NAT2 genotypes and NER-deficient Chinese hamster ovary (CHO) cells transfected with human CYP1A2 and human *NAT2*4*, *NAT2*5B* or *NAT2*7B* have been used to investigate *N*-acetylation of different xenobiotics. *In vitro* and *in situ* *N*-acetylation products of hydralazine and isoniazid (INH) as drugs and 4-aminobiphenyl (ABP), β-naphthylamine (BNA), and 4, 4'-methylene bis (2-chloroaniline) (MOCA) as carcinogens were measured using high performance liquid chromatography (HPLC).

Cell viability was measured using alamar blue assay. Our findings showed that *N*-acetylation rates of ABP, BNA and MOCA in rapid acetylators are higher than slow acetylators. Also, CHO cells expressing *NAT2*4* (rapid acetylator) showed higher *N*-acetylation rates of hydralazine, INH, BNA and MOCA than cells expressing slow alleles *NAT2*5B* or *NAT2*7B*. *N*- acetylation rate of hydralazine in CHO cells expressing *NAT2*5B* was insignificantly higher compared to *NAT2*7B N*-acetylation rates of hydralazine. However, For BNA, *N*- acetylation rate in CHO cells expressing *NAT2*5B* was insignificantly lower compared to *NAT2*7B* suggesting genetic heterogeneity within the slow NAT2 phenotype. Treatment of cells with ABP, BNA and MOCA resulted in concentration dependent cytotoxicity in human hepatocytes and CHO cells. These data suggest that individual susceptibility to side effects or carcinogenicity can be modified by human NAT2 genotype. Moreover, NAT2 slow acetylator phenotype is not homogeneous, but rather multiple slow acetylator phenotypes exist resulting from different mechanisms inferred by various SNPs. Therefore, the investigations of NAT2 genotype/phenotype relationship could be more precise if heterogeneity within the "slow" NAT2 acetylator phenotype is incorporated into future lab-based, pre-clinical and clinical studies. These results are important for future studies to determine the role of NAT2 genotype on the toxic effects of aromatic amines such as DNA damage, DNA adducts and mutagenicity.

TABLE OF CONTENTS

LIST OF TABLES

LIST OF FIGURES

INTRODUCTION

Arylamine *N*-acetyltransferases (NATs) are xenobiotic metabolizing enzymes that play an important role in the metabolism and detoxification of many drugs and carcinogens [1]. Two NAT genes (NAT1 and NAT2) have been annotated in humans, both are located on chromosome 8 between 170-360Kb at 8p22 (Figure 1) [2]. NAT1 and NAT2 genes consist of 873 bp with similar structure. However, they exhibit different physiological roles and substrate affinities [3]. NAT1 shows substrate specificity for p-aminobenzoic acid (PABA), while NAT2 shows substrate specificity for sulfamethazine [4].

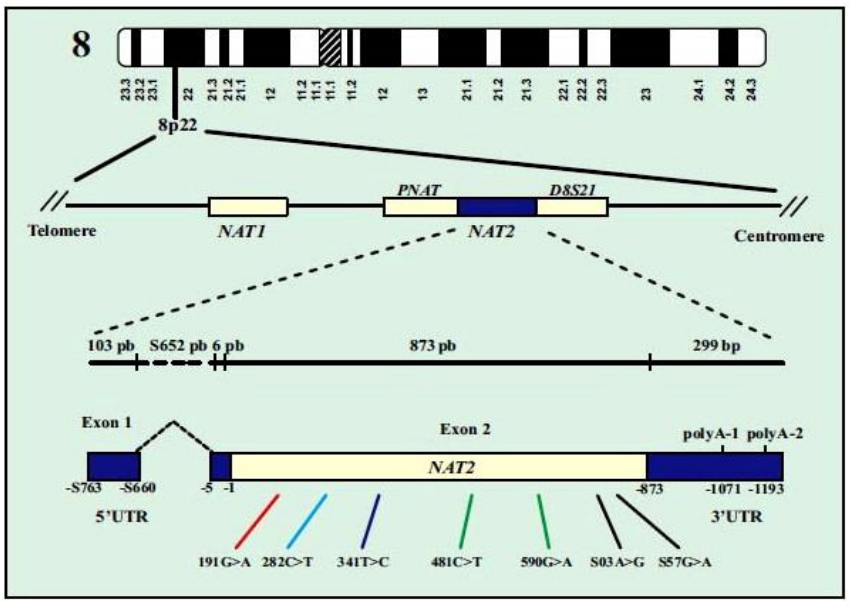

Figure (1): Schematic representation of *NAT* genes on human chromosome 8p22. Adapted from [2].

Although NAT2 has restricted tissue expression, NAT1 is expressed in almost all tissues of the body. Recent studies have suggested a novel role for NAT1 in cancer cell growth, survival, and resistance to chemotherapy [5, 6]. Regarding NAT2, it is a typical xenobiotic metabolizing enzyme expressed mainly in the small and large intestine and the liver. Also, its mRNA was detected in diverse human tissues [7].

NAT1 and NAT2 catalyze *N*-acetylation or *O*-acetylation of drugs, aromatic and heterocyclic amine carcinogens. NAT2 catalyzes *N*-acetylation of many drugs such as sulfamethazine, isoniazid (INH), hydralazine, procainamide and dapsone [8]. Also, it catalyzes both *N*-acetylation (usually deactivation) and *O*-acetylation (usually activation) of aromatic and heterocyclic amine carcinogens such as: 4 aminobipnenyl (ABP), β-naphthylamine (BNA) and 4,4'-methylenebis (2-chloroaniline) or (MOCA), which can be found in chemical, dye and rubber industries as well as in hair dyes, paints, and cigarette smoke [9].

Both human NATs are polymorphic enzymes (about 28 *NAT1* and 108 *NAT2* alleles) http://nat.mbg.duth.gr/ resulting in three acetylator phenotypes, rapid, intermediate, and slow acetylators [10, 11]. NAT2 genetic polymorphism was first noticed when isoniazid was used as anti-tuberculosis drug. Patients with less ability to acetylate isoniazid or slow NAT2 acetylators, were most likely to experience hepatitis [12].

There are many known polymorphisms in the NAT2 gene resulting from single nucleotide polymorphism or SNPs. These SNPs are associated with decreased enzyme activity and variable stability [13-15]. Figure (2) illustrates *NAT2*4* as the reference allele and the most common NAT2 allelic variants.

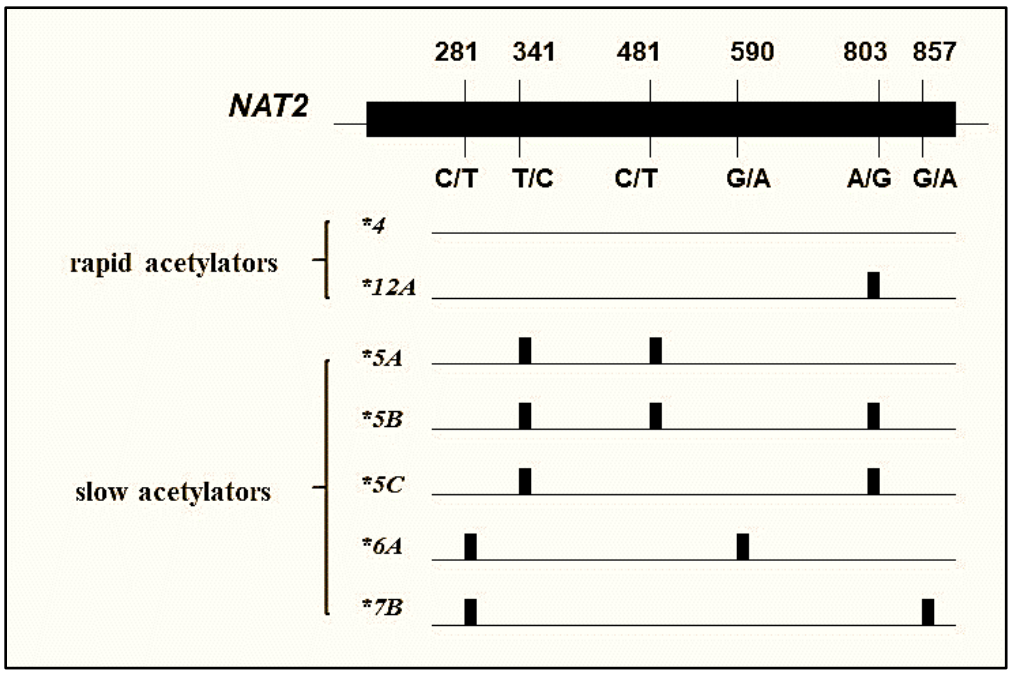

Figure (2): Schematic illustration of NAT2 allelic variants. The reference allele (*NAT2*4*) and the most common allelic variants (*NAT2*12A, 5A, 5B, 6A, 7B*). Adapted from [17].

The difference between allelic frequencies in the different populations are shown in (Table 1). The reference allele *NAT2*4* is associated with the acetylator phenotype, although *NAT2*12* and *NAT2*13* were also identified as rapid acetylators in African populations [10, 16]. The remaining alleles, *NAT2*5*, *NAT2*6*, *NAT2*7*, and *NAT2*14*, and their subtypes are typically associated with

the slow acetylator phenotype [17]. *NAT2*4* makes up 20–25% of alleles in Caucasians. The reference allele *NAT2*4* is higher among African Americans (36–41%), Hispanics (41%), Chinese (50%) and Japanese (70%) relative to Caucasians [18].

*NAT2*5* allele is the most common slow genotype among Hispanics (25%), Africans (27%), and Caucasian (44%) relative to Chinese (1.9-5.5%) [19, 20]. *NAT2*6* is evenly distributed across the different ethnic groups (22-28%), while Chinese have *NAT2*7* (17%) as the common slow allele [21, 22]. *NAT2*14* is exclusively present in sub-Saharan Africa [23].

Table (1): N-acetyltransferase 2 (NAT2) allele frequencies in the different populations

	Africans	**Asians**	**Caucasians**	**Hispanics**
NAT2*4	36-41 %	50-70%	20-25%	41%
NAT2*5	27%	1.9-5.5%	44%	25%
NAT2*6	22%	21%	28%	21.9%
NAT2*7	2%	17%	1.3%	9.2%
NAT2*12	12-20%	2.5%	4%	4.5%
NAT2*14	9%	0.0	0.0	0.0

Increased risk for drug toxicity, therapeutic failure or cancer are associated with the presence of these different genotypes [24]. For instance, patients who inherit the slow NAT2 genotype have an increased risk of developing isoniazid induced liver injury relative to those with the rapid NAT2 genotype [25]. Moreover, carriers of the slow acetylator genotype are linked with higher blood pressure following hydralazine treatment relative to rapid acetylators. However, slow acetylators experience greater adverse effects in form of lupus like syndrome because of the low acetylation rate [26]. This can be explained by the inhibitory effect of hydralazine on the complement system that may contribute to impaired clearance of immune complexes and thus to systemic lupus erythematosus [1].

Regarding cancer susceptibility, slow NAT2 acetylation status has been associated with a high risk of developing urinary bladder cancer, since they have a decreased capacity to detoxify aromatic amines by *N*-acetylation [27, 28]. *N*-acetylation of aromatic amines such as 4-aminobiphenyl (ABP) is generally considered as a detoxification step. It competes with P450-catalyzed *N*-hydroxylation followed by *O*-acetylation of *N*-hydroxy-amine catalyzed by NAT2 that generates acetoxy-derivatives that are highly unstable, leading to the formation of an arylnitrenium ions that binds to DNA leading to mutagenesis and carcinogenesis [29] (Figure 3).

Therefore, rapid acetylators have faster detoxification of aromatic amines so they can be excreted from the body while slow acetylators are more likely to metabolic bioactivation via O-acetylation pathway. The later leads to formation of

an arylnitrenium ions and DNA adducts then carcinogenesis if DNA is not repaired by repair pathway [30].

4-aminobiphenyl (ABP), is an environmental and occupational contaminant that can cause urinary bladder cancer in humans through inhalation and dermal penetration. It is mainly generated through the combustion of fossil fuels and from rubber, coal, textile, hair dyes industries [31, 32]. The International Agency for Research on Cancer (IARC) has classified ABP as a group I carcinogen [33].

Despite the cessation of commercial ABP production and use, smokers are still exposed to 2–5 ng ABP for each cigarette smoked [34] Also, bladder cancer biopsies from smokers have significantly higher levels of 4-ABP–DNA adducts than nonsmokers [34]. Moreover, increased levels of ABP hemoglobin adducts have also been found in the erythrocytes of smokers. DNA adducts result from activation pathway through hydroxylation followed by *N*-acetylation of ABP [34].

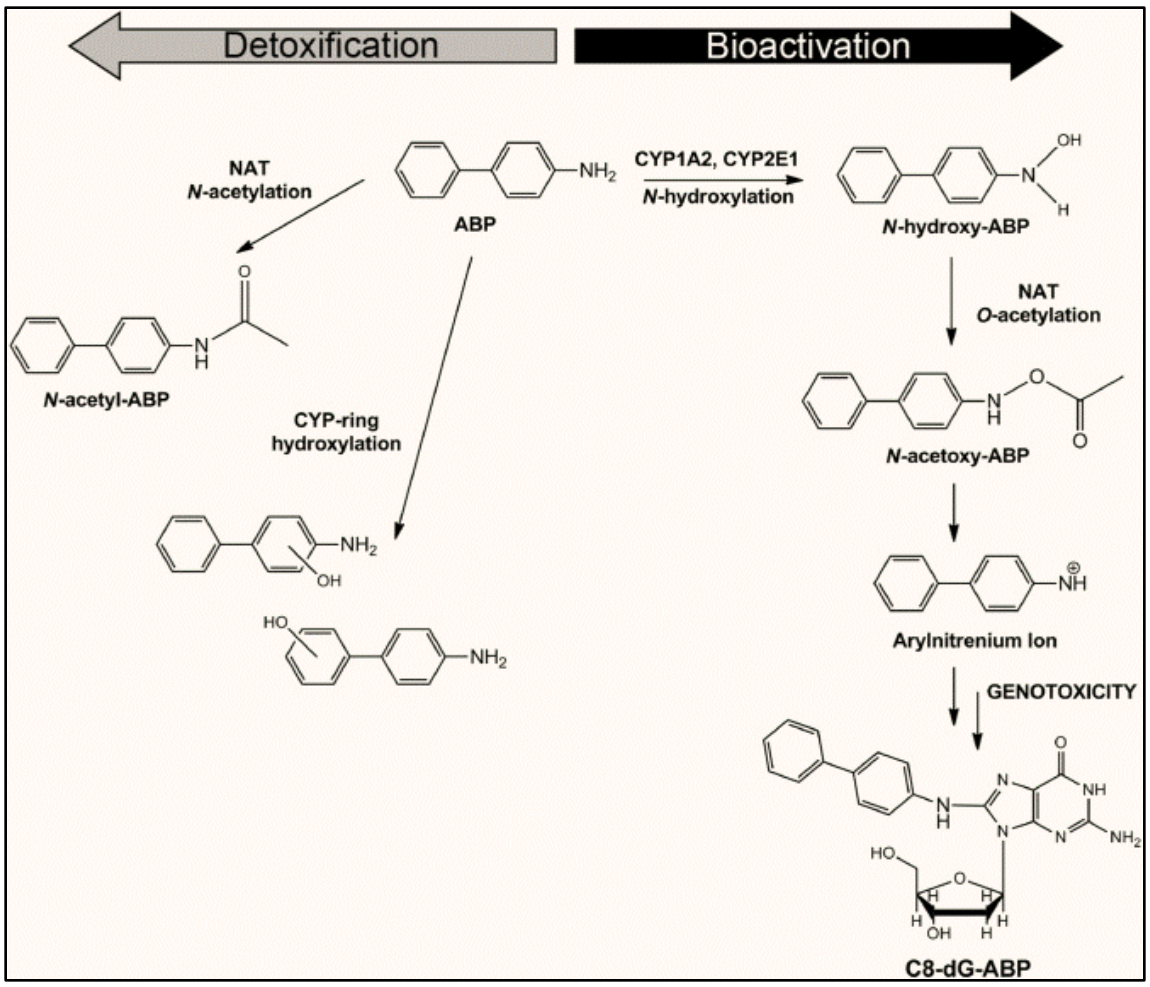

Figure (3): Pathways of detoxification and bioactivation of ABP as an example of aromatic amines. Adapted from [30].

Although, some of aromatic amines have affinity to be acetylated with NAT1 and NAT2, human NAT2 has a three to four-fold higher affinity than NAT1 for urinary bladder carcinogens such as ABP, BNA and MOCA [10, 35]. This may explain how NAT2 genetic polymorphism, regardless of NAT1 acetylator type, may

influence cancer risk among humans exposed to these carcinogens even in low doses [36].

Both rapid and slow NAT2 acetylator phenotypes have been associated with increased cancer in different target organs related to arylamine exposure [37]. For instance, many studies have associated increased urinary bladder cancer risk with inheritance of the NAT2 slow phenotype, especially, the *NAT2*5B* genotype. Slow acetylators are less likely to detoxify ABP and the procarcinogen is more likely to undergo metabolic activation via O-acetylation leading to increased formation of arylnitrenium ions and DNA adducts then carcinogenesis, if not repaired by DNA repair pathways [38-40]. On the other hand, the risk of colorectal cancer from well-done cooked meat, containing higher levels of meat derived carcinogens (i.e., heterocyclic aromatic amines or HAAs), was higher among rapid acetylators compared to slow acetylators [41-44]. These data suggest the association of cancer risk with NAT2 phenotype may be exposure and organ specific.

Moreover, epidemiological studies show the implication of NAT2 genetic polymorphism in the development of malignancies involving the breast [22], prostate [45], liver [46], and lung [47]. However, except for the smoking-related urinary bladder cancer, these studies have been unable to establish a consistent association between the acetylator status and human cancers [48].

Although previous studies have shown aromatic amines such as ABP undergo *N*-acetylation to acetyl metabolites in animals and humans, very little is

known regarding whether their metabolism is subjected to the NAT2 genetic polymorphism. Also, earlier studies have not provided a clear evidence for the association between *N*-acetylation and cytotoxicity or genotoxicity of some aromatic amines. Therefore, more laboratory-based experiments are needed to investigate the role of NAT2 genetic polymorphism in *N*-acetylation of aromatic amines. It is our hypothesis that different NAT2 alleles can decrease *N*-acetylation rates of these aromatic amines and the associated cytotoxicity compared to the reference rapid allele *NAT2*4.*

In the current study we selected isoniazid, and hydralazine as drugs and ABP, BNA, and MOCA as carcinogens to investigate the effect of NAT2 polymorphism on their *N*-acetylation rates.

HYDRALAZINE:

Hydralazine is a potent vasodilator widely used to treat hypertension during pregnancy as well as heart failure [49]. Recently, it has been shown that hydralazine may have an epigenetic role in cancer treatment through its ability to cause reversible heritable changes in gene expression without alterations in the DNA sequence [50, 51]. Hydralazine acts as a DNA methylation inhibitor by reducing the expression of the DNA methyltransferases which are involved in aberrant cytosine methylation in mammalian DNA [52, 53]. Clinical trials have revealed a protective role of hydralazine, either alone or with combination with valproate, in relation to many types of cancer including cancer cervix [54] T-cell lymphoma [55].

Two pathways have been proposed for hydralazine metabolism in humans. First, direct acetylation through NAT2, forming the metabolite 3-methyl-s-triazolo (3,4-a)-phthalazine (MTP) leading to detoxification. Second, hydralazine may also undergo bioactivation to form N-acetylhydrazinophthalazinone (NAc-HPZ) via an oxidative intermediate (HPZ) (Figure 4) [56].

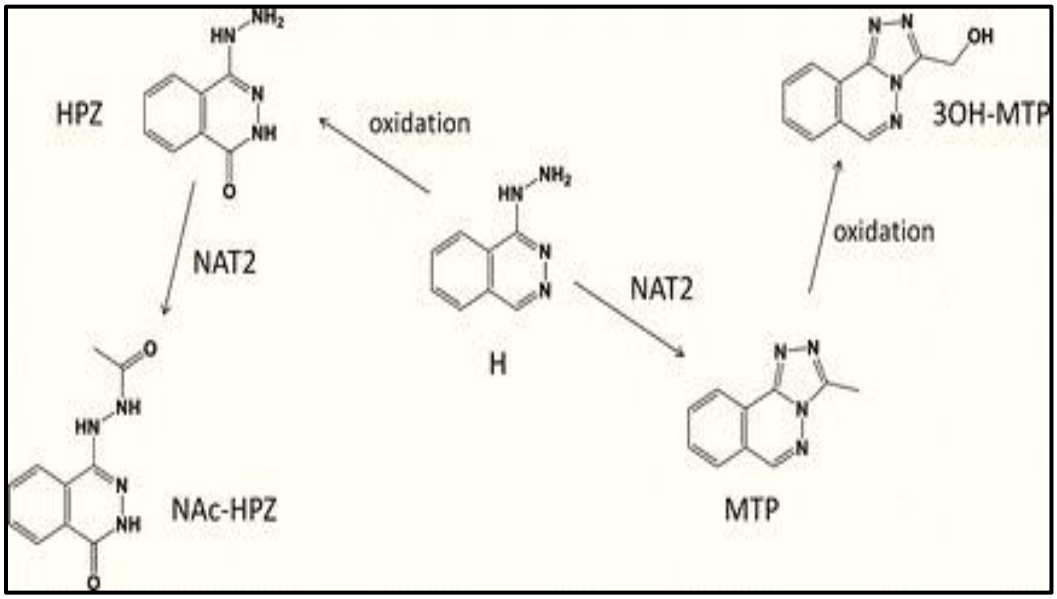

Figure (4): Metabolism of hydralazine in humans. (H) hydralazine, (MTP) 3-methyl-s-triazolo (3,4-a)-phthalazine, (3-OH-MTP) hydroxymethyl- triazolophthalazine, (NAc-HPZ) N-acetyl hydrazinophthalazinone [56].

Our laboratory revealed *N*-acetylation of hydralazine in human hepatocytes is higher in rapid acetylators compared to intermediate and slow acetylators [57].

ISONIAZID (INH):

Isoniazid (INH) is one of the current highly effective therapies against Mycobacterium tuberculosis. The major pathway for metabolizing INH involves *N*-acetylation to acetyl-isoniazid by NAT2 and this is considered as detoxification. However, if AcINH is converted to AcHz and hydroxylation via CYP2E1 occurs, this will lead to formation of toxic reactive metabolites (Figure 5) [58]. The rate of acetylation is constant in every individual but varies according to NAT2 genotype [59]. Doll and co-workers mentioned that *N*-acetylation of INH is genotype-dependent in human cryopreserved hepatocytes both in vitro and in situ following incubations at different concentrations of INH [60].

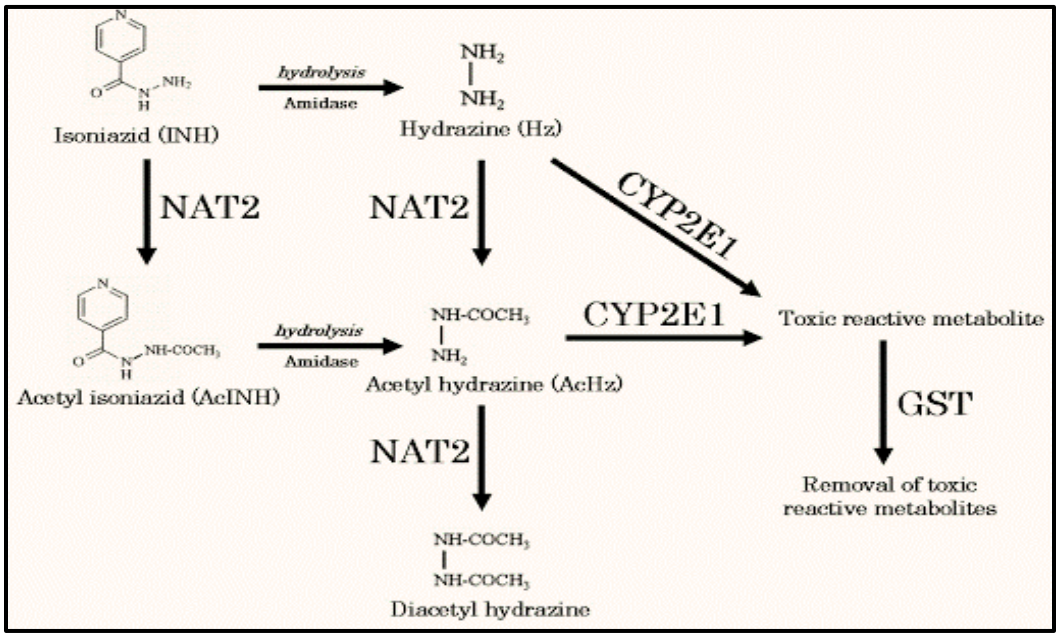

Figure (5): Metabolic pathways of isoniazid in humans. INH, Isoniazid; AcINH, acetylisoniazid; Hz, hydrazine; AcHz, acetylhydrazine. Adapted from [58].

In addition, a recent meta-analysis revealed isoniazid induced hepatitis is more likely to occur in patients with NAT2 slow acetylator genotype compared to rapid and intermediate acetylators across all social ethnic variations including Africans, Asians, Hispanic and Caucasians. This suggests it should be required to closely monitor patients with tuberculosis carrying the NAT2 slow acetylator genotype is required to detect hepatotoxicity induced by INH-based treatment [61].

β-NAPHTHYLAMINE (BNA):

Regarding 2-Naphthylamine or β-naphthylamine (BNA), it was formerly used commercially as an intermediate in the manufacturing of dyes, and as an antioxidant in the rubber industry. Also, environmental exposure occurs due to cigarette smoking. BNA amounts in mainstream and side stream cigarette smoke range from 1–22 ng/cigarette and 113.5–171.6 ng/cigarette, respectively [62]. It has been classified as a definite human carcinogen for bladder cancer by the International Agency for Research on Cancer and can be absorbed through the lungs or skin [63].

BNA undergoes *N*- and/ or *O*-acetylation via NATs. *O*-acetylation leads to formation of nitrenium ions that can bind to DNA forming DNA adducts (Figure 6). Previous studies have illustrated the association between BNA exposure due to smoking or occupation as well as NAT2 slow genotype alleles (*NAT2*6A* and/or **7B* alleles) and increased bladder cancer risk [63-66].

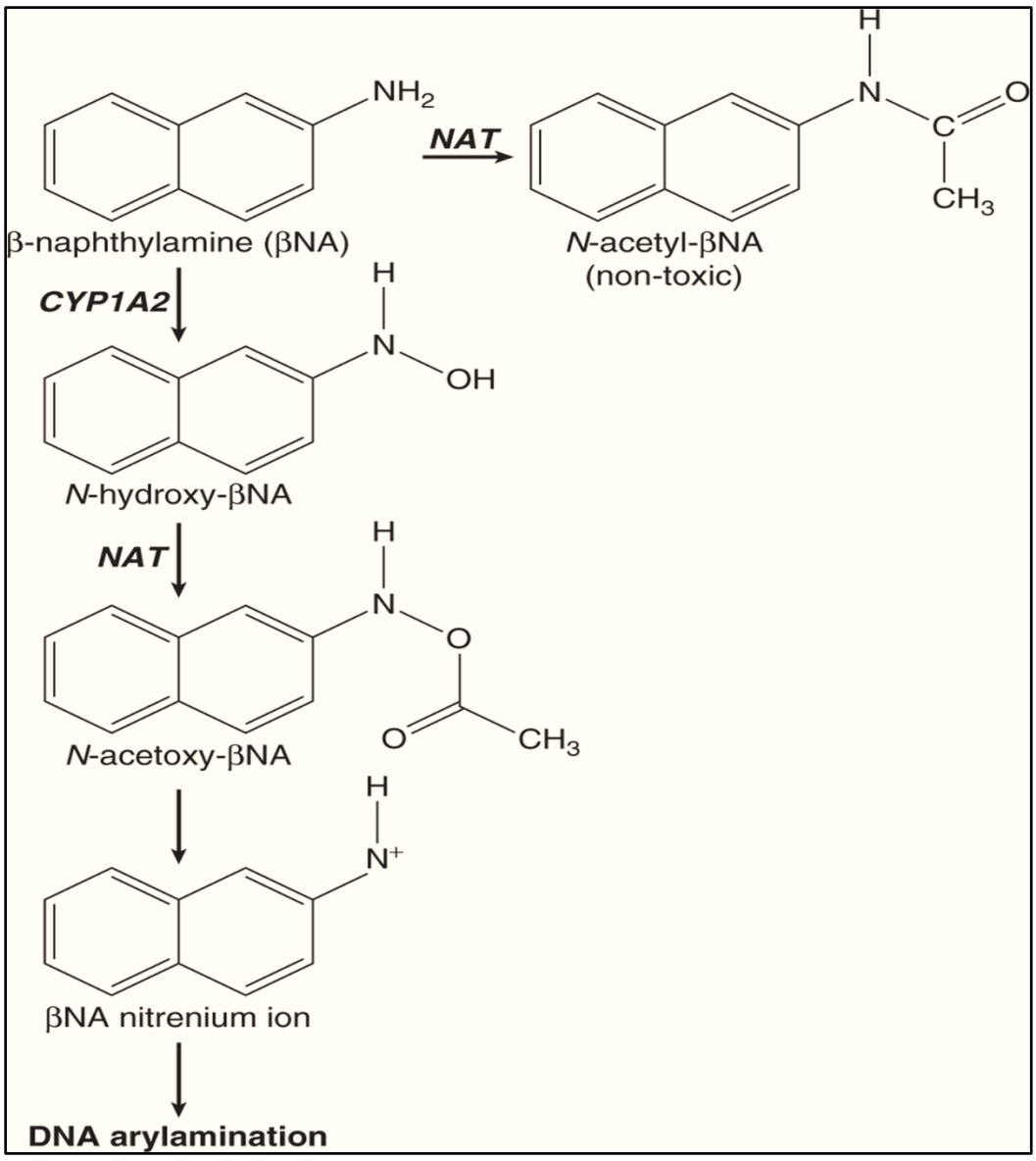

Figure (6): Proposed metabolic activation and detoxification pathways for the aromatic amine β-naphthylamine [67].

4, 4’-METHYLENE BIS (2-CHLOROANILINE) OR MOCA:

MOCA is used primarily in polyurethane industry. MOCA has been linked to hepatomas in mice and rats, lung, and mammary tumors in rats as well as bladder cancer in dogs [68-70]. As it is one of the aromatic amines, MOCA undergoes detoxification through an *N*-acetylation process catalyzed by NAT1 and NAT2 (Figure 7). However, in a previous study done by our lab, MOCA exhibited about 4-fold higher affinity for recombinant human NAT2 relative to NAT1. Also, *N*-acetylation rates of MOCA by human *NAT2*5, NAT2*6, NAT2*7*, and *NAT2*14* were much lower than the reference *NAT2*4* allozyme. [71].

In another study, industrial workers who were exposed to MOCA and had the NAT2 rapid alleles (*4, *12 A, B, C) had less oxidative damage compared to slow acetylators [72].

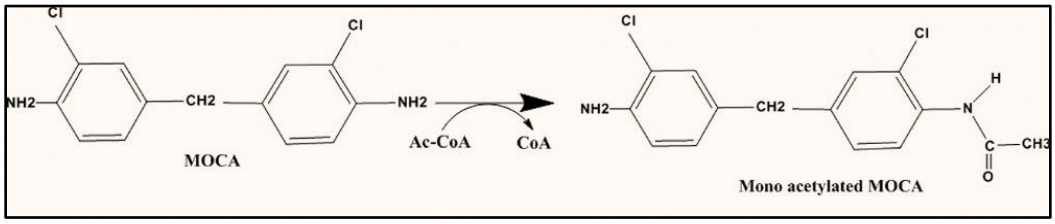

Figure (7): *N*-acetylation of MOCA to form the acetylated product [71].

Since DNA damage and mutagenesis are harmful consequences of both environmental exposure and carcinogen metabolism, they are informative biomarkers to investigate genetic variation in carcinogen metabolism. One important mechanism of DNA damage following exposure to carcinogens is the oxidative stress induced by reactive oxygen species (ROS) [73]. These ROS can bind to DNA, which may lead to oxidative DNA damage and ultimately many pathological conditions such as age dependent cataract, diabetes mellitus, chronic hepatitis [74-78] and cancer [79-82].

ROS are produced by the metabolism of environmental arylamine genotoxins such as chemical carcinogens and environmental agents [83]. ROS can lead to deleterious and extensive DNA damage including single strand breaks and DNA adduct formation. Modified bases such as 8-hydroxy-deoxyguanosine (8-OHdG) can be used as a marker to evaluate DNA damage caused by oxidative stress [84, 85].

Many studies showed the relationship between exposure to arylamine carcinogens and oxidative DNA damage. A study done previously among MOCA exposed workers showed that 8-OHdG concentration of rapid and intermediate acetylators was lower than that of the control group [72]. Also, Zhang et al., stated that 2-Amino-9H-pyrido[2,3-b] indole (AαC), which is present in high quantities in cigarette smoke and fried food**,** can increase level of (8-OH-dG) in HepG2 cells [86].

In addition, NO-naphthol, a metabolite of BNA caused oxidative DNA damage that includes formation of 8-OHdG [87]. Moreover, reactive oxygen species including H_2O_2 may result in cytotoxicity upon exposure to certain drugs such as hydralazine which could explain the associated hepatitis in some patients [88].

Several studies evaluated the role of aromatic amines in relation to mutagenicity. For instance, BNA and MOCA increase mutant formation in bacterial strains [89]. Also, our lab reported heterocyclic aromatic amines such as 2-Amino-9*H*-pyrido[2,3-*b*] indole or AαC can induce mutations in a dose-dependent manner. These mutations were found to be higher in cells transfected with *NAT2*4* than cells transfected with *NAT2*5B* [90]. More recently, Baldauf and coworkers reported mutagenesis induced by ABP and 2-aminofluorene (AF) was significantly higher in the Chinese hamster ovary (CHO) cells that were stably transfected with human CYP1A2/NAT2*4 compared to cells expressing human CYP1A2/NAT2*5B [91]. CHO cells lack nucleotide excision repair (NER) and allows the evaluation of CYP1A2 with NAT2 role in metabolism in the absence of NAT1.

Most of the previously mentioned studies have inferred NAT2 phenotype from genetic classification of the population into rapid, intermediate, and slow acetylators. However, clinical studies suggest different NAT2 alleles lead to heterogeneity of the acetylation status within the same phenotype [15]. One study showed antituberculosis drug-induced hepatotoxicity risk is particularly high among carriers of the *NAT2*6/*6* allele. This suggests *NAT2*6/*6* carriers individuals may constitute a subcategory of “ultra or very slow” acetylators [92].

Another study done in 504 north American subjects of Caucasian origin indicated there were variations in the *N*-acetylation NAT2 status among slow acetylator individuals. NAT2*6/*6 homozygotes show roughly a 30% reduction on enzyme activity as compared to NAT2*5/*5 homozygotes although both are considered slow acetylators [93]. Nonetheless, the role of these allelic variants in metabolism of arylamine carcinogens have yet to be investigated. Previous experimental studies investigated the effect of NAT2 polymorphism on arylamine carcinogens in rabbit or rat hepatocytes [94, 95]. In the current study, we investigated *N*-acetylation of ABP, BNA and MOCA as arylamine carcinogens in cryopreserved human hepatocytes that included rapid, intermediate, and slow acetylator genotypes. Human hepatocytes are an important model system to study the synergistic effects of CYP1A2 and NATs genes on the metabolism of different xenobiotics.

Also, we investigated the *N*-acetylation of hydralazine, INH, ABP, BNA and MOCA in Chinese hamster ovary (CHO) cells. To compare the effect of NAT2 allelic variants on the heterogeneity within the same phenotype, UV5-CHO cells were stably transfected with human CYP1A2 and either *NAT2*4* (as rapid acetylator), *NAT2*5B* (as common slow acetylator in Caucasians) or *NAT2*7B* (as common slow acetylator in Asians). The stable expression of CYP1A2 and NAT2 can reveal the individual role of NAT2 heterogeneity independent of possible confounding by NAT1. In addition, since UV5-CHO cell line lacks nucleotide excision repair (NER) due to a mutation in the XPD (ERCC2) gene, it is hypersensitive to bulky adduct mutagens [96].

Previous studies showed that the gene-gene interaction between different xenobiotic metabolizing enzymes particularly NATs an CYP1A2 can determine the individual risk to develop cancer. For instance, Cascorbi and coworkers showed individuals who carry *NAT2*4* and *NAT1*10* are at lower risk to develop bladder cancer when exposed to carcinogens either by smoking or occupational exposure [97].

Also, a meta-analysis, demonstrated inheritance of NAT1 rapid/NAT2 slow genotypes coupled with cigarette smoking jointly increased susceptibility to bladder cancer relative to nonsmokers [98]. More recently, Doaei and coworkers reported possession of NAT2 G857A SNP combined with CYP1A2 154 A > C genetic variant elevated colon and rectal cancer risk, especially among people who consumed high levels of meat [99]. However, these previous studies could not refer to the role of NAT2 genetic polymorphism in *N*-acetylation of arylamine carcinogens that is considered as the toxification pathway of many environmental carcinogens.

Therefore, we believe use of human hepatocytes containing both NATs and CYP1A2 will reflect the interaction between different xenobiotic metabolizing enzymes. In addition, NER-deficient UV5-CHO cell lines expressing human CYP1A2 and NAT2 alleles will advance the study of functional effects and the individual risks associated with NAT2 genetic polymorphism.

The objective of this study was to compare metabolism and cytotoxicity of different xenobiotics in cryopreserved human hepatocytes and CHO cells stably

transfected with human CYP1A2 and NAT2. The results could provide further evidence that the NAT2 genetic polymorphism modifies aromatic amine-induced mutagenesis and DNA damage and warrant consideration in human risk assessments following aromatic amine exposures.

MATERIALS AND METHODS

The outline of the experimental design and methods are presented in (Figure 8). Human hepatocytes with different NAT2 genotypes were used to measure in vitro and in situ N-acetyltransferase activity towards SMZ, ABP, BNA and MOCA. Also, CHO cells were stably transfected with CYP1A2 and *NAT2*4*, *5B or *7B and used to measure in vitro and in situ N-acetyltransferase activity towards hydralazine, Isoniazid, BNA and MOCA. Cell viability assays were done to evaluate the cytotoxicity induced by aromatic amines.

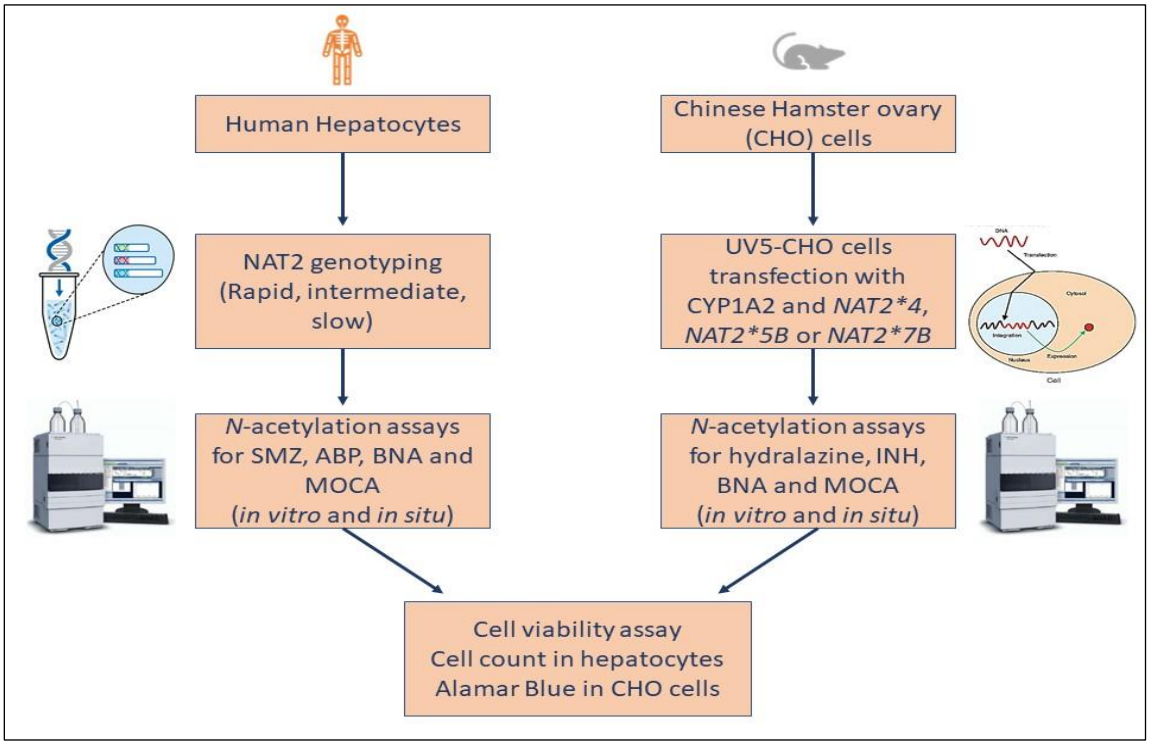

Figure (8): Flow chart of the experimental design and methods

SOURCE AND PROCESSING OF CRYOPRESERVED HUMAN HEPATOCYTES:

Cryopreserved human hepatocytes were received from Bioreclamation IVT, (Baltimore, MD) and stored in liquid nitrogen until use. Upon removal from liquid nitrogen, hepatocytes were thawed according to the manufacturer's instructions by warming a vial of the hepatocytes at 37°C for 90 seconds and transferring to a 50 mL conical tube containing 45 mL of InVitroGRO HT medium (Bioreclamation IVT). The suspension was centrifuged at 50 x g at room temperature for 5 min. The supernatant was discarded and cells washed once in ice-cold PBS before lysing the cells in ice-cold 20 mM $NaPO_4$, 1 mM dithiothreitol, 1 mM EDTA, 0.2% triton-X-100, 1 mM phenylmethylsulfonyl fluoride, 1 µM pepstatin A, and 1 µg/mL aprotinin. The lysate was centrifuged at 15,000 x g for 20 min and the supernatant was aliquoted and stored at -70°C. To mitigate possible instability of human NAT2, supernatant aliquots were thawed only once and used immediately to carry out the enzymatic reactions.

DETERMINATION OF NAT2 GENOTYPE AND DEDUCED PHENOTYPE:

Genomic DNA was isolated from pelleted cells prepared from human cryopreserved hepatocyte samples as described above using the QIAamp DNA Mini Kit (QIAGEN, Valencia, CA) according to the manufacturer's instructions. NAT2 genotypes and deduced phenotypes were determined as described previously [100]. Controls (no DNA) were run to ensure that there was no amplification of contaminating DNA (one for each plate) and samples were run once for every SNP.

Individuals possessing two NAT2 alleles associated with rapid acetylation activity (*NAT2*4*) were classified as rapid acetylators; individuals possessing one of these alleles and one allele associated with slow acetylation activity (*NAT2*5*, *NAT2*6*, and *NAT2*7*) were classified as intermediate acetylators, and those individuals that possessed two slow acetylation alleles were classified as slow acetylators. Cryopreserved hepatocytes with rapid, intermediate, and slow NAT2 acetylator genotype were selected at random for measurements of *N*-acetylation as described below.

MEASUREMENT OF SULFAMETHAZINE, ABP, BNA AND MOCA *N*-ACETYLTRANSFERASE ACTIVITY *IN VITRO*:

N-acetyltransferase assays containing hepatocyte lysate (< 2 mg of protein/ml), SMZ (300 µM), ABP (10 – 100 µM), BNA (10 – 100 µM) and MOCA (10 – 100 µM) and acetyl coenzyme A (AcCoA) (1000 µM) were incubated at 37°C for 10 minutes. Reactions were terminated by the addition of 1/10 volume of 1 M acetic acid and the reaction tubes were centrifuged in a small biofuge at 15,000 x g for 10 minutes to precipitate protein. The amount of the acetylated products was determined following separation and quantitation by high performance liquid chromatography (HPLC). For all substrates and their acetylated products, separation was accomplished by injection (40µL) onto a 125 x 4 mm Lichrosher 100 RP-100 5µM C18 HPLC column (Table 2 shows the HPLC parameters for the methods used in the current study). The amount of acetyl-SMZ produced was determined following separation and quantitation by HPLC as described previously

[101]. The amount of acetyl-ABP produced was determined following separation and quantitation by high performance liquid chromatography as described previously [102]. The amount of acetyl-BNA produced was determined following separation and quantitation by HPLC subjected to a gradient of 85% 20 mM sodium perchlorate pH 2.5/15% acetonitrile to 35% 20 mM sodium perchlorate pH 2.5/65% acetonitrile over 10 min, then to 85% 20 mM sodium perchlorate pH 2.5/15% acetonitrile over 5 min. Retention times for BNA and acetyl-BNA were 3.97 and 10.1 min respectively. The UV detector was set at 260 nm (Table 2). The amount of acetyl-MOCA was determined following separation and quantitation by HPLC subjected to a gradient of 100% 20 mM sodium perchlorate pH 2.5/0% acetonitrile to 0% 20 mM sodium perchlorate pH 2.5/100% acetonitrile over 10 min, then to 100% 20 mM sodium perchlorate pH 2.5/0% acetonitrile over 5 min. Retention times for acetyl-MOCA and MOCA were 18.6 and 19.1 min respectively. The UV detector was set at 280 nm (Table 2). For all samples, protein concentrations were determined using the Bio-Rad protein assay kit (Bio-Rad, Richmond, CA).

Table (2): Parameters of HPLC methods used for separation of different substrates

HPLC parameters	SMZ	ABP	BNA	MOCA	Hydralazine	INH
Column	Lichrosher 100 RP- C18 (125 x 4 mm; pore size:5 µM)				Discovery C18 (250 x 4 mm; pore size 5µM)	
Injection volume	40 uL					
Mobile Phase	20 mM sodium perchlorate (A): acetonitrile (B); pH 2.5				55 mM sodium phosphate (A): methanol (B); pH 4	25 mM sodium phosphate/20 mM heptanosulfonate (A): acetonitrile (B); pH 3
Gradient System (A: B)	91:9 then 71:29 over 5 min	85:15 then 35:65 over 10 min	85:15 then 35:65 over 10 min	100:0 then 0:100 over 10 min	95:5 then 40:60 over 20 min	90:10 for the whole time (Isocratic)
Wavelength	260 nm	260 nm	260 nm	280 nm	260 nm	266 nm

Cryopreserved human hepatocytes were selected at random with rapid, intermediate, and slow genotypes. Table (3) summarize the different alleles used in the current study for the in vitro assays.

Table (3): The individual NAT2 genotypes used for measurement of *in vitro* N-acetyltransferase activity in cryopreserved human hepatocytes

NAT2 genotype	**Deduced phenotype**	**SMZ (n)**	**ABP (n)**	**BNA (n)**	**MOCA (n)**
*NAT2*4/*4*	Rapid	10	8	7	5
*NAT2*4/*5B*	Intermediate	14	5	6	5
*NAT2*4/*6A*	Intermediate	8	3	3	2
*NAT2*4/*7B*	Intermediate	2	0	0	3
*NAT2*5B/*6A*	Slow	14	5	6	0
*NAT2*5B/*5B*	Slow	9	2	2	2
*NAT2*6A/*6A*	Slow	3	0	1	1
*NAT2*7B/*7B*	Slow	2	2	2	1
*NAT2*5B/*7B*	Slow	1	0	0	0

MEASUREMENT OF SULFAMETHAZINE, ABP, BNA AND MOCA *N*-ACETYLTRANSFERASE ACTIVITY *IN SITU*:

Cryopreserved human hepatocytes previously identified as rapid, intermediate, or slow NAT2 acetylator genotypes were thawed as described above and transferred to 50 mL conical tubes containing 12 mL of InVitroGRO CP media. One mL of hepatocyte/ media mixture was transferred to each well of 12 well Biocoat® collagen coated plates to allow cells to attach for 24 hours at 37ºC. Following culture in growth media for 24 hours, the cells were washed 3 times with 500 µL 1X PBS and replaced with media and SMZ, ABP, BNA or MOCA with concentrations of 10-100 µM. Hepatocytes were incubated for up to 24 hours after which media was removed and protein precipitated by addition of 1/10 volume of 1 M acetic acid. Media was centrifuged at 15,000 x g for 10 min and the supernatant used to separate and quantitate all substrates and their *N*-acetylated products by HPLC as described above (Table 2).

Cell number was determined after 24 hours of incubation with each substrate and activity was calculated in nmoles of acetylated product /24h/million cells. Cell number was used to compare the possible toxic effect of each substrate on hepatocytes. Also, comparison of that toxic effect was done between the different between genotypes. Table (4) summarizes the different alleles used in the current study for the *in-situ* assays.

Table (4): The individual NAT2 genotypes used for *in situ* N-acetyltransferase activity in cryopreserved human hepatocytes.

NAT2 genotype	Deduced phenotype	SMZ (n)	ABP (n)	BNA (n)	MOCA (n)
*NAT2*4/*4*	Rapid	6	6	6	5
*NAT2*4/*5B*	Intermediate	4	5	5	5
*NAT2*4/*6A*	Intermediate	2	1	0	0
*NAT2*4/*7B*	Intermediate	0	0	0	0
*NAT2*5B/*6A*	Slow	6	6	5	5
*NAT2*5B/*5B*	Slow	1	1	1	0
*NAT2*6A/*6A*	Slow	1	1	1	0
*NAT2*7B/*7B*	Slow	1	1	1	0
*NAT2*5B/*7B*	Slow	0	0	1	0

CHINESE HAMSTER OVARY (CHO) CELL CULTURE:

The UV5-CHO cell line, a nucleotide excision repair deficient derivative of the AA8 line [103], was obtained from the ATCC. Since UV5-CHO lacks nucleotide excision repair due to a mutation in the XPD (ERCC2) gene, it is hypersensitive to bulky adduct mutagens and belongs to the excision repair cross complementation group 2. Cells were grown in alpha-modified minimal essential medium (Cambrex) without L-glutamine, ribosides, and deoxyribosides supplemented with 10% fetal bovine serum (Hyclone), 100 units/ml penicillin, 100 micrograms/ml streptomycin (Cambrex), and 2 mM L-glutamine (Cambrex) at 37 °C in 5% CO2. Media were supplemented with appropriate selective agents to maintain stable transfectants.

CONSTRUCTION AND CHARACTERIZATION OF UV5/CHO CELL LINES:

The construction of UV5-CHO cells expressing human *CYP1A2* and *NAT2*4*, *NAT2*5B* or *NAT2*7B* has been reported and characterized [104]. The construction scheme is illustrated in (Figure 9). Briefly, pFRT/lacZeo plasmid was transfected into nucleotide excision repair deficient UV5 cell lines to generate a UV5 cell line containing a single integrated FRT site (UV5FRT). Purified human NADPH cytochrome P450 reductase (POR) and CYP1A2 polymerase chain reaction (PCR) products were digested and ligated into similarly treated pIRES vector and transformed into DH5α competent cells.

The pIRES plasmid containing cDNAs of human *CYP1A2* and POR was transfected into the newly established UV5FRT cell line. The colonies of these cells were expanded, and intact geneticin-resistant cells were assayed for 7-ethoxyresorufin O-deethylase (EROD) activity. EROD catalytic activity is

undetectable (<0.2 pmoles/min/10^6 cells) in untransfected UV5 cells, whereas CYP1A2-transfected cells (with and without further transfection with NAT2) have EROD catalytic activities about 3 pmol/min/10^6 cells.

The open reading frames of *NAT2*4*, *NAT2*5B* and *NAT2*7B* were amplified by PCR and inserted into the pcDNA5/FRT vector. The pcDNA5/FRT plasmid containing human *NAT2*4*, *NAT2*5B*, or *NAT2*7B* was co-transfected with pOG44, a Flp recombinase expression plasmid, into UV5FRT/CYP1A2 cells. Integration of the pcDNA5/FRT construct into the FRT site was confirmed by PCR. The *NAT2*4*-, *NAT2*5B*- and *NAT2*7B*-transfected cells were characterized for *N*-acetylation of sulfamethazine, a NAT2-selective substrate.

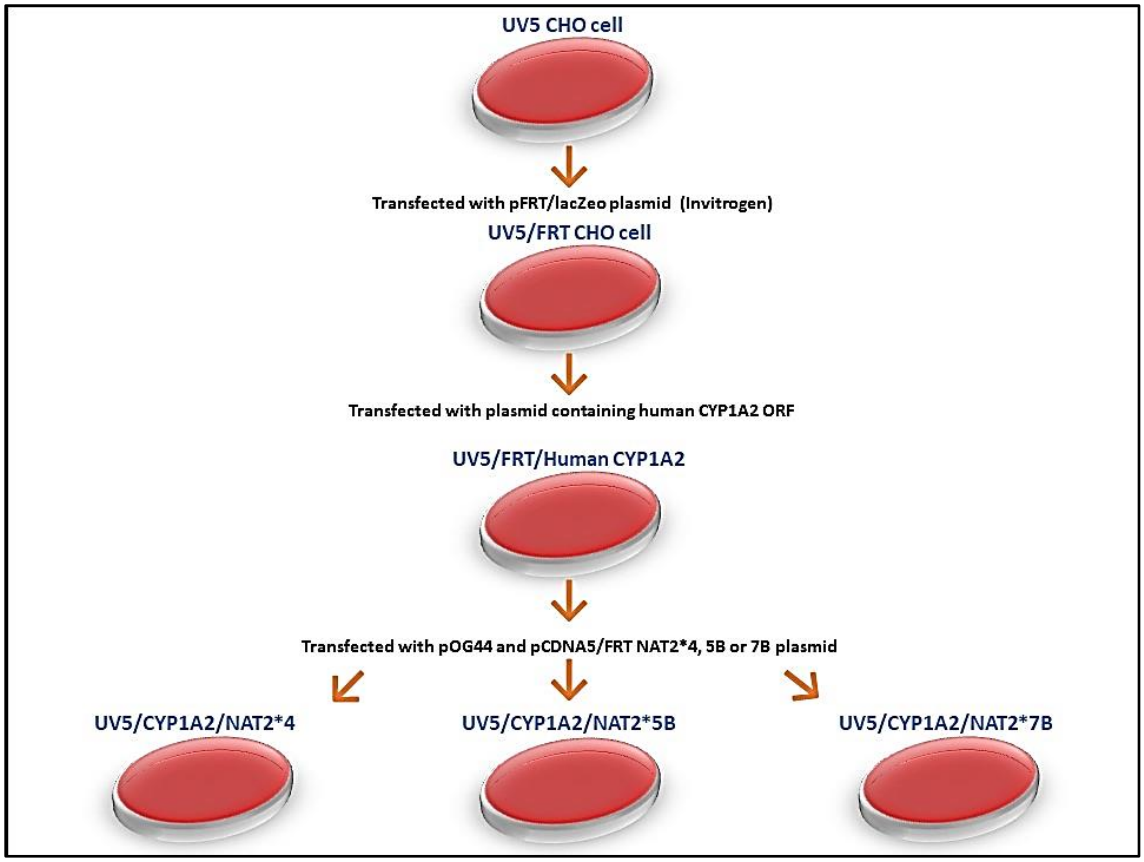

Figure (9): Chinese hamster ovary (CHO) cells construction. Adapted from [104]

MEASUREMENT OF HYDRALAZINE, INH, BNA AND MOCA *N*-ACETYLTRANSFERASE ACTIVITY *IN VITRO:*

N-acetyltransferase assays containing CHO cell lysates of different genotypes, hydralazine (10 – 1000 µM), INH (10 – 1000 µM), BNA (10 – 1000 µM) and MOCA (10 – 1000 µM) and acetyl coenzyme A (300 – 1000 µM) were incubated at 37°C for 60 minutes. Reactions were terminated by the addition of 1/10 volume of 1 M acetic acid and the reaction tubes were centrifuged in a small biofuge at 15,000 x g for 10 minutes to precipitate protein. The amount of the acetylated products was determined following separation and quantitation by HPLC (Table 2).

For hydralazine, INH and their acetylated products, separation was accomplished by injection (40µL) onto a 250 x 4 mm Discovery 5µM C18 HPLC column. Separation of hydralazine and acetyl-hydralazine or 3-methyl-s-triazolo [3,4a]-phthalazine (MTP) was done using a gradient of 95% 55 mM sodium perchlorate pH 4/5% methanol to 40% 55 mM sodium perchlorate pH 4/60% methanol over 20 min, then to 95% 55 mM sodium perchlorate pH 4/5% methanol over 3 min. Retention times for hydralazine and MTP were 8.9 and 19.9 min respectively. The UV detector was set at 260 nm.

Separation of INH and acetyl-INH was done using an isocratic gradient of 90% 25mmol/L sodium phosphate, 20mmol/L heptane sulfonate pH3/10 % acetonitrile. Acetyl-INH was quantitated by measuring the absorbance at 266 nm. Retention times for acetyl-INH and INH were 4.65 and 6.57 min, respectively.

For BNA, MOCA and their acetylated products, separation was accomplished by injection (40µL) onto a 125 x 4 mm Lichrosher 100 RP-100 5µM C18 HPLC column. The amounts of acetyl-BNA and acetyl-MOCA produced were determined using the same methods mentioned before. To determine the apparent Km and Vmax for BNA and MOCA, reactions were run in the presence of BNA (7.8 -1000 µM) or MOCA (100, 200, 300 µM) with fixed concentration of AcCoA (300 µM).

For all samples, protein concentrations of cell lysates were determined using the Bio-Rad protein assay kit (Bio-Rad, Richmond, CA) and activity was calculated in nmoles of acetylated product /ml/min/mg protein.

MEASUREMENT OF BNA AND MOCA *N*-ACETYLTRANSFERASE ACTIVITY *IN SITU:*

Cryopreserved CHO cells with different genotypes were thawed and transferred to 50 mL conical tubes containing 12 mL of alpha-modified minimal essential medium (Cambrex) without L-glutamine, ribosides, and deoxyribosides supplemented with 10% fetal bovine serum (Hyclone), 100 units/ml penicillin, 100 micrograms/ml streptomycin (Cambrex), and 2 mM L-glutamine (Cambrex). One mL of cell/ media mixture was transferred to each well of 12 well plates to allow cells to attach for 24 hours at 37ºC.

Following culture for 24 hours, the cells were washed 3 times with 500 µL 1X PBS and replaced with media and BNA or MOCA with concentrations of 10-

1000 µM. Cells were incubated for up to 24 hours after which media was removed and protein precipitated by addition of 1/10 volume of 1 M acetic acid. Media was centrifuged at 15,000 x g for 10 min and the supernatant used to separate and quantitate all substrates and their acetylated products by HPLC as described above. Cell number was determined after 24 hours of incubation with each substrate and activity was calculated in nmoles of acetylated product /24h/million cells.

Cell viability assay:

Cytotoxic effect of BNA and MOCA on CHO cell lysates of different genotypes was assessed using Alamar Blue test [105]. Briefly, control medium was removed; the cells were rinsed with PBS and 2 mL of an Alamar Blue (AB) solution (5% [v/v] solution of AB dye) prepared in fresh medium (without FBS or supplements) was added to each well. Following 1-hour incubation, AB fluorescence was quantified at the respective excitation and emission wavelength of 530 and 590 nm using a Tecan Genios microplate reader. The results were averaged over 3 different independent experiments (n = 3) with 3 replicates per experiment (3 × 12 well plates). Finally, for each plate the reading was also done in triplicate (values obtained from 3 different wells were averaged). For each experiment, wells containing only the AB solution without cells were also prepared and incubated for 1 hour.

STATISTICAL ANALYSIS:

Differences in *N*-acetylation rates of all substrates among different genotypes in hepatocytes and CHO cells were tested for significance by Kruskal-Wallis test followed by Dunn's post-hoc test. For kinetics of BNA and MOCA, Michaelis–Menten kinetic constants were calculated by linear regression (GraphPad Software, Inc, San Diego, CA).

RESULTS

Arylamine N-acetyltransferases (NATs) are xenobiotic metabolizing enzymes that play an important role in the metabolism and detoxification of many drugs and carcinogens. Two NAT genes (NAT1 and NAT2) have been annotated in humans. Both NATs catalyze *N*- or *O*-acetylation using AcCoA as a cofactor (Figure 10). Our hypothesis is that different NAT2 genotypes affects *N*-acetylation of xenobiotics in cryopreserved human hepatocytes and CHO cells.

Previous studies in our lab have shown NAT2 genetic polymorphism dependent *N*-acetylation of arylhydrazines as hydralazine [57] and isoniazid [60] in human hepatocytes and arylamines as ABP in CHO cells [106]. Also, apparent K_m and V_{max} for SMZ and ABP [37] and for hydralazine [57] were previously measured in our lab.

In the current study, we measured *in vitro* and *in situ* NAT2 activity towards SMZ (a specific substrate for NAT2 used as a control), ABP, BNA and MOCA in cryopreserved human hepatocytes. In addition, we measured *in vitro* and *in situ* NAT2 activity towards hydralazine, isoniazid, BNA and MOCA in CHO cells stably transfected with human CYP1A2 and either *NAT2*4* (as rapid acetylator), *NAT2*5B* (as common slow acetylator in Caucasians) or *NAT2*7B* (as common slow acetylator in Asians).

Also, this study included determination of the cytotoxic effect of carcinogens: ABP, BNA and MOCA. So, we measured cell viability in human hepatocytes exposed to ABP, BNA, or MOCA. For CHO cells, we measured cell viability following treatment with BNA and MOCA as ABP induced cytotoxicity was previously studied in [106]. Table (5) illustrates a summary of the experiments done in the current study.

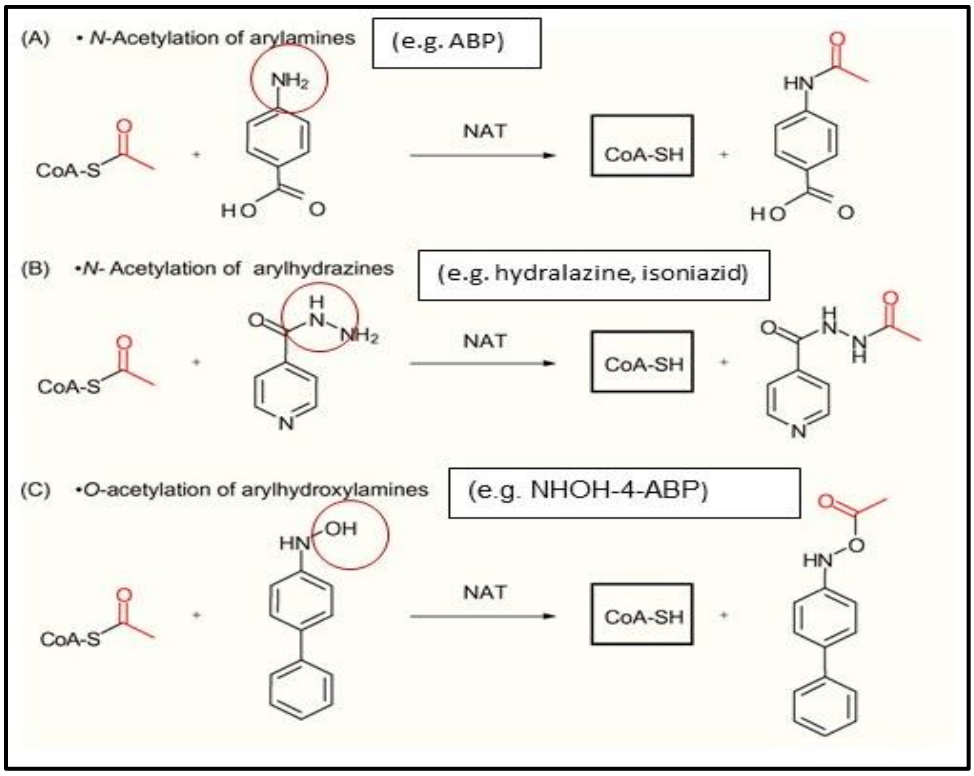

Figure (10): Reactions catalyzed by N-acetyltransferases. Reactions (A), (B) and (C) lead to the hydrolysis of acetyl CoA as well as the acetylation of the acetyl acceptor molecule. Reactions (A) and (B) inactivate the substrate, reactions (C) leads to substrate activation. Adapted from [107].

Table (5): Summary of the experiments done in the current study

Substrate	*In vitro* and *in situ* NAT2 in hepatocytes	Concentration and time dependence	Cytotoxicity in hepatocytes	In vitro NAT2 in CHO cells	In situ NAT2 in CHO cells	K_m and V_{max}	Cytotoxicity in CHO cells
SMZ	Figures (11, 16)	Figure (15 a)	Not included	In previous study [106]		In previous study [37]	Not included
ABP	Figures (12, 17)	Figure (15 b)	Figures (20, 21)				In previous study [106]
BNA	Figures (13, 18)	Figure (15 c)	Figures (22, 23)	Figures (30, 31)	Figure (36)	Figure (34)	Figures (38, 39)
MOCA	Figures (14, 19)	Figure (15 d)	Figures (24, 25)	Figures (32, 33)	Figure (37)	Figure (35)	Figures (40, 41)
Hydralazine	In previous study [57]		Not included	Figures (26, 27)	need to be done	In previous study [57]	Not included
Isoniazid	In previous study [60]			Figures (28, 29)		Need to be done	

IN VITRO N-ACETYLTRANSFERASE ACTIVITY IN CRYOPRESERVED HUMAN HEPATOCYTES:

SULFAMETHAZINE (SMZ):

N-acetylation rates towards SMZ in the cryopreserved human hepatocytes from rapid, intermediate, and slow NAT2 acetylators were measured using HPLC. They exhibited a robust and highly significant NAT2 genotype dependent metabolism ($P < 0.0001$). *N*-acetylation rate of SMZ was about 2- and 10-fold higher in rapid NAT2 acetylators than that of intermediate or slow NAT2 acetylators, respectively. The highest levels of *N*-acetylated product were observed in rapid acetylator, lower levels in intermediate acetylator, and the lowest levels in slow acetylator hepatocytes (Figure 11).

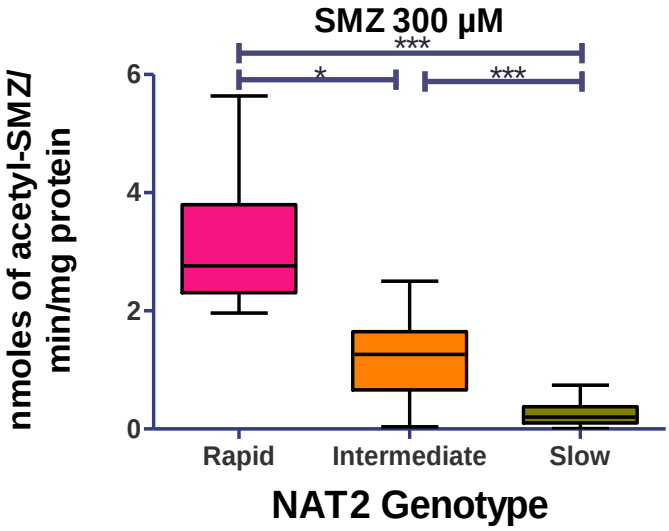

Figure (11): *In vitro N*-acetyltransferase catalytic activities towards SMZ (300 µM). Data illustrates box plot of rapid (n=10), intermediate (24), and slow (n=29) acetylators. Individuals possessing two NAT2 alleles associated with rapid acetylation activity (NAT2*4) were classified as rapid; individuals possessing one of these alleles and one allele associated with slow acetylation activity (NAT2*5, NAT2*6, and NAT2*7) were classified as intermediate, and those individuals that possessed two slow acetylation alleles were classified as slow. Statistical significance was determined using Kruskal-Wallis test followed by Dunn's Multiple Comparison Test. SMZ *N*-acetyltransferase activities differed significantly ($p < 0.0001$) between rapid, intermediate, and slow acetylators.

4-AMINOBIPHENYL (ABP):

Regarding ABP, *N*-acetyltransferase activities differed significantly between rapid, slow, and intermediate acetylators at 10 µM and 100 µM ($p < 0.01$). *N*-acetylation rate of ABP in rapid acetylators was about 6- and 14-fold higher than slow acetylators at 10 µM and at 100 µM, respectively (Figure 12).

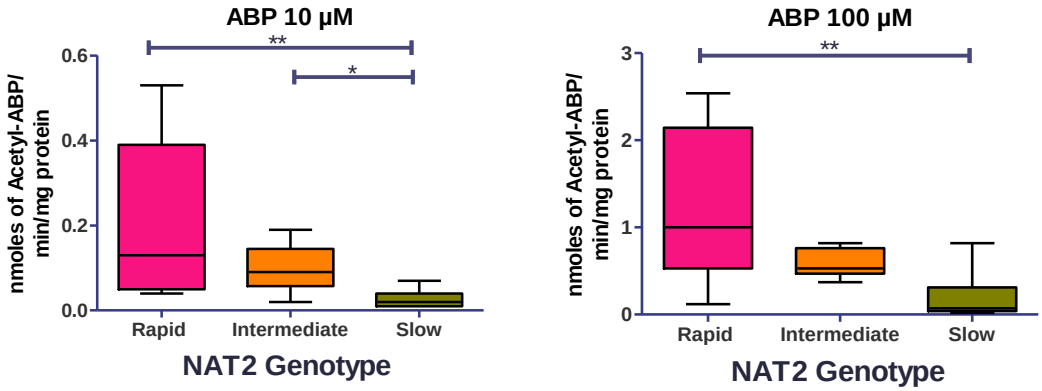

Figure (12): *In vitro N*-acetyltransferase catalytic activities towards ABP (10-100 µM). Data illustrates box plot of rapid (n=8), intermediate (n=8), and slow (n=9) acetylators. Statistical significance was determined using Kruskal-Wallis test followed by Dunn's Multiple Comparison Test. ABP *N*-acetyltransferase activities differed significantly between rapid, intermediate, and slow acetylators 10 µM ($p = 0.0023$; rapid vs. slow $p < 0.01$ and intermediate vs. slow $p < 0.05$) or 100 µM ($p = 0.0023$; rapid vs. slow $p < 0.01$).

β-NAPHTHYLAMINE (BNA):

For BNA, *N*-acetyltransferase activities differed significantly between rapid, slow, and intermediate acetylators at 10 ($p< 0.001$) and 100 µM ($p< 0.01$). *N*-acetylation rate of BNA in rapid acetylators was about 5- and 6-fold higher than slow acetylators at 10 µM and at 100 µM respectively (Figure 13).

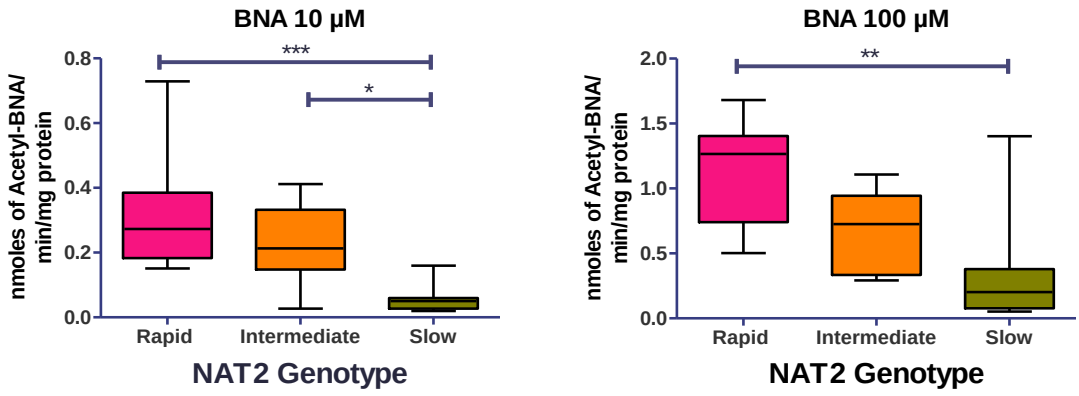

Figure (13): *In vitro N*-acetyltransferase catalytic activities towards BNA (10-100 µM). Data illustrates box plot of rapid (n=7), intermediate (n=9), and slow (n=11) acetylators. Statistical significance was determined using Kruskal-Wallis test followed by Dunn's Multiple Comparison Test. BNA *N*-acetyltransferase activities differed significantly between rapid, intermediate, and slow acetylators at 10 µM ($p= 0.0005$; rapid vs. slow $p < 0.001$ and intermediate vs. slow $p< 0.05$) or 100 µM ($p= 0.0013$; rapid vs. slow $p< 0.01$).

4, 4'-METHYLENE BIS (2-CHLOROANILINE) OR MOCA:

For MOCA, *N*-acetyltransferase activities differed significantly between rapid, slow, and intermediate acetylators at 10 µM and 100 µM ($p < 0.01$). *N*-acetylation rate of MOCA in rapid acetylators was about 8- and 10-fold higher than slow acetylators at 10 µM and at 100 µM, respectively (Figure 14).

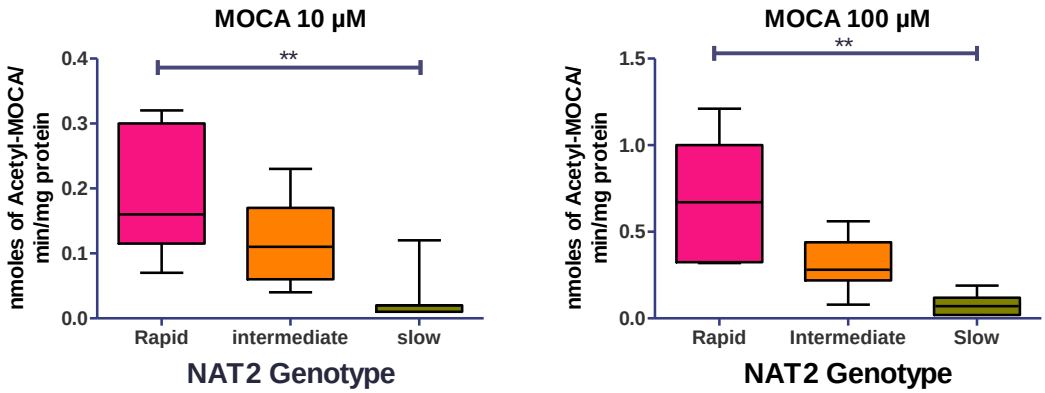

Figure (14): *In vitro N*-acetyltransferase catalytic activities towards MOCA (10-100 µM). Data illustrates box plot of rapid (n=5), intermediate (n=7), and slow (n=7) acetylators. Statistical significance was determined using Kruskal-Wallis test followed by Dunn's Multiple Comparison Test. MOCA *N*-acetyltransferase activities differed significantly between rapid, intermediate, and slow acetylators at 10 µM ($p = 0.0041$; rapid vs. slow $p < 0.01$) or 100 µM ($p = 0.0018$; rapid vs. slow $p < 0.01$).

Figures (11-14) showed *in vitro N*-acetylation rate of SMZ differed significantly among rapid, intermediate, and slow NAT2 acetylators. However, *in vitro N*-acetylation rates of ABP, BNA and MOCA were significantly higher in rapid NAT2 acetylators compared to slow acetylators only. No significant difference was

between rapid and intermediate NAT2 acetylators. This difference in *N*-acetylation rates for these carcinogens can affect the individual cancer risk.

IN SITU N-ACETYLTRANSFERASE ACTIVITY IN CRYOPRESERVED HUMAN HEPATOCYTES:

In situ N-acetylation rates for SMZ, ABP, BNA, and MOCA in cryopreserved hepatocytes was concentration dependent (Figure 15: a, b, c, d).

For SMZ, BNA and MOCA, there was significant correlation between time and the rate of production of the acetylated products at both concentrations 10 and 100 µM ($p < 0.05$). The single exception was at BNA 10 µM that can be explained with the decreased rate of production of acetylated BNA after 10 hours. Spearman Correlation coefficient or $r = 1.0$ for SMZ at both concentrations ($p = 0.0167$), $r = 1.0$ for BNA 100 µM ($p=0.0167$) and $r = 0.9747$ and 1.0 for MOCA 10 and 100 µM, respectively ($p=0.0167$). For ABP, $r = 1.0$ however, the correlation between time and rate of *N*-acetylation was insignificant at both concentrations ($p > 0.05$). It is likely that the rate of reaction started to decrease over time due to ABP consumption.

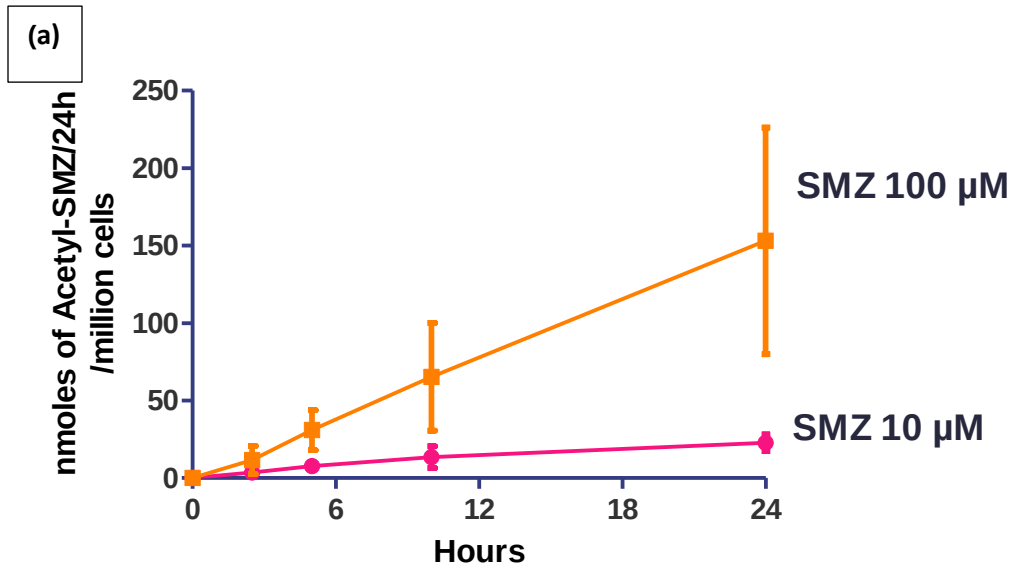
(a)
nmoles of Acetyl-SMZ/24h
/million cells
250
200
150
100
50
0
0
6
12
18
24
Hours
SMZ 100 µM
SMZ 10 µM

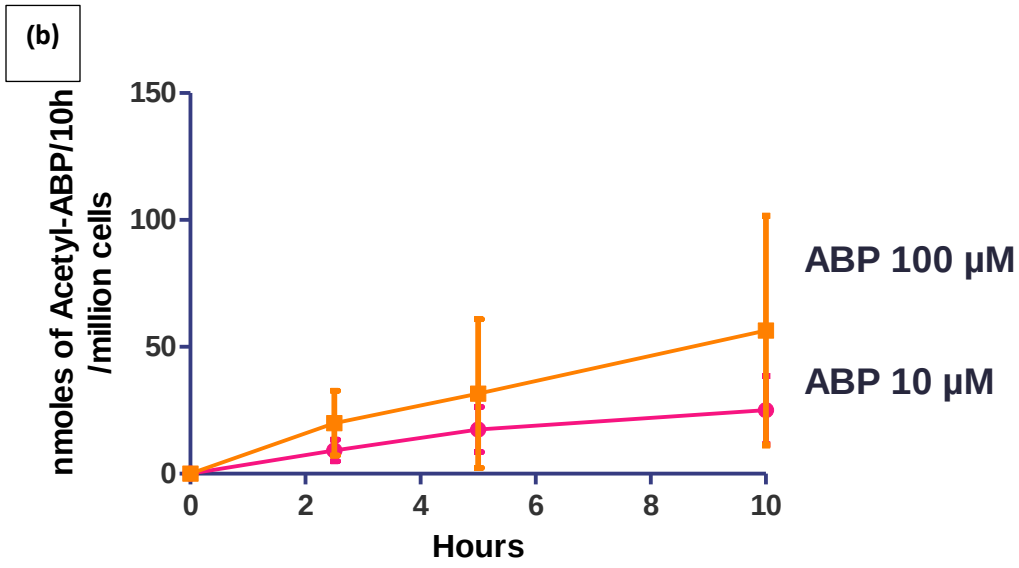
(b)
nmoles of Acetyl-ABP/10h
/million cells
150
100
50
0
0
2
4
6
8
10
Hours
ABP 100 µM
ABP 10 µM

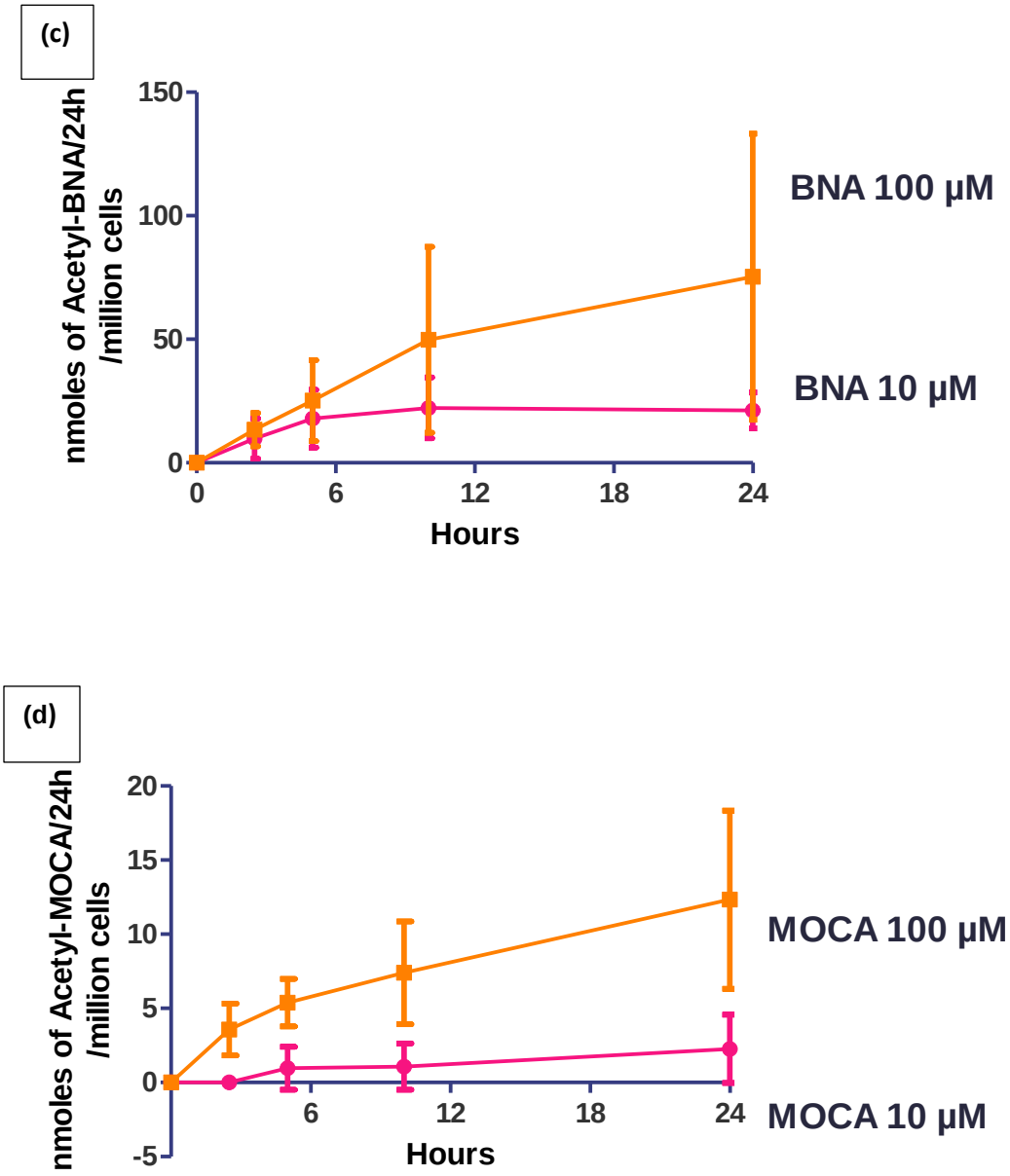

Figure (15): Concentration- and time-dependent *N*-acetylation of (a) SMZ, (b) ABP, (c) BNA, and (d) MOCA in cryopreserved human hepatocytes *in situ*. Each data point illustrates the mean ± SD of 6 replicates of SMZ, ABP and BNA treated hepatocytes and 5 replicates of MOCA treated hepatocytes. Correlation between time and the rate of production of N-acetylated products was determined using Spearman's correlation test. Significant correlation ($p < 0.05$) was found in case of SMZ, BNA and MOCA not ABP.

Also, the *in-situ N*-acetylation rates of SMZ, ABP, BNA and MOCA were measured using cryopreserved human hepatocytes with different NAT2 genotypes and the results are shown below in detail.

Sulfamethazine (SMZ):

N-acetylation rate of SMZ in rapid acetylators was about 22- and 20-fold higher ($p< 0.001$) than slow acetylator hepatocytes, following incubation with SMZ 10 µM and 100 µM respectively (Figure 16).

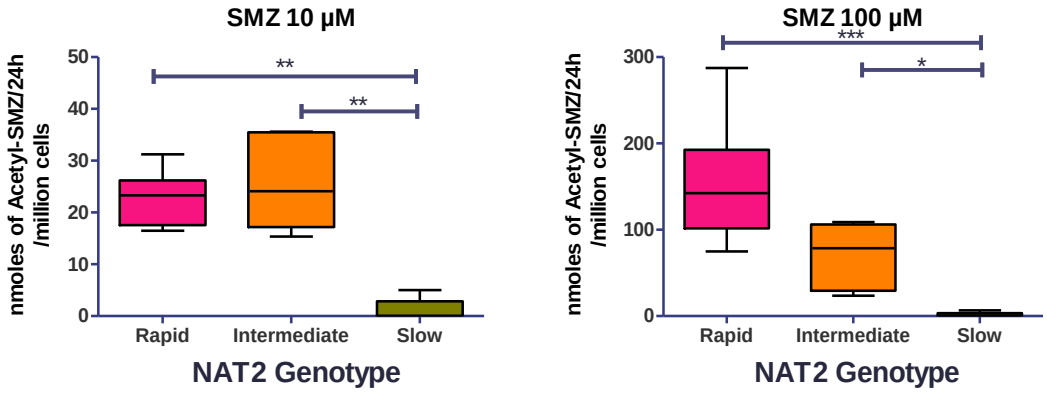

Figure (16): *N*-acetylation rate of SMZ *in situ* in cryopreserved human hepatocytes from rapid, intermediate, and slow acetylators. Data illustrates box plot of rapid (n=6), intermediate (n=6), and slow (n=9) acetylators. Statistical significance was determined using Kruskal-Wallis test followed by Dunn's Multiple Comparison Test. SMZ *N*-acetylation rates differed significantly at 10 µM ($p= 0.0005$; rapid vs. slow $p< 0.01$; intermediate vs slow $p< 0.01$) or at 100 µM ($p= 0.0002$; rapid vs. slow $p< 0.001$; intermediate vs. slow $p< 0.05$).

4-AMINOBIPHENYL (ABP):

N-acetylation of ABP differed significantly between rapid and slow; and between intermediate and slow acetylators ($p < 0.01$). *N*-acetylation rate in rapid acetylators was about 6- and 4-fold higher than slow acetylator hepatocytes, following incubation with ABP 10 µM and 100 µM respectively (Figure 17).

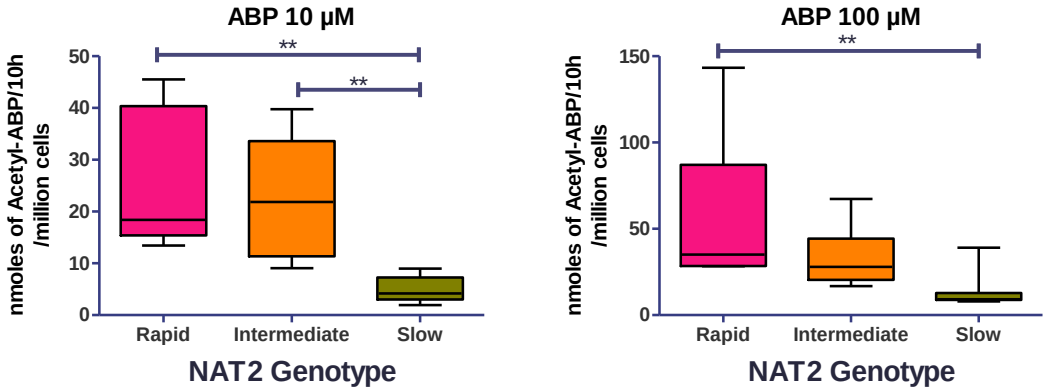

Figure (17): *N*-acetylation rate of ABP *in situ* in cryopreserved human hepatocytes from rapid, intermediate, and slow acetylators. Data illustrates box plot of rapid (n=6), intermediate (n=6), and slow (n=9) acetylators. Statistical significance was determined using Kruskal-Wallis test followed by Dunn's Multiple Comparison Test. ABP *N*-acetylation rates differed significantly at 10 µM ($p = 0.0006$; rapid vs. slow $p < 0.01$; intermediate vs. slow $p < 0.01$) or at 100 µM ($p = 0.0034$; rapid vs. slow $P < 0.01$).

β-NAPHTHYLAMINE (BNA):

N-acetylation differed significantly between rapid and slow; and between intermediate and slow acetylators ($p < 0.01$). *N*-acetylation rate in rapid acetylators was about 3- and 4- fold higher than slow acetylator hepatocytes, following incubation with BNA 10 µM and 100 µM respectively (Figure 18).

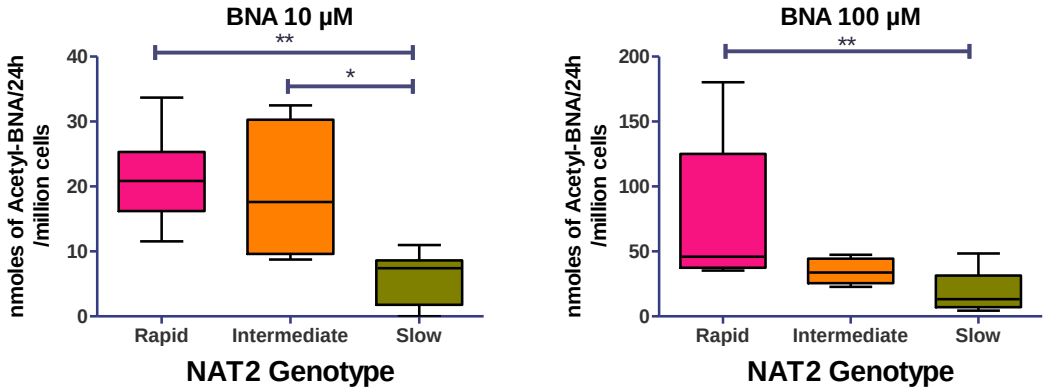

Figure (18): *N*-acetylation rate of BNA *in situ* in cryopreserved human hepatocytes from rapid, intermediate, and slow acetylators. Data illustrates box plot of rapid (n=6), intermediate (n=5), and slow (n=9) acetylators. Statistical significance was determined using Kruskal-Wallis test followed by Dunn's Multiple Comparison Test. BNA *N*-acetylation rates differed significantly at 10 µM ($p = 0.0016$; rapid vs. slow $p < 0.01$; intermediate vs. slow $p < 0.05$) or at 100 µM ($p = 0.0099$; rapid vs. slow $p < 0.01$).

4, 4’-METHYLENE BIS (2-CHLOROANILINE) OR MOCA:

N-acetylation of MOCA was detected in rapid acetylators. N-acetyl MOCA was below detection limit in intermediate and slow acetylators (Limit of detection was 13 pmole/24h/million cells) (Figure 19).

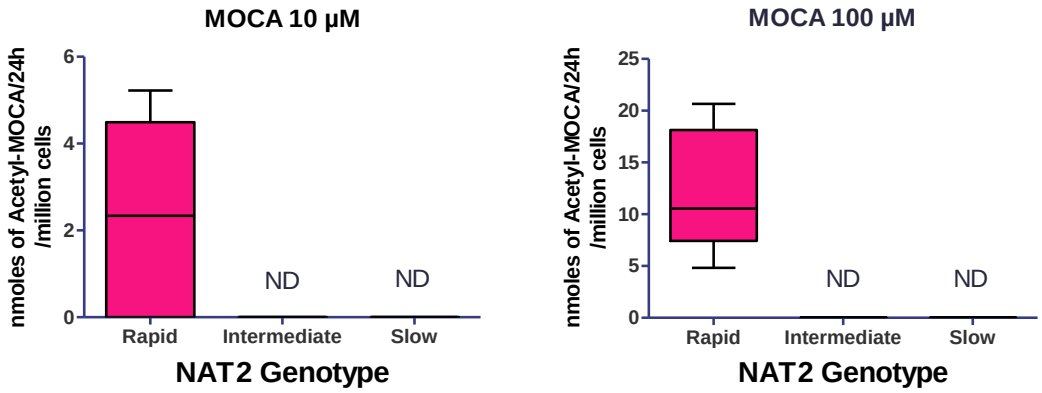

Figure (19): *N*-acetylation rate of MOCA *in situ* in cryopreserved human hepatocytes from rapid, intermediate, and slow acetylators. Data illustrates box plot of rapid (n=5), intermediate (n=5), and slow (n=5) acetylators. ND = Not detected (Limit of detection was 13 pmole//24h/million cells)

Both *in vitro* and *in situ* NAT2 activity assays showed NAT2 genotype dependent *N*-acetylation of carcinogens as ABP, BNA, and MOCA suggesting a role of NAT2 genotype polymorphism in modification of cancer risk following exposure to these carcinogens.

CELL TOXICITY RESULTS:

We have measured the percent of cell survival in cryopreserved human hepatocytes following treatment with ABP, BNA and MOCA.

4-AMINOBIPHENYL (ABP):

Treatment of cryopreserved human hepatocytes using ABP for 24 hours led to concentration dependent cytotoxicity in all NAT2 genotypes. Cell survival following ABP 100 µM treatment differed significantly ($p < 0.05$) in all genotypes (Figure 20). However, there was no significant difference ($p > 0.05$) between different genotypes (Figure 21).

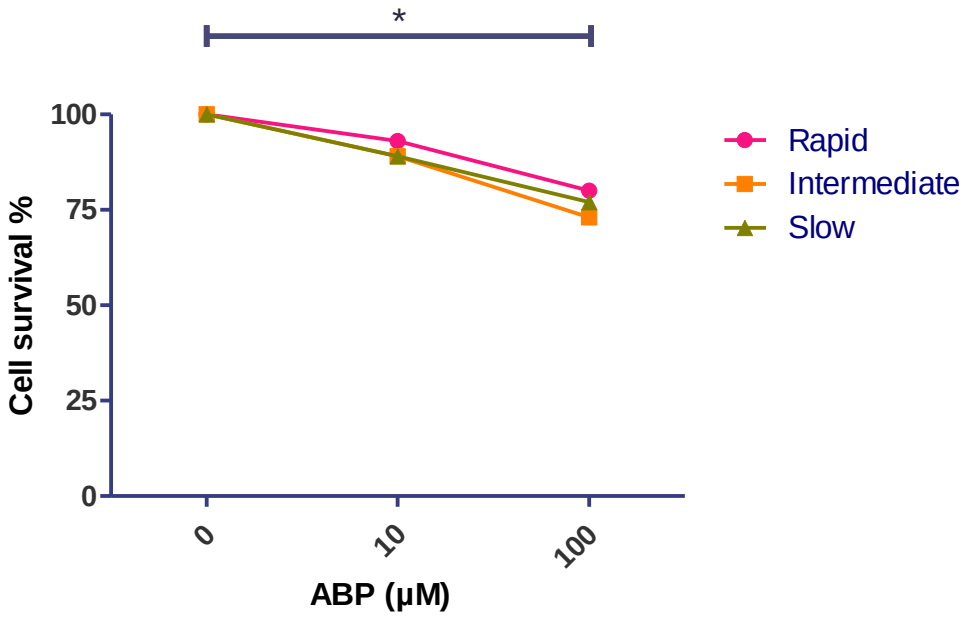

Figure (20): Cell survival following treatment with ABP. Percent cell survival on the ordinate is plotted versus ABP treatment concentration on the abscissa. Statistical significance was determined using Kruskal-Wallis test followed by Dunn's Multiple Comparison Test. Each data point represents Median for 5 experiments in Rapid (circles), Intermediate (squares), Slow (triangles). For all genotypes, cell survival differed significantly following treatment with 100 µM.*= $p < 0.05$

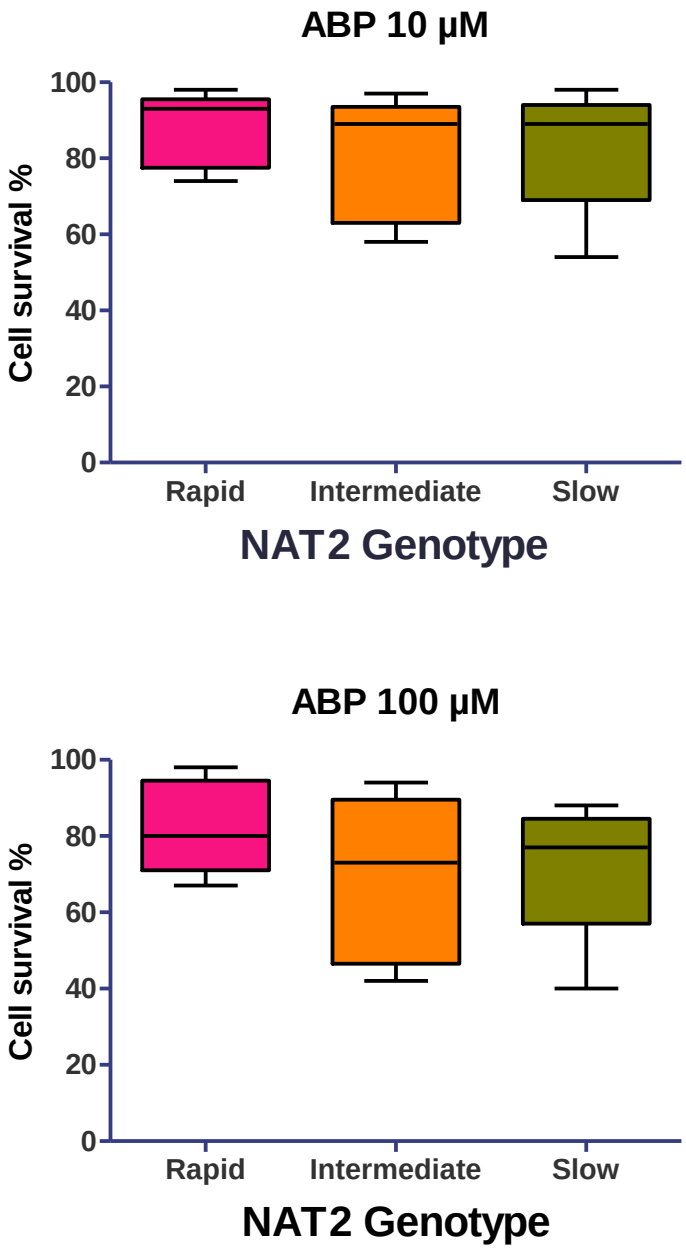

Figure (21): Effect of ABP treatment on cell survival: at 10 µM (Top panel) and at 100 µM (Bottom panel) in cryopreserved human hepatocytes. Statistical significance was determined using Kruskal-Wallis test followed by Dunn's Multiple Comparison Test. Data illustrates box plot of 5 experiments. There was no significant difference between different genotypes at both concentrations ($p > 0.05$).

B-NAPHTHYLAMINE (BNA):

Treatment of cryopreserved human hepatocytes using BNA for 24 hours led to concentration dependent cytotoxicity in all NAT2 genotypes. Cell survival following BNA 100 µM treatment differed significantly in all genotypes ($p < 0.05$) (Figure 22). However, there was no significant difference ($p > 0.05$) between different genotypes (Figure 23).

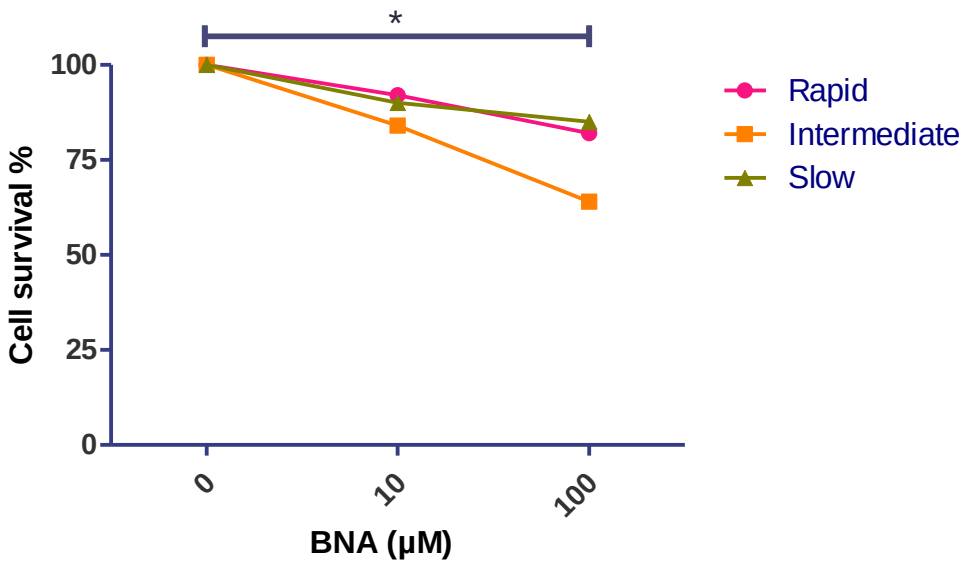

Figure (22): Cell survival following treatment with BNA. Percent cell survival on the ordinate is plotted versus BNA treatment concentration on the abscissa. Statistical significance was determined using Kruskal-Wallis test followed by Dunn's Multiple Comparison Test. Each data point represents Median for 5 experiments in Rapid (circles), Intermediate (squares), Slow (triangles). For all genotypes, cell survival differed significantly following treatment 100 µM.

*= $p < 0.05$

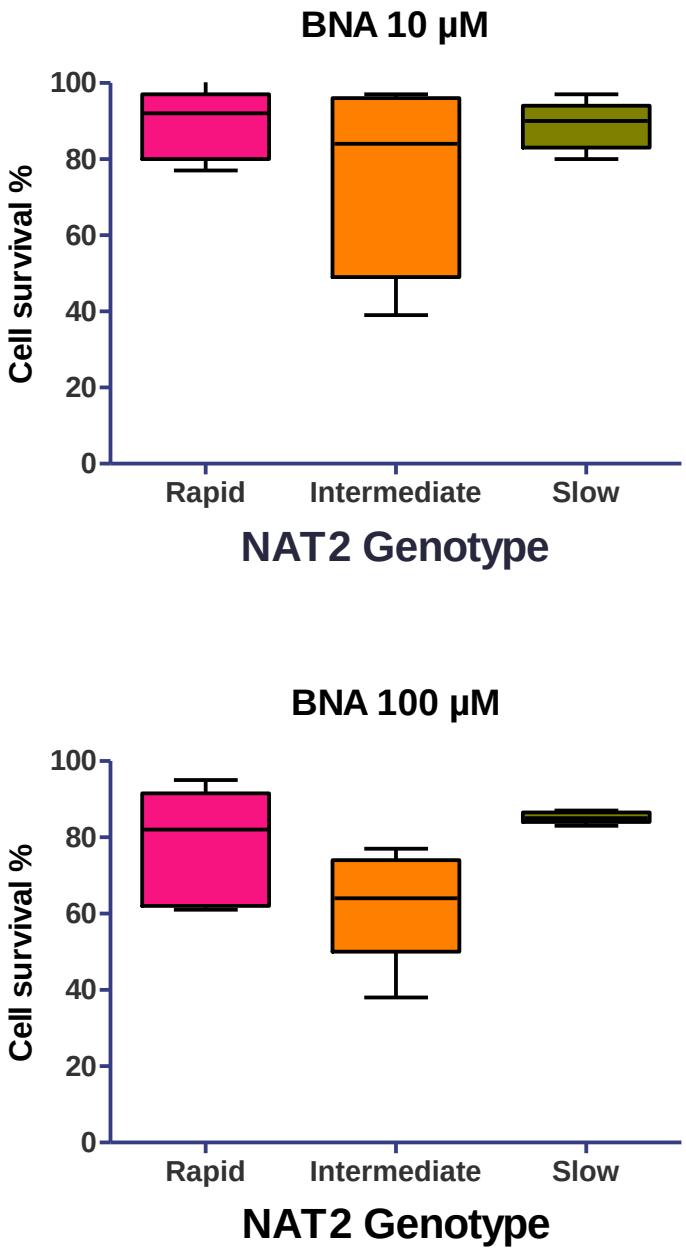

Figure (23): Effect of BNA treatment on cell survival: at 10 µM (Top panel) and at 100 µM (Bottom panel) in cryopreserved human hepatocytes. Statistical significance was determined using Kruskal-Wallis test followed by Dunn's Multiple Comparison Test. Data illustrates box plot of 5 experiments. There was no significant difference between different genotypes at both concentrations ($p > 0.05$).

4, 4'-METHYLENE BIS (2-CHLOROANILINE) OR MOCA:

Treatment of cryopreserved human hepatocytes using MOCA for 24 hours led to concentration dependent cytotoxicity in all NAT2 genotypes. Cell survival following MOCA 100 µM treatment differed significantly ($p < 0.05$ in all genotypes) (Figure 24). However, there was no significant difference ($p > 0.05$) between different genotypes (Figure 25).

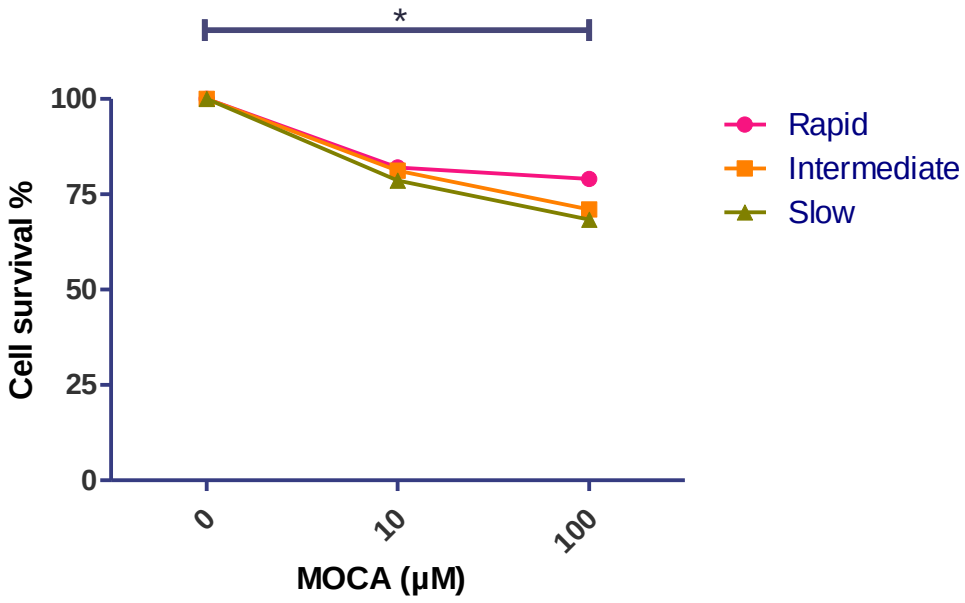

Figure (24): Cell survival following treatment with MOCA. Percent cell survival on the ordinate is plotted versus MOCA treatment concentration on the abscissa. Statistical significance was determined using Kruskal-Wallis test followed by Dunn's Multiple Comparison Test. Each data point represents Median for 5 experiments in Rapid (circles), Intermediate (squares), Slow (triangles). For all genotypes, cell survival differed significantly following treatment with 100 µM.

*= $p < 0.05$

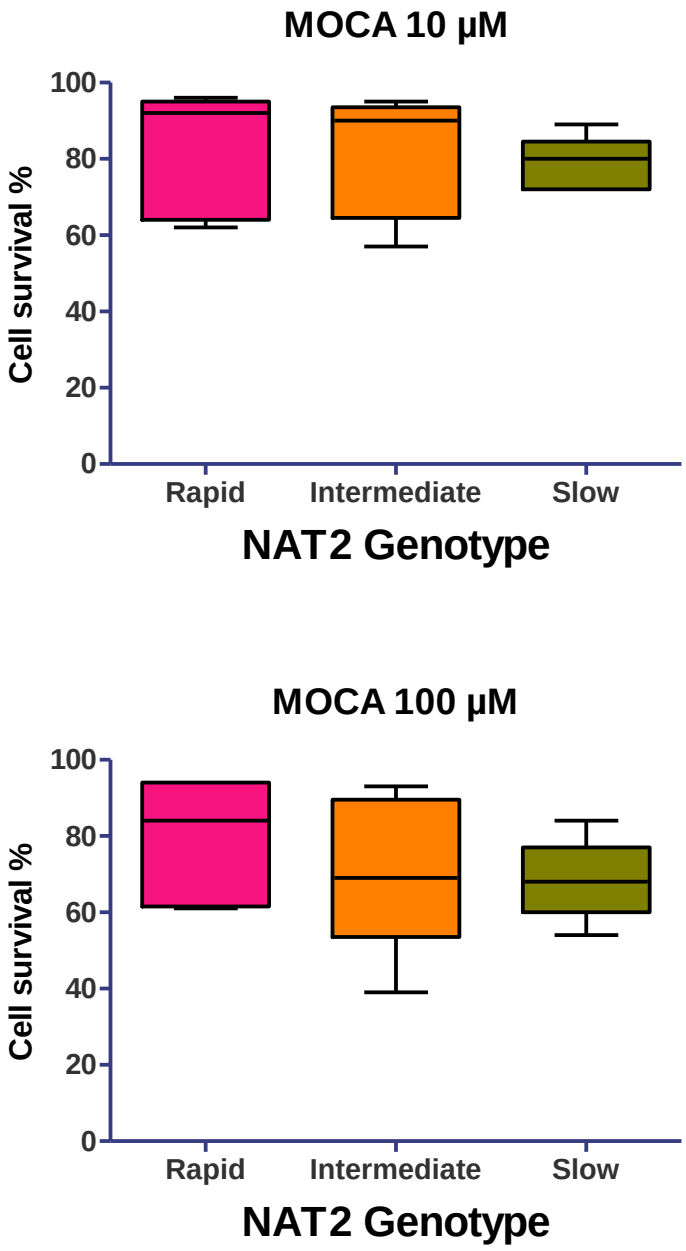

Figure (25): Effect of MOCA treatment on cell survival: at 10 µM (Top panel) and at 100 µM (Bottom panel) in cryopreserved human hepatocytes. Statistical significance was determined using Kruskal-Wallis test followed by Dunn's Multiple Comparison Test. Data illustrates box plot of 5 experiments. There was no significant difference between different genotypes at both concentrations ($p > 0.05$).

IN VITRO N-ACETYLTRANSFERASE ACTIVITY IN CHINESE HAMSTER OVARY (CHO) CELLS:

For hydralazine, INH, BNA and MOCA, *in vitro* NAT2 activity was done using three different concentrations: 10, 100, 1000 µM and AcCoA 300 and 1000 µM to investigate the role of NAT2 genotype polymorphism in *N*-acetylation. *N*-acetyltransferase activities were normalized to reaction minutes and mg protein.

HYDRALAZINE:

For Hydralazine 10 µM or 100 µM and AcCoA 300 µM, NAT2 catalytic in UV5/CYP1A1/NAT2*4 cells was line was about 5-fold higher than UV5/CYP1A1/NAT2*7B cells ($p < 0.05$). For Hydralazine 1000 µM and AcCoA 300 µM, NAT2 catalytic activity in UV5/CYP1A1/NAT2*4 cells was about 4-fold higher than UV5/CYP1A1/NAT2*7B cells ($p < 0.05$) (Figure 26).

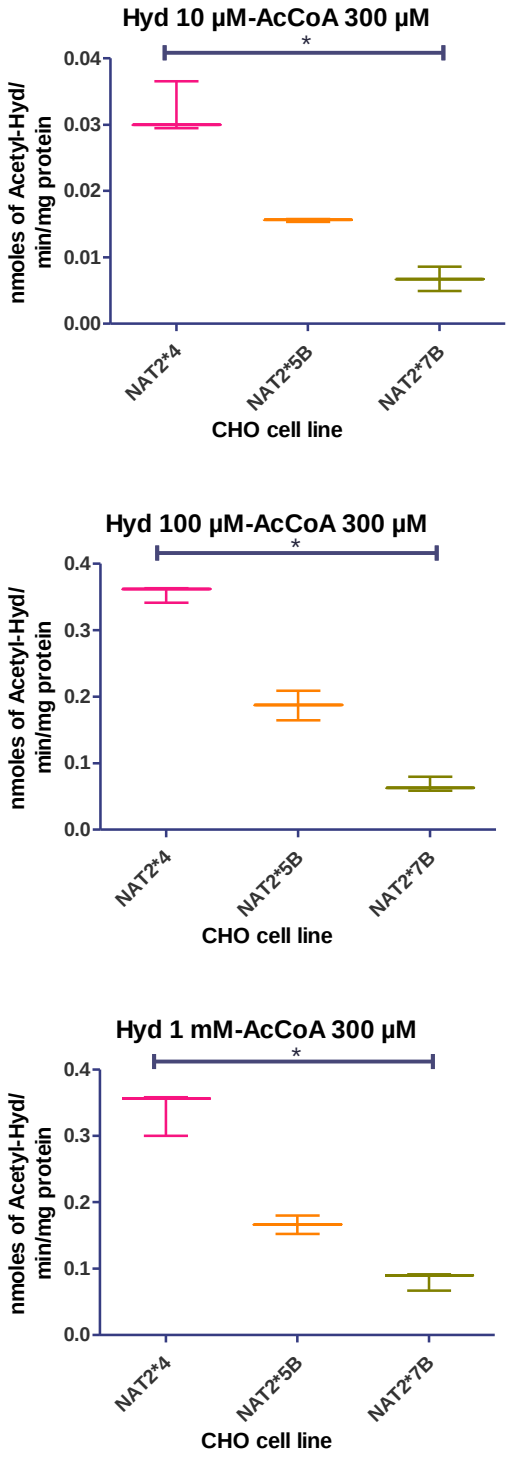

Figure (26): *N*-acetylation rate of hydralazine *in vitro* in CHO cell lines using AcCoA 300 µM. Statistical significance was determined using Kruskal-Wallis test followed by Dunn's Multiple Comparison Test. Data illustrates box plot of three replicates. *= p< 0.05

For hydralazine 10 µM and AcCoA 1000 µM, No significant difference between *N*-acetylation rate of hydralazine in the three genotypes ($p > 0.05$). For hydralazine 100 or 1000 µM and AcCoA 1000 µM, NAT2 catalytic activity in UV5/CYP1A1/NAT2*4 cells was about 13-fold higher than UV5/CYP1A1/NAT2*7B cells ($p < 0.05$) (Figure 27).

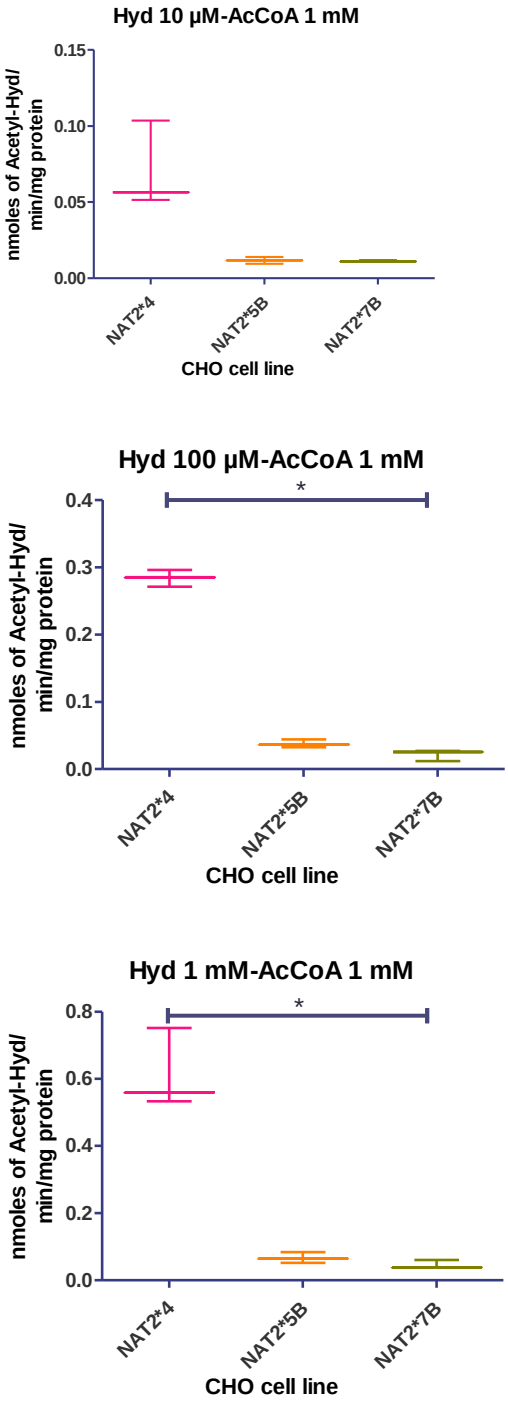

Figure (27): *N*-acetylation rate of hydralazine *in vitro* in CHO cell lines using AcCoA 1000 µM. Statistical significance was determined using Kruskal-Wallis test followed by Dunn's Multiple Comparison Test. Data illustrates box plot of three replicates. *= p< 0.05

ISONIAZID (INH):

For isoniazid 10 µM and AcCoA 300 µM, NAT2 catalytic was undetected in all CHO cell lines (The detection limit was 0.1 pmole/min/mg). For isoniazid 100 µM and AcCoA 300 µM, NAT2 catalytic activity in UV5/CYP1A1/NAT2*4 cells was about 4-fold higher than UV5/CYP1A1/NAT2*5B cells ($p < 0.05$) while there is no detectable activity in UV5/CYP1A1/NAT2*7B cell line. For isoniazid 1000 µM and AcCoA 300 µM, NAT2 catalytic activity in UV5/CYP1A1/NAT2*4 cells was about 5-fold higher than UV5/CYP1A1/NAT2*7B cells ($p < 0.05$) (Figure 28).

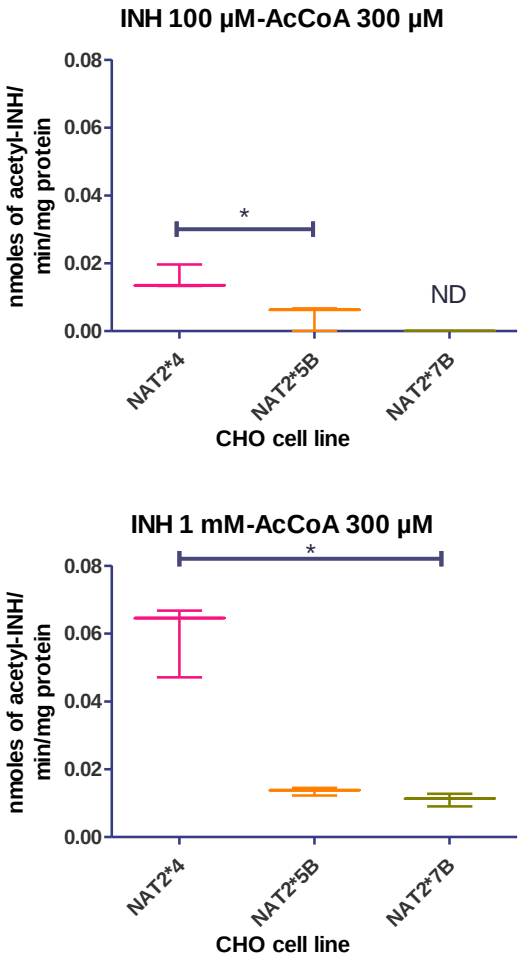

Figure (28): *N*-acetylation rate of isoniazid *in vitro* in CHO cell lines using AcCoA 300 µM. Statistical significance was determined using Unpaired T-test (INH 100 µM) and Kruskal-Wallis test followed by Dunn's Multiple Comparison Test (INH 1000 µM). Data illustrates box plot of three replicates. *= p< 0.05, ND= not detected (The detection limit was 0.1 pmole/min/mg)

For AcCoA 1000 µM, NAT2 catalytic activity in UV5/CYP1A1/NAT2*4 cells was 4-, 11- 12- fold higher than in UV5/CYP1A1/NAT2*7B cells with isoniazid 10, 100, 1000 µM, respectively (p< 0.05) (Figure 29).

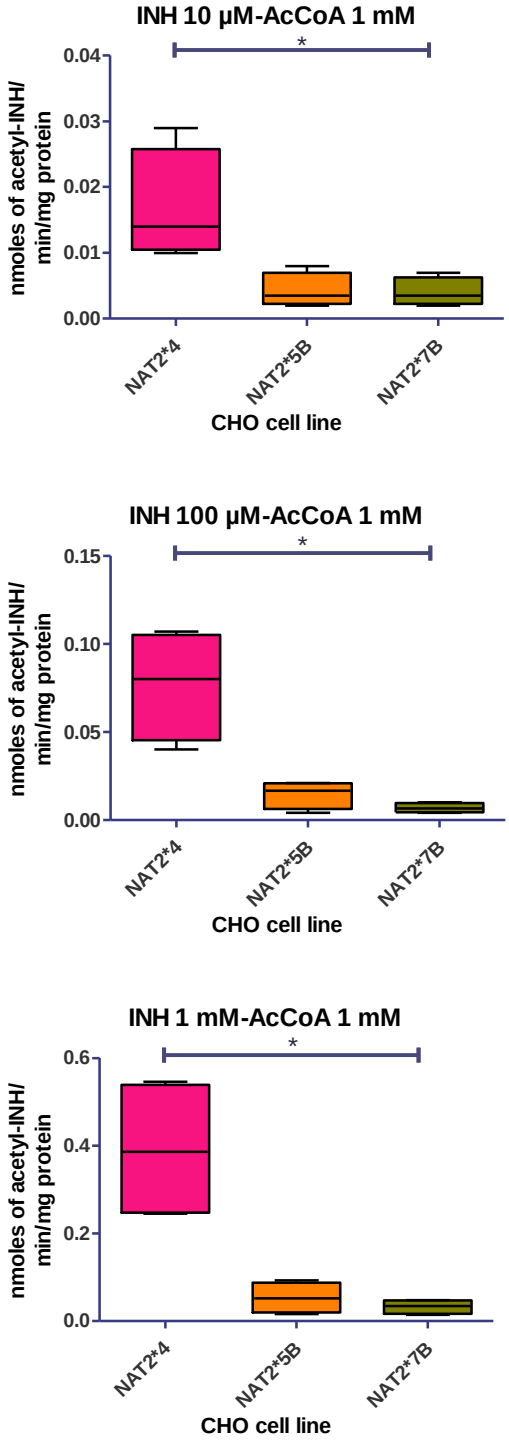

Figure (29): *N*-acetylation rate of isoniazid *in vitro* in CHO cell lines using AcCoA 1000 µM. Statistical significance was determined using Kruskal-Wallis test followed by Dunn's Multiple Comparison Test. Data illustrates box plot of four replicates. *= p< 0.05

N-acetylation rates of hydralazine and INH differed significantly between UV5/CYP1A1/NAT2*4 cells (contains rapid NAT2 allele) and UV5/CYP1A1/NAT2*7B but not UV5/CYP1A1/NAT2*5B although both contain slow NAT2 alleles.

β-NAPHTHYLAMINE (BNA):

In vitro BNA NAT2 activity was not detected in the UV5 and UV5/CYP1A1 cell lines (Limit of detection was 0.03 pmoles/min/mg).

For BNA 10 µM or 100 µM and AcCoA 300 µM, NAT2 catalytic activity towards BNA in UV5/CYP1A1/NAT2*4 cells was about 7-fold higher than in the UV5/CYP1A1/NAT2*5B cells ($p < 0.05$). For BNA 1000 µM and AcCoA 300 µM, NAT2 catalytic activity towards BNA in UV5/CYP1A1/NAT2*4 cells was about 4-fold higher than the UV5/CYP1A1/NAT2*5B cells ($p < 0.05$). In all BNA concentrations, there was no significant difference between UV5/CYP1A1/NAT2*5B and UV5/CYP1A1/NAT2*7B cell lines ($p > 0.05$) (Figure 30).

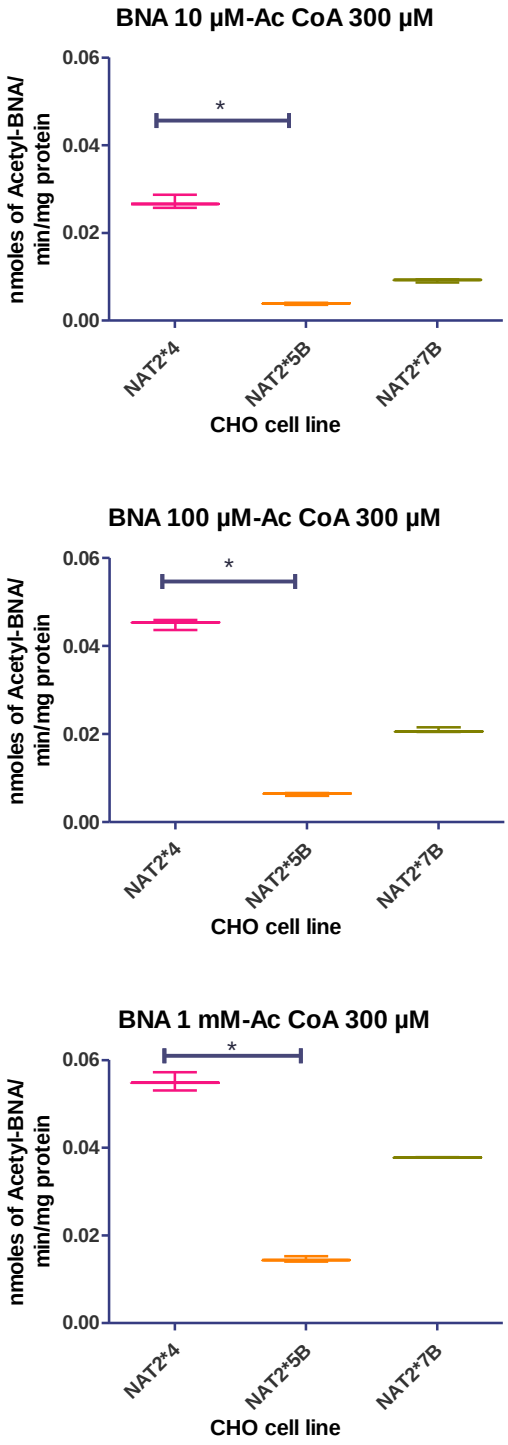

Figure (30): *N*-acetylation rate of BNA *in vitro* in CHO cell lines using AcCoA 300 µM. Statistical significance was determined using Kruskal-Wallis test followed by Dunn's Multiple Comparison Test. Data illustrates box plot of three replicates. *= p< 0.05

For BNA 10 µM and AcCoA 1000 µM, NAT2 catalytic activity towards BNA in UV5/CYP1A1/NAT2*4 cells was about 37-fold higher than in the UV5/CYP1A1/NAT2*7B cells ($p < 0.05$). For BNA 100 µM and AcCoA 1000 µM, NAT2 catalytic activity towards BNA in UV5/CYP1A1/NAT2*4 cells was about 9- and 14-fold higher than in the UV5/CYP1A1/NAT2*5B and UV5/CYP1A1/NAT2*7B cell lines respectively ($p < 0.05$). For BNA 1000 µM and AcCoA 1000 µM, NAT2 catalytic activity towards BNA in UV5/CYP1A1/NAT2*4 cells was about 8-and 9-fold higher than in the UV5/CYP1A1/NAT2*5B and UV5/CYP1A1/NAT2*7B cell lines respectively ($p < 0.05$). In all BNA concentrations, there was no significant difference between UV5/CYP1A1/NAT2*5B and UV5/CYP1A1/NAT2*7B cell lines ($p > 0.05$) (Figure 31).

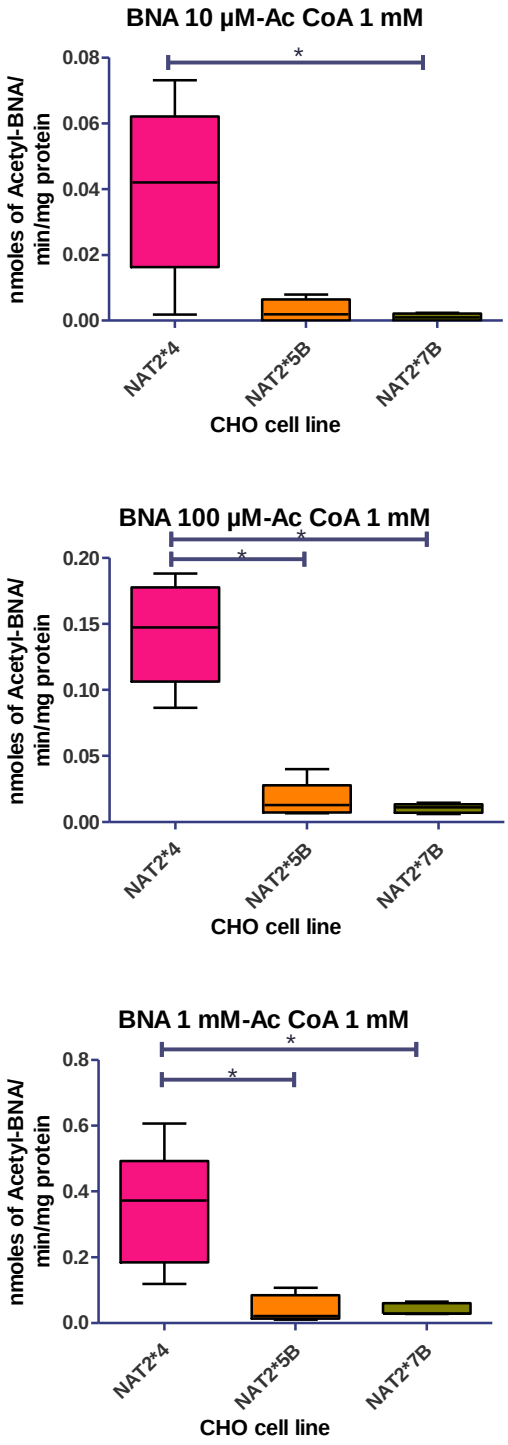

Figure (31): *N*-acetylation rate of BNA *in vitro* in CHO cell lines using AcCoA 1000 µM. Statistical significance was determined using Kruskal-Wallis test followed by Dunn's Multiple Comparison Test. Data illustrates box plot of five replicates. *= p< 0.05

4, 4’-METHYLENE BIS (2-CHLOROANILINE) OR MOCA:

For MOCA 10 µM or 100 µM and AcCoA 300 µM, *in vitro* NAT2 catalytic activity towards MOCA in UV5/CYP1A1/NAT2*4 cells was about 4-fold higher than in the UV5/CYP1A1/NAT2*5B cells ($p < 0.05$). For MOCA 1000 µM and AcCoA 300 µM, NAT2 catalytic activity towards MOCA had no significant difference between the three genotypes ($p > 0.05$). Also, increasing MOCA concentration from 100 µM to 1000 µM with steady AcCoA concentration did not lead to further increase in the rate of production of the acetylated MOCA (Figure 32).

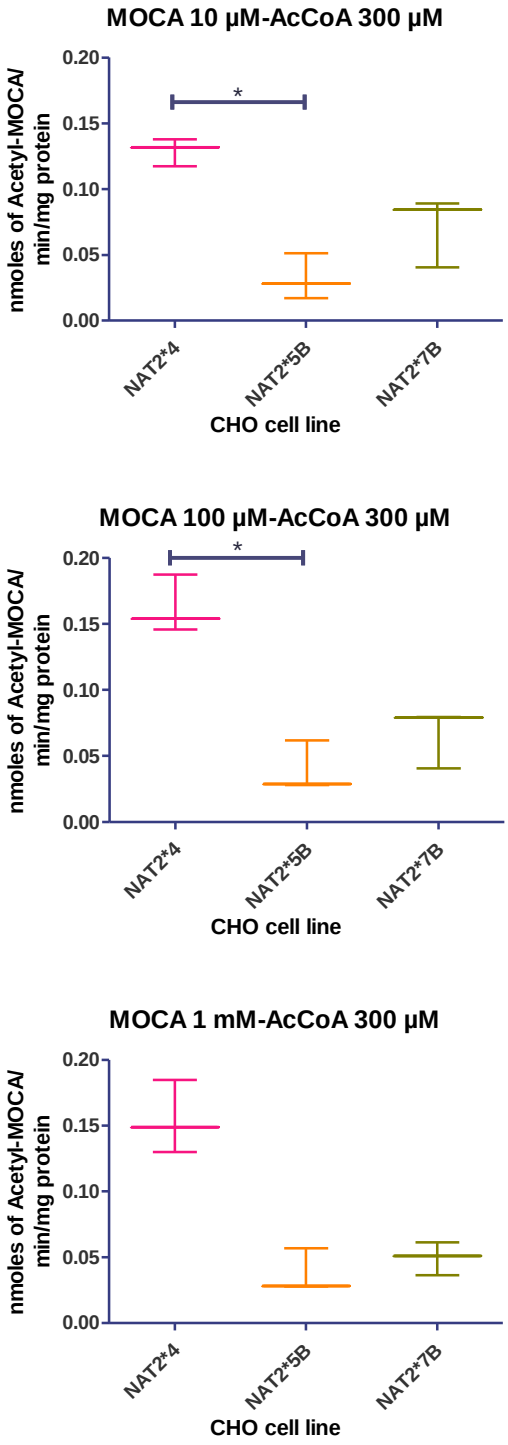

Figure (32): *N*-acetylation rate of MOCA *in vitro* in CHO cell lines using AcCoA 300 µM. Statistical significance was determined using Kruskal-Wallis test followed by Dunn's Multiple Comparison Test. Data illustrates box plot of three replicates. *= $p < 0.05$

For MOCA 10, 100 or 1000 µM and AcCoA 1000 µM, NAT2 catalytic activity towards MOCA showed no significant difference between the three genotypes ($p > 0.005$) (Figure 33).

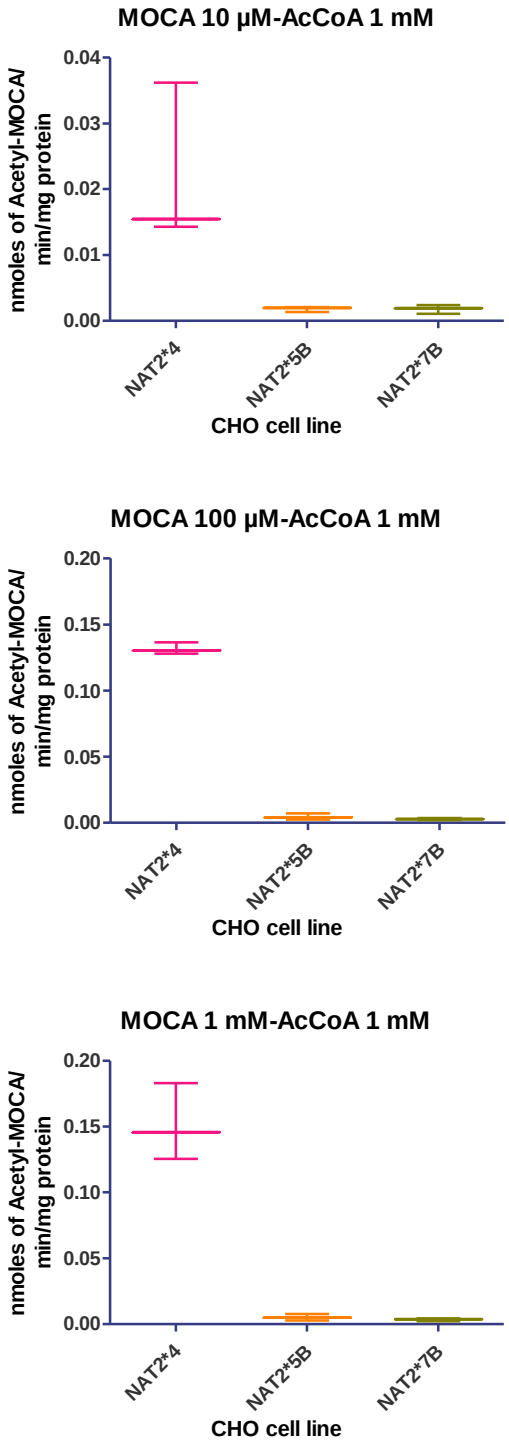

Figure (33): *N*-acetylation rate of MOCA *in vitro* in CHO cell lines using AcCoA 1000 µM. Statistical significance was determined using Kruskal-Wallis test followed by Dunn's Multiple Comparison Test. Data illustrates box plot of three replicates.

In vitro N-acetylation rates of hydralazine and isoniazid showed higher level in *NAT2*4* compared to *NAT2*7B* not *NAT2*5B* although both are slow. For BNA, CHO cells expressing *NAT2*5B* and *NAT287B* showed different significance when compared to *NAT2*4*. At AcCoA 300 µM, *N*-acetylation rate in *NAT2*4* was significantly higher than *NAT2*5B* and not *NAT2*7B*. However, at AcCoA 1000 µM, *N*-acetylation rate of *NAT2*4* was significantly higher than both NAT2*5B and *NAT2*7B*. For MOCA, *NAT2*4* is significantly higher than *NAT2*5B* and not *NAT2*7B*. All these finding suggest *N*-acetylation rate of some substrates differ according to AcCoA concentration within the same slow NAT2 genotype.

KINETICS OF CHO CELLS EXPRESSING *NAT2*4*, *NAT2*5B* AND *NAT2*7B*:

Previous studies have measured apparent K_m and V_{max} of SMZ, ABP [37], and hydralazine [57]. Table (6) summarizes the apparent K_m and V_{max} of SMZ, ABP and hydralazine previously reported by our lab.

Table (6): Kinetic parameters for SMZ, ABP, and hydralazine acetylation

Substrate	**K_m (µM)**	**V_{max} (nmole/min/mg protein)**
SMZ [37]	116	11.5
ABP [37]	25.8 ± 3.1	2.41 ± 0.16
Hydralazine [57]	20.1 ± 8.8	153 ± 15

In the current study, Kinetics of BNA and MOCA acetylation were tested in CHO cells expressing *NAT2*4*, *NAT2*5B* or *NAT2*7B*

BNA KINETICS:

To determine apparent K_m and V_{max} values for BNA, *in vitro* N-acetyltransferase reactions were run in the presence of a range of BNA (7.8–1000 µM) and fixed concentration of AcCoA (300 µM). Apparent K_m did not vary significantly between *NAT2*4*, *NAT2*5B* and *NAT2*7B* ($p > 0.05$).

However, V_{max} which is the rate of production of acetylated BNA for UV5/CYP1A1/NAT2*4 cells was about 7-fold greater ($p < 0.05$) than in the UV5/CYP1A1/NAT2*5B cell line (Table 7, Figure 34).

Table (7): Kinetic parameters for BNA acetylation by *NAT2*4*, *NAT2*5B* and *NAT2*7B* in CHO cells

Enzyme	K_m (μM)	V_{max} (nmole/min/mg protein)
NAT2*4	9.65 ± 2.7	0.0522 ± 0.0032
NAT2*5B	9.2 ± 1.8	0.0078 ± 0.0003
NAT2*7B	130.9 ± 15.9	0.0313 ± 0.0012

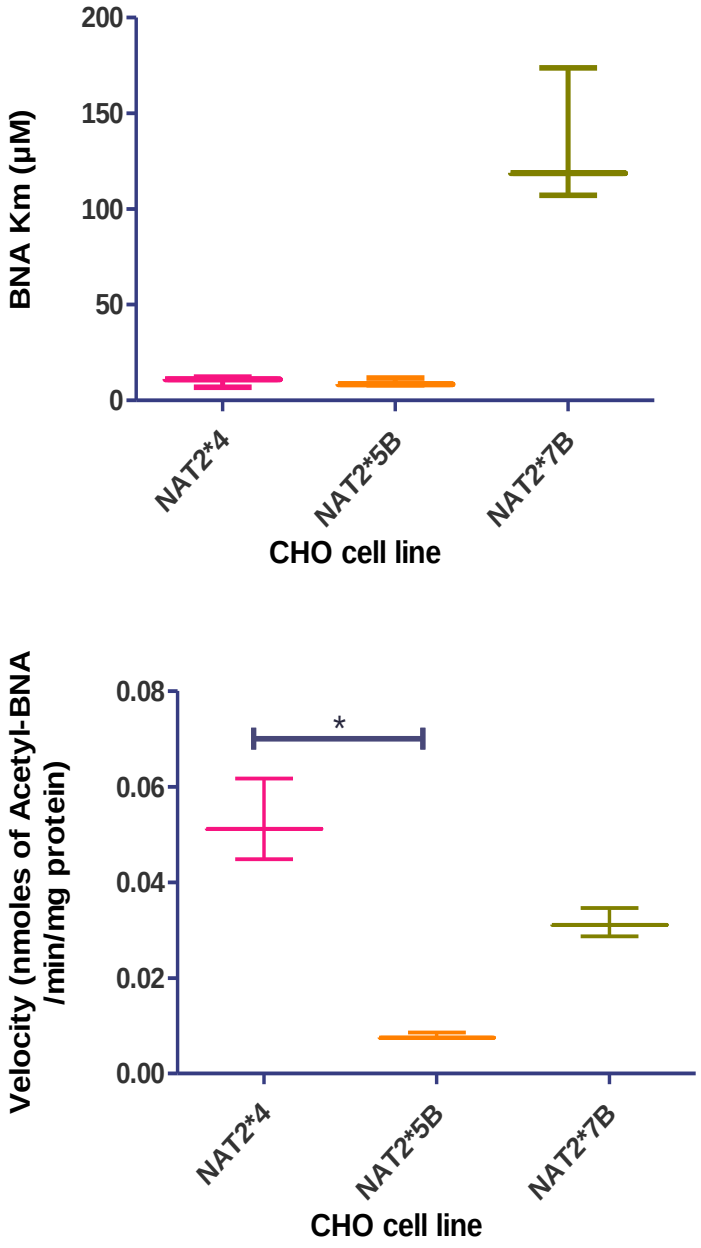

Figure (34): Different CHO cells genotypes affinity towards BNA. No significant difference in apparent K_m between NAT2*4, NAT2*5B and NAT2*7B (Top panel). The rate of production of N-Acetyl BNA was lower in NAT2*5B than NAT2*4 as indicated by the lower V_{max} (Bottom panel). Statistical significance was determined using Kruskal-Wallis test followed by Dunn's Multiple Comparison Test. Data illustrates box plot of three replicates. *= $p < 0.05$

MOCA KINETICS:

To determine apparent K_m and V_{max} values for MOCA, *in vitro* N-acetyltransferase reactions were run in the presence of a range of MOCA (25–300 µM) and fixed concentration of AcCoA (300 µM). Apparent K_m values of MOCA did not vary significantly between *NAT2*4*, *NAT2*5B* and *NAT2*7B* ($p > 0.05$).

However, V_{max} which is the rate of production of acetylated MOCA for UV5/CYP1A1/NAT2*4 cells was about 42-fold higher ($p < 0.05$) than in the UV5/CYP1A1/NAT2*7B cell line (Table 8 and Figure 35).

Table (8): Kinetic parameters for MOCA acetylation by NAT2*4, NAT2*5B in CHO cells

Enzyme	K_m (µM)	V_{max} (nmole/min/mg protein)
NAT2*4	16.04 ± 5.2	0.0849 ± 0.0022
NAT2*5B	37.72 ± 30.54	0.0026 ± 0.0004
NAT2*7B	6.64 ± 2.76	0.0020 ± 0.0001

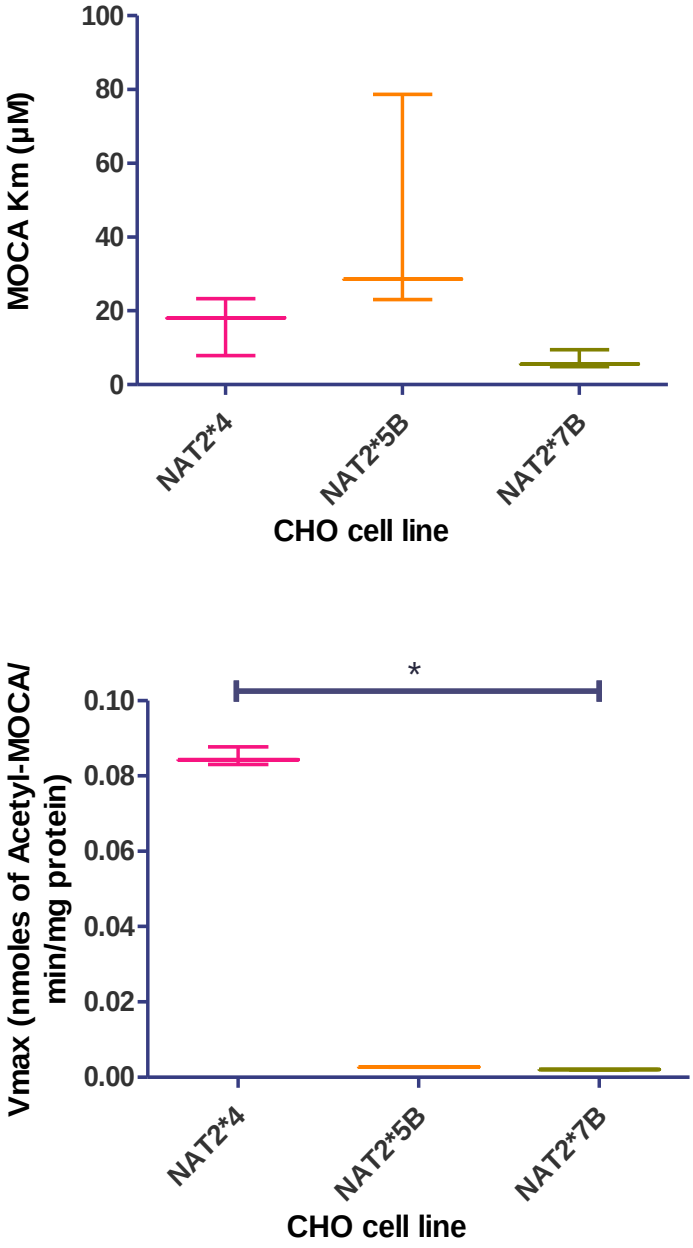

Figure (35): Different CHO cells genotypes affinity towards MOCA. No significant difference in apparent K_m between NAT2*4, NAT2*5B and NAT2*7B (Top panel). The rate of production of N-Acetyl MOCA was lower in NAT2*7B than NAT2*4 as indicated by the lower V_{max} (Bottom panel). Statistical significance was determined using Kruskal-Wallis test followed by Dunn's Multiple Comparison Test. Data illustrates box plot of three replicates. *= $p< 0.05$

IN SITU N-ACETYLTRANSFERASE ACTIVITY IN CHINESE HAMSTER OVARY (CHO) CELLS:

In the current study, we have used CHO cells expressing CYP1A2 and *NAT2*4, NAT2*5B* or *NAT2*7B* to measure *in situ* N-acetyltransferase activity towards BNA and MOCA. Future studies are needed to measure *in situ N*-acetylation for other substrates: SMZ, ABP, hydralazine and INH in CHO cells.

β-NAPHTHYLAMINE (BNA):

For BNA 10 µM and 100 µM NAT2 catalytic activity towards BNA in UV5/CYP1A1/NAT2*4 cells was about 8- and 9-fold higher, respectively than in the UV5/CYP1A1/NAT2*5B cell line ($p < 0.05$). For BNA 1000 µM, NAT2 catalytic activity towards BNA showed no significant difference between the three cell lines ($p > 0.05$) (Figure 36).

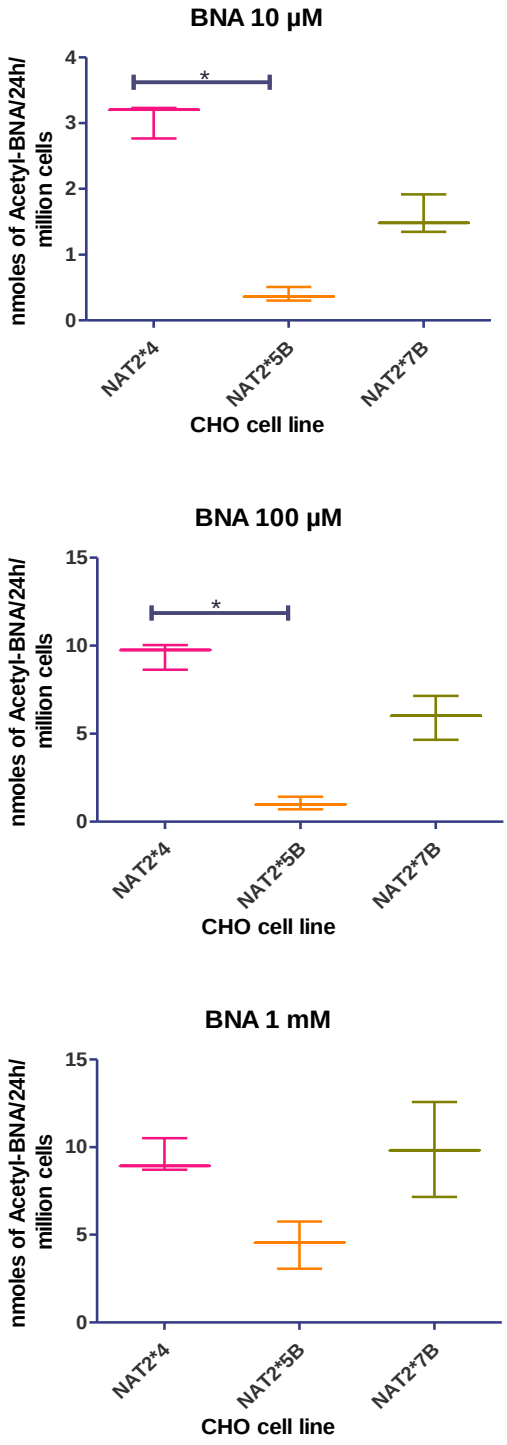

Figure (36): *N*-acetylation rate of BNA *in situ* in CHO cell lines. Statistical significance was determined using Kruskal-Wallis test followed by Dunn's Multiple Comparison test. Data box plot of three experiments. *= $p< 0.05$

4, 4'-METHYLENE BIS (2-CHLOROANILINE) OR MOCA:

For MOCA 10 µM and 100 µM, NAT2 catalytic activity towards MOCA in UV5/CYP1A1/NAT2*4 cells was about 30- and 39- fold higher than in the UV5/CYP1A1/NAT2*5B cell line ($p < 0.05$) (Figure 37). However, for MOCA 1000 µM, NAT2 catalytic activity towards MOCA was not detected in all genotypes (Data not shown).

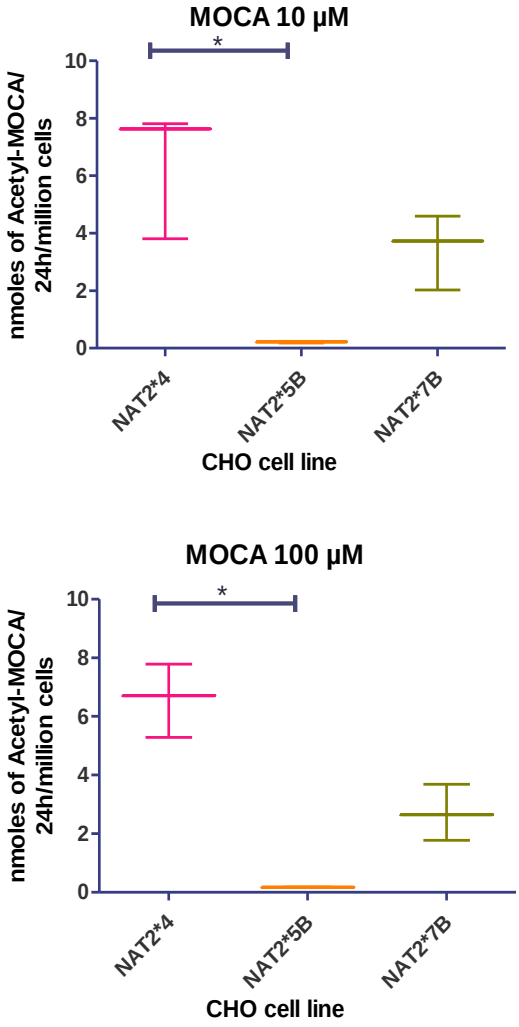

Figure (37): *N*-acetylation rate of MOCA *in situ* in CHO cell lines. Statistical significance was determined using Kruskal-Wallis test followed by Dunn's Multiple Comparison test. Data illustrates box plot of three experiments, *= $p < 0.05$

CELL VIABILITY ASSAY:

Arylamine carcinogens can induce cytotoxicity and/or genotoxicity. Previous study, done in our lab, showed that arylamine carcinogens as ABP and AF have cytotoxic effect on CHO cells [91]. In the current study, we treated CHO cells with BNA and MOCA for 24 hours then alamar blue assay was done to measure percent of cell viability.

β-NAPHTHYLAMINE (BNA):

BNA (10-1000 µM) treatment for 24 hours resulted in dose-dependent reduction in the viability of the UV5/CYP1A1/NAT2*4, UV5/CYP1A1/NAT2*5B and UV5/CYP1A1/NAT2*7B transfected CHO cell lines. Cell survival following BNA 1000 µM treatment differed significantly ($p < 0.05$ in all cell lines) (Figure 38). However, there was no significant difference ($p > 0.05$) between different genotypes (Figure 39).

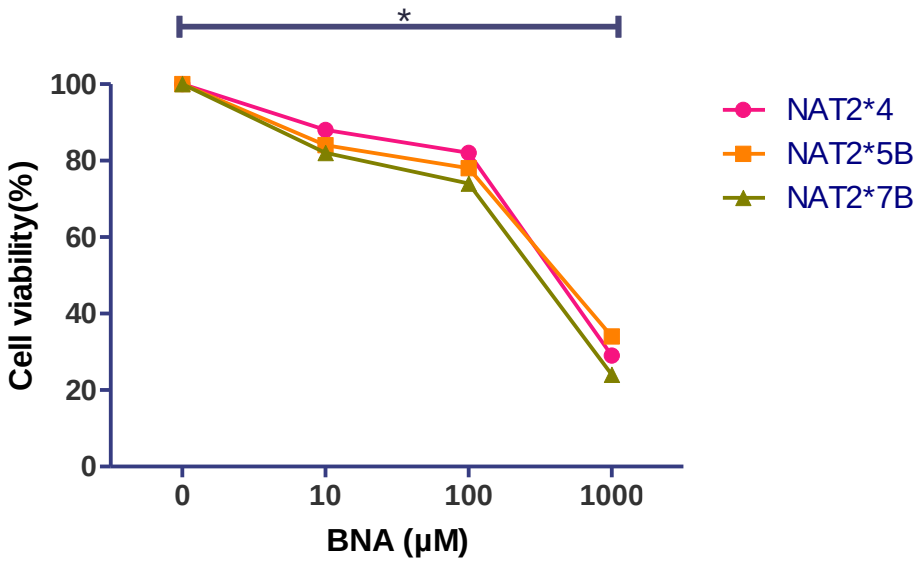

Figure (38): Cell viability in CHO cell lines following treatment with BNA. Percent cell viability on the ordinate is plotted versus BNA treatment concentration on the abscissa. Statistical significance was determined using Kruskal-Wallis test followed by Dunn's Multiple Comparison test. Each data point represents Median for three experiments in UV5/CYP1A1/NAT2*4 (circles), UV5/CYP1A1/NAT2*5B (squares), UV5/CYP1A1/NAT2*7B (triangles). For all cell lines, cell viability differed significantly following treatment with 1000 µM.

*= $p < 0.05$

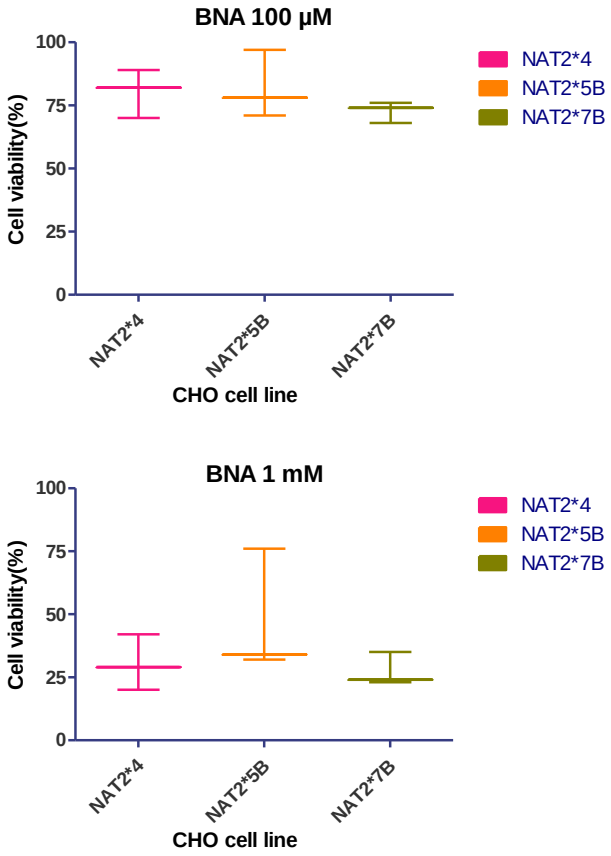

Figure (39): Effect of BNA treatment on cell viability: at 100 µM (Top panel) and at 1000 µM (Bottom panel) in CHO cell lines. Statistical significance was determined using Kruskal-Wallis test followed by Dunn's Multiple Comparison test. Data illustrates box plot of three experiments. There was no significant difference between different genotypes at both concentrations ($p > 0.05$).

4, 4'-METHYLENE BIS (2-CHLOROANILINE) OR MOCA:

Treatment of CHO cells using MOCA (10-1000 µM) for 24 hours resulted in dose-dependent reduction in viability of the UV5/CYP1A1/NAT2*4, UV5/CYP1A1/NAT2*5B and UV5/CYP1A1/NAT2*7B transfected CHO cell lines. Cell survival following MOCA 1000 µM treatment differed significantly ($p < 0.05$ in all cell lines) (Figure 40). However, there was no significant difference between different genotypes (Figure 41).

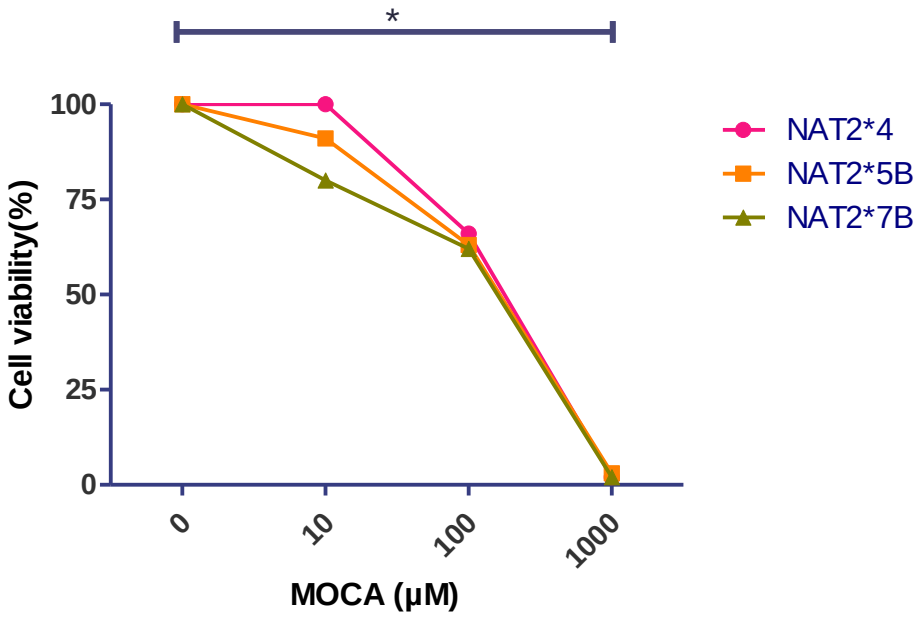

Figure (40): Cell viability in CHO cell lines following treatment with MOCA. Percent cell viability on the ordinate is plotted versus MOCA treatment concentration on the abscissa. Each data point represents Each data point represents Median for three experiments in UV5/CYP1A1/NAT2*4 (circles), UV5/CYP1A1/NAT2*5B (squares), UV5/CYP1A1/NAT2*7B (triangles). For all cell lines, cell viability differed significantly following treatment 100-1000 µM.

*= $p < 0.05$

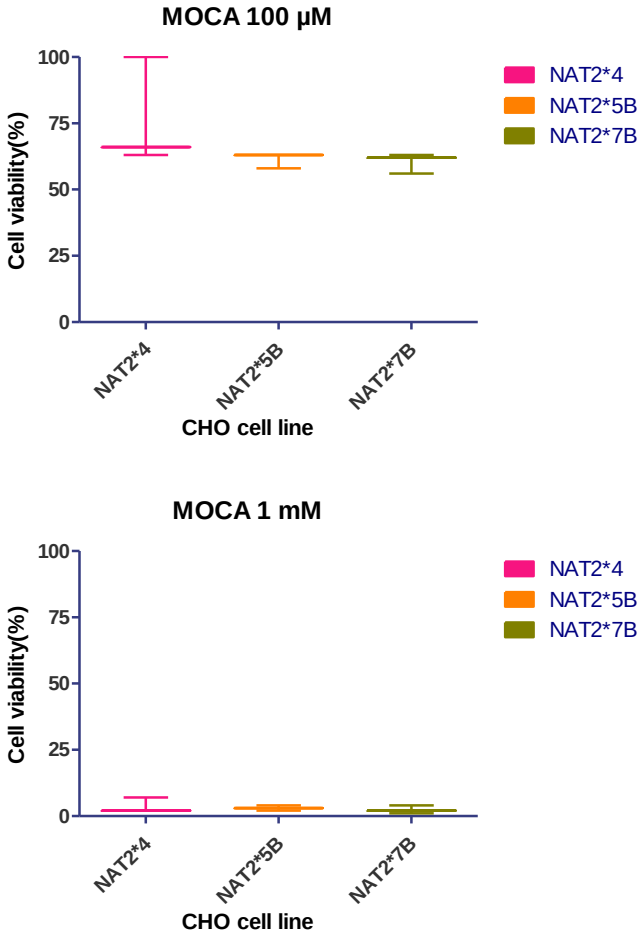

Figure (41): Effect of MOCA treatment on cell viability: at 100 µM (Top panel) and at 1000 µM (Bottom panel) in CHO cell lines. Statistical significance was determined using Kruskal-Wallis test followed by Dunn's Multiple Comparison test. Data illustrates box plot of three experiments. There was no significant difference between different genotypes at both concentrations ($p > 0.05$).

DISCUSSION

Human NAT2 genotype and phenotype relationship is well established in previous studies, and it is documented as a gene dosage relationship. Following recombinant expression of human NAT2 alleles in bacteria and yeast, *NAT2*4* allele is the reference allele with high activity, *NAT2*5* allele showed the greatest reduction in *N*-acetylation, followed by the *NAT2*14 allele* cluster followed by the *NAT2* 6* cluster followed by the *NAT2* 7* cluster [108, 109]. However, more recent studies in cryopreserved human hepatocytes have shown that the N-acetyltransferase activity is lower in hepatocytes homozygous for *NAT2*6A* than *NAT2*5B* [110]. Due to these variable findings, we need more lab based experimental studies thus providing better understanding the role of NAT2 genetic variants. The objective of the present study was to investigate the effect of different NAT2 genotypes on *N*-acetylation of SMZ, hydralazine, INH, ABP, BNA and MOCA in cryopreserved human hepatocytes expressing different rapid, intermediate and slow NAT2 alleles and CHO cells expressing *NAT2*4* (as rapid acetylator) *NAT2*5B* and *NAT2*7B* (as slow acetylators). It is our hypothesis that *N*-acetylation rates of these xenobiotics are NAT2-genotype dependent and that *N*-acetylation activity is associated with cytotoxicity and/or genotoxicity.

N-ACETYLATION IN CRYOPRESERVED HUMAN HEPATOCYTES:

The trimodal capacity of *N*-acetylation of many drugs and carcinogens metabolized by NAT2 has been previously identified in cryopreserved human hepatocytes both *in vitro* and *in situ*. Doll et al., [3] reported SMZ *N*-acetyltransferase catalytic activities carried out at 300 µM *in vitro* differed significantly with respect to the NAT2 acetylator genotype.

SULFAMETHAZINE (SMZ):

In the current study, *in vitro N*-acetylation of SMZ as an aromatic amine drug yielded rapid, intermediate, and slow acetylator phenotypes ($p< 0.0001$) (Figure 11). This is consistent with the trimodal (rapid, intermediate, and slow) distribution of *N*-acetylation capacity in human populations mentioned before for SMZ [111]. However, for *in situ N*-acetylation of SMZ, there was no significant difference between the rapid and intermediate acetylators at 10 or 100 µM (Figure 16). It is possible SMZ *N*-acetylation *in situ* was not NAT2-genotype dependent might be due to use of SMZ at concentrations that were below the apparent K_M for recombinant human NAT2 previously reported by our lab [37].

ABP, BNA and MOCA are arylamine procarcinogens that undergo *N*- and/or *O*- acetylation catalyzed by NAT1 and NAT2. However, human NAT2 has a three- to four-fold higher affinity than NAT1 for urinary bladder carcinogens such as ABP, BNA and MOCA [10, 112]. This finding is consistent with our hypothesis that NAT2 genetic polymorphism in cryopreserved human hepatocytes and CHO cells can affect the rate of acetylation of ABP, BNA and MOCA. Previous studies done in

our lab have used a congenic Syrian hamster model that showed NAT2 acetylation polymorphism clearly sequestered the *N*-acetylation of urinary bladder carcinogens such as ABP and BNA into three phenotypes in hepatic and extrahepatic tissues [113, 114].

4-AMINOBIPHENYL (ABP):

For ABP, a previous study reported *in vitro N*-acetylation of ABP (1 mM) in hepatocytes among rapid acetylators was 2-fold higher than slow acetylators. This suggests NAT2 polymorphism may have a modest impact on ABP metabolism [3]. In the current study, *N*-acetylation rates in the cryopreserved human hepatocytes from rapid, intermediate, and slow NAT2 acetylators exhibited NAT2 genotype-dependent *N*-acetylation of ABP. *In vitro* ABP NAT activities differed significantly between rapid and slow acetylators at 10 μM or 100 μM ($P = 0.0023$) (Figure 12). Moreover, the differences between rapid and slow acetylator hepatocytes were more robust at 10 μM (8-fold) and 100 μM (6-fold) than previously reported at 1 mM (two-fold) [3]. *N*-acetylation of ABP *in situ* also differed significantly between human hepatocytes from rapid and slow acetylators at 10 μM (about 5-fold, $p = 0.0006$) and 100 μM (about 4-fold, $p = 0.0034$) (Figure 17).

These findings are the first to be reported for an aromatic amine carcinogen in human hepatocytes that mirror those recently reported for therapeutic drugs such as hydralazine [57], isoniazid [60] and solithromycin [115]. A previous study [106] in genetically engineered Chinese hamster ovary (CHO) cells have clearly

shown the effect of NAT2 acetylation polymorphism on ABP-induced genotoxicity in the form of DNA adducts and mutants. Cells transfected with *NAT2*4* allele (rapid acetylator) showed higher levels of *N*-acetylation and mutagenicity than cells transfected with *NAT2*5B* or *NAT2*7B* (slow acetylators).

β-NAPHTHYLAMINE (BNA):

In the current study, *in vitro N*-acetylation of BNA varied significantly among rapid, intermediate, and slow NAT2 genotypes at 10 μM ($p = 0.0005$) or 100 μM ($p = 0.0013$) (Figure 13). The highest levels were observed in rapid acetylator, lower levels in intermediate acetylator, and the lowest levels in slow acetylator hepatocytes. Moreover, the differences between rapid and slow acetylator hepatocytes were more robust at 10 μM (7-fold, $p< 0.001$) than 100 μM (3.5-fold, $p< 0.01$). Also, *in situ N*-acetylation of BNA differed significantly between rapid, intermediate, and slow NAT2 genotypes at 10 μM ($p = 0.0016$) or 100 μM ($p = 0.0099$) (Figure 18).

BNA *N*-acetylation in humans has yet to be investigated or reported, but our findings clearly show NAT2 genotype dependent BNA *N*-acetylation as previously shown for *N*-acetylation of other arylamine carcinogens such as 2-aminofluorene, 4-aminobiphenyl and benzidine [116, 117]. Previous studies investigated *N*-acetylation of BNA using rabbit or rat hepatocytes and they showed *N*-acetylation is the major pathway for BNA metabolism and *N*-oxidation is a minor pathway [94, 95]. To our knowledge, this is the first study conducted in cryopreserved human

hepatocytes to investigate the effect of NAT2 genetic polymorphism on *N*-acetylation of BNA.

4, 4'-METHYLENE BIS (2-CHLOROANILINE) OR MOCA:

Also, *in vitro N*-acetylation of MOCA differed significantly among rapid and slow acetylator genotypes at 10 μM (P = 0.0041) or 100 μM (P = 0.0018). The highest levels were observed in rapid acetylator, lower levels in intermediate acetylator, and the lowest levels in slow acetylator hepatocytes. The differences between rapid and slow acetylator hepatocytes were about 7-fold ($p < 0.01$) at 10 μM and 8-fold ($p < 0.01$) at 100 μM (Figure 14). This is consistent with a previous study performed by our lab in which we observed a highly significant ($p < 0.0001$) gene dose-response relationship between NAT2 genotype polymorphism and *in vitro N*-acetylation of MOCA using cryopreserved human hepatocytes and MOCA 300 μM [71]. In our current study, *in situ N*-acetylation of MOCA was not detectable in intermediate and slow acetylators incubated with 10 or 100 μM (Figure 19). Further studies are needed to explain that.

The *N*-acetylation activity of all three arylamine procarcinogens (i. e., ABP, BNA or MOCA) across all NAT2 genotypes was lower than SMZ *N*-acetylation activity (Figures 11-14). Although *N*-acetylation of these carcinogens was significantly higher in rapid NAT2 acetylators compared to slow NAT2 acetylators. However, there were no significant differences in *N*-acetylation of carcinogens between rapid and intermediate NAT2 genotypes in contrast to what was found in

SMZ. This insignificant difference can be explained with the fact of catalysis of arylamine carcinogens by NAT1 in addition to NAT2. NAT1 with its variant alleles is considered as additional factor that affects *N*-acetylation of these carcinogens [10, 71]. Future studies will assess the role of NAT1 different alleles in *N*-acetylation of these carcinogens.

Furthermore, we found *in situ N*-acetylation rates of SMZ, BNA and MOCA were both time and concentration dependent *in situ* in cryopreserved human hepatocytes (Figure 15). The single exception was at BNA 10 µM where the *N*-acetylation rate for BNA µM started to decrease after 6 hours suggesting additional studies are needed at shorter time points. This is consistent with other previously described studies for isoniazid and hydralazine that showed an increase in the *N*-acetylation rate with increase in concentration and incubation time in cryopreserved human hepatocytes [57, 60]. For ABP, the correlation between time and rate of production of acetylated ABP was insignificant at both concentrations ($p > 0.05$). It is likely that the rate of reaction started to decrease over time due to ABP consumption.

Previous studies demonstrated aromatic amines such as ABP and BNA can induce cytotoxicity in bacteria [118], rabbit hepatocytes [94] or CHO cells expressing human NAT2 [91, 106]. To our knowledge, the current study is the first study to investigate the cytotoxic effects of aromatic amines in human hepatocytes. Our findings showed treatment of cryopreserved human hepatocytes using ABP, BNA or MOCA for 24 hours led to concentration dependent cytotoxicity in all NAT2 genotypes (Figures 20, 22, 24). There is no significant difference between different

genotypes except for BNA at 100 µM (Figures 21, 23, 25) suggesting ABP, BNA, MOCA might induce cytotoxicity in human hepatocytes regardless of the NAT2 acetylator status.

N-ACETYLATION IN CHINESE HAMSTER OVARY (CHO) CELLS:

Chinese hamster ovary or CHO cells are considered a good model to display the different human NAT2 genotypes and how this can affect *N*-acetylation of different drugs and carcinogens. This model is a good fit for our study for many reasons. First, CHO cells enabled stable expression of human NAT2 alleles so they can reveal the individual role of NAT2 in *N*-acetylation independent of NAT1. Next, they enable stable expression of CYP1A2 which is a keystone for activation of these carcinogens through *N*-hydroxylation and further *O*-acetylation by NAT2. Last, they lack nucleotide excision repair or NER due to a mutation in the XPD (ERCC2) gene. This lack of NER makes the CHO cells hypersensitive to bulky DNA adducts and mutagens [91]. This characteristic allows us to capture CYP1A2/NAT2 dependent genotoxic effects.

In the current study, we used CHO cells transfected with human CYP1A2 and either human *NAT2*4* (rapid acetylator), *NAT2*5B* (common Caucasian slow acetylator), or *NAT2*7B* (common Asian slow acetylator) alleles. We have tested hydralazine and isoniazid as examples of drugs and BNA and MOCA as examples of carcinogens.

HYDRALAZINE:

For hydralazine, using AcCoA concentration of 300 or 1000 µM, UV5/CYP1A1/NAT2*4 has higher *N*-acetylation rate than UV5/CYP1A1/NAT2*7B not UV5/CYP1A1/NAT2*5B although both later alleles are considered slow NAT2 alleles. (Figure 26, 27). This can be explained by the presence of NAT2 SNP G857A which is characteristic of *NAT2*7* allele. This SNP might influence the accessibility of some substrates and AcCoA, leading to substrate-dependent activity changes observed here and in previous studies [109,119,120]. Zang and coworkers showed that G857A SNP displayed an 8-fold lower apparent K_m to SMZ but a 3-fold higher apparent K_m to AcCoA compared to the reference allele *NAT2*4* [121].

ISONIAZID (INH):

For isoniazid, UV5/CYP1A1/NAT2*4 had higher *in vitro N*-acetylation rate compared to UV5/CYP1A1/NAT2*5B and UV5/CYP1A1/NAT2*7B at both 300 µM AcCoA. At 1000 µM AcCoA, UV5/CYP1A1/NAT2*4 had higher *in vitro N*-acetylation rate compared to UV5/CYP1A1/NAT2*7B and not UV5/CYP1A1/NAT2*5B (Figures 28, 29).

β-NAPHTHYLAMINE (BNA):

In vitro NAT2 activity towards BNA using AcCoA 300 µM showed significant differences in *N*-acetylation rates between UV5/CYP1A1/NAT2*4 and UV5/CYP1A1/NAT2*5B and not UV5/CYP1A1/NAT2*7B. Also, *N*-acetylation rate of UV5/CYP1A1/NAT2*7B increased with increase in BNA concentration. (Figure 30). However, at AcCoA concentration 1000 µM*,* *N*-acetylation rate was significantly higher in UV5/CYP1A1/NAT2*4 compared to UV5/CYP1A1/NAT2*5B and UV5/CYP1A1/NAT2*7B. Also, no remarkable increase in *N*-acetylation rate by increasing BNA concentration (Figure 31)*.* This suggest *N*-acetylation rate of BNA is AcCoA dependent even within the same slow genotype.

This can be explained with different BNA and AcCoA kinetics between different slow NAT2 alleles. To investigate that, we measured the apparent K_m and V_{max} for BNA in CHO cells. Our findings showed that UV5/CYP1A1/NAT2*7B had an apparent K_m of 130.9 µM value which is about 13-fold higher than that of the other two genotypes reflecting the lower affinity of UV5/CYP1A1/NAT2*7B towards BNA. However, V_{max} which is the rate of production of *N*-acetyl BNA for UV5/CYP1A1/NAT2*4 cells was about 5.5-fold higher ($p< 0.05$) than in the UV5/CYP1A1/NAT2*5B cell line. On the other hand, there was no significant difference in Vmax for the UV5/CYP1A1/NAT2*4 and UV5/CYP1A1/NAT2*7B cell lines (Table 7, Figure 34).

For AcCoA kinetics, we propose *NAT2*7B* has a lower K_m for AcCoA. So, at AcCoA 300 uM, *NAT2*7B* can bind to AcCoA leading to *N*-acetylation rate close to that of NAT2*4 (no significant difference between them). However, at higher

AcCoA concentration, NAT2*5B can bind more effectively to AcCoA. So, further studies are required to confirm the impact of different NAT2 alleles on the AcCoA Km in CHO cells.

In situ N-acetylation rates of BNA were measured following treatment of CHO cells with BNA 10-1000 µM for 24 hours. For BNA, NAT2 catalytic activity in UV5/CYP1A1/NAT2*4 cells was about 8-fold and 9-fold higher ($p< 0.05$) than in the UV5/CYP1A1/NAT2*5B cell line at 10 and 100 µM, respectively. Increasing BNA concentration led to further increase in *N*-acetylation in UV5/CYP1A1/NAT2*7B to the extent that was close to UV5/CYP1A1/NAT2*4 at 1000 µM (Figure 36). This is consistent with the *in vitro* BNA *N*-acetylation results in CHO cells using AcCoA 300 µM (Figure 30).

Treatment of CHO cells with BNA (10-1000 µM) for 24 hours resulted in concentration-dependent reduction in the viability of all CHO cell lines. Cell viability following BNA 1000 µM treatment differed significantly ($p< 0.05$) in all cell lines (Figure 38). No significant difference was observed in cell viability between the different genotypes ($p> 0.05$) suggesting NAT2 genotype may not be the only determinant of aromatic amines induced cytotoxicity in these cell lines (Figure 39).

4, 4'-METHYLENE BIS (2-CHLOROANILINE) OR MOCA:

For MOCA 10 and 100 µM, *in vitro N*-acetylation rate in UV5/CYP1A1/NAT2*4 cells was significantly about 4-fold higher than that in UV5/CYP1A1/NAT2*5B cells at AcCoA 300 µM not 1000 µM (Figures 32, 33).

Although *N*-acetylation rate in UV5/CYP1A1/NAT2*7B was higher than that of UV5/CYP1A1/NAT2*5B using AcCoA 300 µM, the difference was not significant (Figures 32).

For MOCA kinetics, there was no significant difference in apparent K_m between the three genotypes UV5/CYP1A1/NAT2*4, UV5/CYP1A1/NAT2*5B and UV5/CYP1A1/NAT2*7B. However, the rate of production of N-acetylated MOCA or Vmax for UV5/CYP1A1/NAT2*4 cells was about 42-fold higher ($p< 0.05$) than in the UV5/CYP1A1/NAT2*7B cell line (Table 8 and Figure 35).

In situ NAT2 activity towards MOCA showed there was significant difference in *N*-acetylation rates between UV5/CYP1A1/NAT2*4 and UV5/CYP1A1/NAT2*5B and not UV5/CYP1A1/NAT2*7B cell lines at 10 and 100 µM (Figure 37). Also, there was decrease in the amount of the acetylated product while MOCA concentration increased. This can be explained with cytotoxicity at MOCA 100 µM (cell viability was about 65%). *N*-acetylation of MOCA at 1000 µM could not be measured due to significant loss of cell viability at 1000 µM (cell viability was about 3-5%).

Treatment of CHO cells with MOCA (10-1000 µM) for 24 hours resulted in concentration-dependent reduction in the viability of all CHO cell lines. Cell viability following MOCA 1000 µM treatment differed significantly ($p< 0.05$) in all cell lines (Figure 40). As BNA, no significant difference ($p> 0.05$) was observed in cell viability between the different genotypes following MOCA treatment (Figure 41).

These results are consistent with epidemiological studies. For instance, a meta-analysis done using studies in the Chinese population reported NAT2 slow

acetylation phenotype was significantly associated with an increased risk of bladder cancer [122]. In addition, a meta-analysis, that included studies from different populations, indicated a possible association between the slow NAT2 genotype, occupational exposure to aromatic amines or polycyclic aromatic hydrocarbons, and development of bladder cancer in different populations [123].

It also seems that possession of the slow NAT2 genotype and exposure to smoke derived carcinogens such as ABP and BNA jointly modify the risk of developing bladder cancer relative to nonsmoker slow acetylators [124].

Moreover, our findings in CHO cells expressing human *NAT2*5B* and *NAT2*7B* refer to the probability of heterogenicity within the same slow NAT2 genotype as both alleles had different *N*-acetylation activity while decreasing the AcCoA concentration. This is consistent with previous study done in our lab that showed NAT2 catalytic activity towards ABP was lower than the UV5/CYP1A1/NAT2*5B cell line when compared to the cell line expressing UV5/CYP1A1/NAT2*7B [106]. In addition, a clinical study done in 504 north American subjects of Caucasian origin indicated there were variations in the *N*-acetylation NAT2 status among slow acetylator individuals. *NAT2*6/*6* homozygotes had about 30% reduction in enzyme activity as compared to *NAT2*5/*5* homozygotes although both are considered slow acetylators [93].

NAT2 genotypes used in the present study did not affect cytotoxicity in CHO cells following BNA or MOCA exposure. However, further lab-based studies can determine the genotoxicity or mutagenicity induced by aromatic amines and its correlation with different NAT2 genotypes.

CONCLUSIONS AND SUMMARY

STRENGTHS OF THIS WORK:

Although previous studies were done in bacteria, rabbit, or rat hepatocytes to study the effect of NAT2 genetic polymorphism on metabolism of xenobiotics, they are not accurate enough to anticipate the metabolic profile of xenobiotics in humans. In this study, we have used cryopreserved human hepatocytes that contain a combination of drug metabolizing enzymes including CYP1A2 and both NATs. They provide the closest in vitro model to human liver to study the effect of different NAT2 genes on *N*-acetylation of arylamines carcinogens (e.g. ABP, BNA and MOCA) that are hazardous to be studied in humans. Also, we have utilized CHO cells transfected with CYP1A2 and different NAT2 alleles. This advantageous mammalian resource mimics the human cells, providing further study of the individual role of NAT2 regardless of the NAT1 acetylation activity.

Our findings clearly illustrate NAT2 genotype-dependent *N*-acetylation of ABP, BNA and MOCA in human hepatocytes and hydralazine, INH, BNA and MOCA in CHO cells transfected with human NAT2. These results suggest the individual susceptibility to side effects or toxicity of these chemicals can be modified by human NAT2 genotype.

Moreover, the results refer to the different *N*-acetylation rates among the allelic variants normally associated with slow acetylator phenotype suggesting NAT2 slow acetylator phenotype is not homogeneous. Instead, multiple slow acetylator phenotypes exist resulting from different mechanisms inferred by various SNPs. Therefore, the investigations of NAT2 genotype/phenotype relationship could be more precise and reproducible if heterogeneity within the "slow" NAT2 acetylator phenotype is considered and incorporated into the study design.

WEAKNESSES AND LIMITATIONS:

Poor availability of in human hepatocytes and restricted proliferation capacity in vitro hindered the study of some NAT2 genotypes as NAT2*7 which can affect substrate affinity. Larger sample size for the various genotypes would give more accurate findings.

Use of high concentration of arylamine carcinogens led to significant loss of cell viability. This may explain the undetectable amount of the acetylated product for some carcinogens. To mitigate that, future studies should include treatment of cells with less carcinogen's concentrations or incubation of carcinogen with cells for shorter periods (less than 24 hours).

In the present study, we did not investigate AcCoA kinetics to detect the effect of different NAT2 alleles on AcCoA affinity. This would provide an explanation for variable *N*-acetylation rates with different AcCoA concentrations.

FUTURE DIRECTIONS:

Future studies should include investigation of genotoxic effects induced by aromatic carcinogens in human hepatocytes and CHO cells expressing different NAT2 genotypes. These effects include DNA damage, adducts, and formation of mutants. Also, further studies are needed to determine the mechanisms underlying cytotoxicity and/or genotoxicity. This could include detection of apoptotic proteins as caspase-8 or measurement of oxidative stress biomarkers that may be involved.

REFERENCES

1. McDonagh EM, Boukouvala S, Aklillu E, Hein DW, Altman RB, Klein TE. PharmGKB summary: very important pharmacogene information for n-acetyltransferase 2. *Pharmacogenet genomics*. 2014; 24(8): 409-425.
2. Teixeira RL, Lopes MQ, Suffys PN and Santos AR (2013). Tuberculosis pharmacogenetics: state of the art. Bassam H. Mahboub, Mayank G. Vats (Eds.), Tuberculosis – current issues in diagnosis and management (1 ed.), In Tech – Open Science, Rijeka (2013), pp. 105-126.
3. Doll MA, Zang Y, Moeller T, Hein DW. Codominant expression of *N*-acetylation and *O*-acetylation activities catalyzed by N-acetyltransferase 2 in human hepatocytes. *J Pharmacol Exp Ther.* 2010; 334(2): 540-544.
4. Sim E, Hickman D, Coroneos E, Kelly SL. Arylamine N-acetyltransferase. *Biochem Soc Trans.* 1992; 20(2): 304-309.
5. Butcher NJ and Minchin RF. Arylamine N-acetyltransferase 1: a novel drug target in cancer development. *Pharmacol Rev.* 2012; 64: 147-165.
6. Stepp MW, Doll MA, Carlisle SM, States JC, Hein DW. Genetic and small molecule inhibition of arylamine N-acetyltransferase 1 reduces anchorage-independent growth in human breast cancer cell line MDA-MB-231. *Mol Carcinog.* 2018; 57(4): 549-558.
7. Windmill KF, Gaedigk A, Hall PM, Samaratunga H, Grant DM, McManus ME. Localization of N-acetyltransferases NAT1 and NAT2 in human tissues. *Toxicol Sci*. 2000; 54(1):19-29.
8. Adithan C, Subathra A. NAT2 gene polymorphism: covert drug interaction causing phenytoin toxicity. *Indian J Med Res*. 2016;143(5):542–544.
9. Chung KT. The etiology of bladder cancer and its prevention. *J Cancer Sci Ther.* 2013; 5: 346-361.
10. Hein DW. N-acetyltransferase 2 genetic polymorphism: effects of carcinogen and haplotype on urinary bladder cancer risk. *Oncogene* 2006; 25: 1649-1658.
11. Husain A, Zhang X, Doll MA, States JC, Barker DF, Hein DW. Identification of N- acetyltransferase 2 (NAT2) transcription start sites and quantitation of NAT2-specific mRNA in human tissues. *Drug Metab and Dispos.* 2007; 35: 721-727.
12. Weber WW, Hein DW. Clinical pharmacokinetics of isoniazid. *Clin Pharmacokinet*. 1979 ;4(6):401–422.
13. Zhou X, Ma Z, Dong D, Wu B. Arylamine N-acetyltransferases: a structural perspective. *Br J of Pharmacol.* 2013; 169(4): 748-760.
14. Butcher NJ, Boukouvala S, Sim E, Minchin RF. Pharmacogenetics of the arylamine N-acetyltransferases. *Pharmacogenomics J.* 2002; 2:30–42.
15. Hein DW. N-acetyltransferase SNPs: emerging concepts serve as a paradigm for understanding complexities of personalized medicine. *Expert Opin Drug Metab Toxicol*. 2009; 5:353–366.

16. Sabbagh A, Darlu P, Crouau-Roy B, Poloni ES. Arylamine N-acetyltransferase 2 (NAT2) genetic diversity and traditional subsistence: a worldwide population survey. *PLoS One*. 2011;6(4): e18507.
17. Krajinovic M, Richer C, Sinnett H, et al. Genetic polymorphisms of N-acetyltransferases 1 and 2 and gene-gene interaction in the susceptibility to childhood acute lymphoblastic leukemia. *Cancer Epidemiol Biomarkers Prev*. 2000; 9:557–562.
18. Walker K, Ginsberg G, Hattis D, Johns DO, Guyton KZ, Sonawane B. Genetic polymorphism in N-Acetyltransferase (NAT): population distribution of NAT1 and NAT2 activity. *J Toxicol Environ Health B Crit Rev*. 2009; 12:440–472.
19. Guaoua S, Ratbi I, Laarabi FZ, et al. Distribution of allelic and genotypic frequencies of NAT2 and CYP2E1 variants in Moroccan population. *BMC Genet.* 2014;1 5:156.
20. Chen M, Xia B, Chen B, et al. N-acetyltransferase 2 slow acetylator genotype associated with adverse effects of sulphasalazine in the treatment of inflammatory bowel disease*. Can J Gastroenterol.* 2007;21(3):155-158.
21. Ma QW, Lin GF, Chen JG, et al. Polymorphism of N-acetyltransferase 2 (NAT2) gene polymorphism in shanghai population: occupational and non-occupational bladder cancer patient groups. *Biomed Environ Sci.* 2004;17(3):291-298.
22. Baumgartner KB, Schlierf TJ, Yang D, Doll MA, Hein DW. N-acetyltransferase 2 genotype modification of active cigarette smoking on breast cancer risk among hispanic and non-hispanic white women. *Toxicol Sci*. 2009;112(1):211-220.
23. Sabbagh A, Langaney A, Darlu P, Gérard N, Krishnamoorthy R, Poloni ES. Worldwide distribution of NAT2 diversity: implications for NAT2 evolutionary history. *BMC Genet.* 2008; 9:21.
24. Sim E, Abuhammad A, Ryan A. Arylamine N-acetyltransferases: from drug metabolism and pharmacogenetics to drug discovery. *Br J Pharmacol*. 2014; 171(11):2705–2725.
25. Metushi I, Uetrecht J, Phillips E. Mechanism of isoniazid-induced hepatotoxicity: then and now. *Br J Clin Pharmacol*. 2016;81(6):1030–1036.
26. Spinasse LB, Santos AR, Suffys PN, Muxfeldt ES, Salles GF. Different phenotypes of the NAT2 gene influences hydralazine antihypertensive response in patients with resistant hypertension. *Pharmacogenomics*. 2014;15(2):169–178.
27. Marcus PM, Vineis P, Rothman N. NAT2 slow acetylation and bladder cancer risk: a meta-analysis of 22 case-control studies conducted in the general population. *Pharmacogenetics.* 2000;10(2):115–122.
28. García-Closas M, Malats N, Silverman D, et al. NAT2 slow acetylation, GSTM1 null genotype, and risk of bladder cancer: results from the Spanish Bladder Cancer Study and meta-analyses. *Lancet.* 2005;366(9486):649–659.
29. Hein DW, Doll MA, Fretland AJ, et al. Molecular genetics and epidemiology of the NAT1 and NAT2 acetylation polymorphisms. *Cancer Epidemiol Biomarkers Prev*. 2000;9(1):29–42.
30. Wang S, Hanna D, Sugamori KS, Grant DM. Primary aromatic amines and cancer: Novel mechanistic insights using 4-aminobiphenyl as a model carcinogen. *Pharmacol Ther*. 2019; 200:179–189.
31. Feng Z, Hu W, Rom WN, Beland FA, Tang MS. 4-aminobiphenyl is a major etiological agent of human bladder cancer: evidence from its DNA binding spectrum in human p53 gene. *Carcinogenesis*. 2002;23(10):1721–1727.

32. Habil MR, Doll MA, Hein DW. N-acetyltransferase 2 acetylator genotype-dependent N-acetylation of 4-aminobiphenyl in cryopreserved human hepatocytes. *Pharmacogenet Genomics*. 2020 Apr;30(3):61-65.
33. Chung KT. Occurrence, uses, and carcinogenicity of arylamines. *Front Biosci* (Elite Ed). 2015; 7: 322-345.
34. Wang SC, Chung JG, Chen CH, Chen SC. 2- and 4-Aminobiphenyls induce oxidative DNA damage in human hepatoma (Hep G2) cells via different mechanisms. *Mutat Res*. 2006;593(1-2):9–21.
35. Salazar-González RA, Zhang X, Doll MA, Lykoudi A, Hein DW. Role of the human N-acetyltransferase 2 genetic polymorphism in metabolism and genotoxicity of 4, 4'-methylenedianiline. *Arch Toxicol*. 2019;93(8):2237-2246.
36. Vineis P, Alavanja M, Garte S. Dose-response relationship in tobacco-related cancers of bladder and lung: a biochemical interpretation. *Int J Cancer*. 2004;108(1):2–7.
37. Hein DW, Doll MA, Rustan TD, et al. Metabolic activation and deactivation of arylamine carcinogens by recombinant human NAT1 and polymorphic NAT2 acetyltransferases. *Carcinogenesis*. 1993;14(8):1633–1638.
38. Brockmöller J, Cascorbi I, Kerb R, Roots I. Combined analysis of inherited polymorphisms in arylamine N-acetyltransferase 2, glutathione S-transferases M1 and T1, microsomal epoxide hydrolase, and cytochrome P450 enzymes as modulators of bladder cancer risk. *Cancer Res*. 1996;56(17):3915–3925.
39. Okkels H, Sigsgaard T, Wolf H, Autrup H. Arylamine N-acetyltransferase 1 (NAT1) and 2 (NAT2) polymorphisms in susceptibility to bladder cancer: the influence of smoking. *Cancer Epidemiol Biomarkers Prev*. 1997;6(4):225–231.
40. Zhu Z, Zhang J, Jiang W, Zhang X, Li Y, Xu X. Risks on N-acetyltransferase 2, and bladder cancer: a meta-analysis. *Onco Targets Ther*. 2015; 8:3715–3720.
41. Lilla C, Verla-Tebit E, Risch A, et al. Effect of NAT1 and NAT2 genetic polymorphisms on colorectal cancer risk associated with exposure to tobacco smoke and meat consumption. *Cancer Epidemiol Biomarkers Prev*. 2006;15(1):99–107.
42. da Silva TD, Felipe AV, de Lima JM, Oshima CT, Forones NM. N-Acetyltransferase 2 genetic polymorphisms and risk of colorectal cancer. *World J Gastroenterol*. 2011;17(6):760–765.
43. Wang H, Iwasaki M, Haiman CA, et al. Interaction between Red Meat Intake and NAT2 Genotype in Increasing the Risk of Colorectal Cancer in Japanese and African Americans. *PLoS One*. 2015;10(12): e0144955.
44. Procopciuc LM, Osian G, Iancu M. N-acetyl transferase 2/environmental factors and their association as a modulating risk factor for sporadic colon and rectal cancer. *J Clin Lab Anal*. 2017;31(5): e22098.
45. Rovito PJ, Morse PD, Spinek K, Newman N, Jones RF, Wang CY, Haas GP. Heterocyclic amines and genotype of N-acetyltransferases as risk factors for prostate cancer. *Prostate Cancer Prostatic Dis.* 2005; 8:69–74.

46. Farker K, Schotte U, Scheele J, Hoffmann A. Impact of N-acetyltransferase polymorphism (NAT2) in hepatocellular carcinoma (HCC)--an investigation in a department of surgical medicine. *Exp Toxicol Pathol*. 2003;54(5-6):387–391.
47. Gemignani F, Landi S, Szeszenia-Dabrowska N, et al. Development of lung cancer before the age of 50: the role of xenobiotic metabolizing genes. *Carcinogenesis.* 2007;28(6):1287–93.
48. Letašiová S, Medve'ová A, Šovčíková A, et al. Bladder cancer, a review of the environmental risk factors. *Environ Health*. 2012;11 Suppl 1 (Suppl 1): S11.
49. Browne JL, Klipstein-Grobusch K, Franx A, Grobbee DE. Prevention of Hypertensive Disorders of Pregnancy: A Novel Application of the Polypill Concept. *Curr Cardiol Rep*. 2016;18(6):59.
50. Singh V, Sharma P, Capalash N. DNA methyltransferase-1 inhibitors as epigenetic therapy for cancer. *Curr Cancer Drug Targets*. 2013; 13:379-399.
51. Lauschke VM, Barragan I, Ingelman-Sundberg M. Pharmacoepigenetics and Toxicoepigenetics: Novel Mechanistic Insights and Therapeutic Opportunities. *Annu Rev Pharmacol Toxicol.* 2018; 58:1,161-185.
52. Ruiz-Magaña MJ, Martínez-Aguilar R, Lucendo E, Campillo-Davo D, Schulze-Osthoff K, Ruiz-Ruiz C. The antihypertensive drug hydralazine activates the intrinsic pathway of apoptosis and causes DNA damage in leukemic T cells. *Oncotarget*. 2016;7(16):21875–21886.
53. Castillo-Aguilera O, Depreux P, Halby L, Arimondo PB, Goossens L. DNA Methylation Targeting: The DNMT/HMT Crosstalk Challenge. *Biomolecules*. 2017;7(1):3.
54. Coronel J, Cetina L, Pacheco I, et al. A double-blind, placebo-controlled, randomized phase III trial of chemotherapy plus epigenetic therapy with hydralazine valproate for advanced cervical cancer. Preliminary results. *Med Oncol.* 2011; 28 Suppl 1: S540-546.
55. Espinoza-Zamora JR, Labardini-Méndez J, Sosa-Espinoza A, et al. Efficacy of hydralazine and valproate in cutaneous T-cell lymphoma, a phase II study [published correction appears in Expert Opin Investig Drugs. 2017 Apr;26(4):523]. *Expert Opin Investig Drugs*. 2017;26(4):481–487.
56. Garcés-Eisele SJ, Cedillo-Carvallo B, Reyes-Núñez V, et al. Genetic selection of volunteers and concomitant dose adjustment leads to comparable hydralazine/valproate exposure. *J Clin Pharm Ther*. 2014;39(4):368-375.
57. Allen CE, Doll MA, Hein DW. N-Acetyltransferase 2 Genotype-Dependent N-Acetylation of Hydralazine in Human Hepatocytes. *Drug Metab Dispos*. 2017;45(12):1276–1281.
58. Sotsuka T, Sasaki Y, Hirai S, Yamagishi F, Ueno K. Association of isoniazid-metabolizing enzyme genotypes and isoniazid-induced hepatotoxicity intuberculosis patients. *In Vivo*. 2011;25(5):803–812.
59. Zabost A, Brzezińska S, Kozińska M, et al. Correlation of N-acetyltransferase 2 genotype with isoniazid acetylation in Polish tuberculosis patients. *Biomed Res Int.* 2013; 853602.
60. Doll MA, Salazar-González RA, Bodduluri S, Hein DW. Arylamine *N*-acetyltransferase 2 genotype-dependent *N*-acetylation of isoniazid in cryopreserved human hepatocytes. *Acta Pharm Sin B*. 2017;7(4):517–522.

61. Yang S, Hwang SJ, Park JY, Chung EK, Lee JI. Association of genetic polymorphisms of CYP2E1, NAT2, GST and SLCO1B1 with the risk of anti-tuberculosis drug-induced liver injury: a systematic review and meta-analysis. *BMJ Open*. 2019;9(8): e027940.
62. IARC. Tobacco smoke and involuntary smoking. *IARC Monogr Eval Carcinog Risks Hum.* 2004; 83:1–1438.
63. Tomioka K, Saeki K, Obayashi K, Kurumatani N. Risk of Lung Cancer in Workers Exposed to Benzidine and/or Beta-Naphthylamine: A Systematic Review and Meta-Analysis. *J Epidemiol*. 2016; 26(9): 447-458.
64. Blackadar CB. Historical review of the causes of cancer. *World J Clin Oncol*. 2016; 7(1): 54-86.
65. Krech E, Selinski S, Blaszkewicz M, et al. Urinary bladder cancer risk factors in an area of former coal, iron, and steel industries in Germany. *J Toxicol Environ Health A.* 2017; 80(7–8): 430-438.
66. Fontana L, Delort L, Joumard L, et al. Genetic polymorphisms in CYP1A1, CYP1B1, COMT, GSTP1 and NAT2 genes and association with bladder cancer risk in a French cohort. *Anticancer Res.* 2009;29(5):1631–1635.
67. Grant DM. Chemical carcinogenesis in Harrington L, ed. Basic Science of Oncology, Fifth Edition. United Kingdom: McGraw-Hill Education; 2013:73-88
68. Dost A, Straughan JK, Sorahan T. Cancer incidence and exposure to 4,4'-methylene-bis-ortho-chloroaniline (MbOCA). *Occup Med (Lond)*. 2009; 59(6):402–405.
69. Wang C-C, Chen W, Hsiung C, et al. Effect of CYP3A4 genetic polymorphisms on the genotoxicity of 4, 4′-methylene-bis (2-chloroaniline)-exposed workers. *Occup Environ Med*. 2017; 74(1): 30-38.
70. Liu CS, Liou SH, Loh CH, et al. Occupational bladder cancer in a 4,4 -methylenebis(2-chloroaniline) (MBOCA)-exposed worker. *Environ Health Perspect.* 2005;113(6):771–774.
71. Hein DW, Zhang X, Doll MA. Role of N-acetyltransferase 2 acetylation polymorphism in 4, 4'-methylene bis (2-chloroaniline) biotransformation. *Toxicol Lett.* 2018; 283:100–105.
72. Lin IS, Fan PL, Chen HI, Loh CH, Shih TS, Liou SH. Rapid and intermediate N-acetylators are less susceptible to oxidative damage among 4,4'-methylenebis(2-chloroaniline) (MBOCA)-exposed workers. *Int J Hyg Environ Health.* 2013;216(4):515–520.
73. Murata M, Kawanishi S. Mechanisms of oxidative DNA damage induced by carcinogenic arylamines. *Front Biosci (Landmark Ed).* 2011; 16:1132–1143.
74. Wells PG, McCallum GP, Lam KC, Henderson JT, Ondovcik SL. Oxidative DNA damage and repair in teratogenesis and neurodevelopmental deficits. Birth Defects Res C Embryo Today. 2010;90(2):103–109.
75. Dairou J, Malecaze F, Dupret JM, Rodrigues-Lima F. The xenobiotic-metabolizing enzymes arylamine N-acetyltransferases in human lens epithelial cells: inactivation by cellular oxidants and UVB-induced oxidative stress. *Mol Pharmacol.* 2005;67(4):1299–1306.
76. Tamer L, Yilmaz A, Yildirim H, et al. N-acetyltransferase 2 phenotype may be associated with susceptibility to age-related cataract. *Curr Eye Res.* 2005;30(10):835–839.

77. Asmat U, Abad K, Ismail K. Diabetes mellitus and oxidative stress-A concise review. *Saudi Pharm J*. 2016;24(5):547–553.
78. Fujita N, Sugimoto R, Ma N, et al. Comparison of hepatic oxidative DNA damage in patients with chronic hepatitis B and C. *J Viral Hepat*. 2008;15(7):498–507.
79. Jakovcevic D, Dedic-Plavetic N, Vrbanec D, Jakovcevic A, Jakic-Razumovic J. Breast Cancer Molecular Subtypes and Oxidative DNA Damage. *Appl Immunohistochem Mol Morphol.* 2015;23(10):696–703.
80. Wang Z, Li Z, Ye Y, Xie L, Li W. Oxidative Stress and Liver Cancer: Etiology and Therapeutic Targets. *Oxid Med Cell Longev.* 2016; 2016:7891574.
81. Guo C, Li X, Wang R, et al. Association between Oxidative DNA Damage and Risk of Colorectal Cancer: Sensitive Determination of Urinary 8-Hydroxy-2'-deoxyguanosine by UPLC-MS/MS Analysis. *Sci Rep*. 2016; 6:32581.
82. Savina NV, Nikitchenko NV, Kuzhir TD, Rolevich AI, Krasny SA, Goncharova RI. The Cellular Response to Oxidatively Induced DNA Damage and Polymorphism of Some DNA Repair Genes Associated with Clinicopathological Features of Bladder Cancer. *Oxid Med Cell Longev*. 2016; 2016:5710403.
83. Kim YD, Lee CH, Nan HM, Kang JW, Kim H. Effects of genetic polymorphisms in metabolic enzymes on the relationships between 8-hydroxydeoxyguanosine levels in human leukocytes and urinary 1-hydroxypyrene and 2-naphthol concentrations*. J Occup Health*. 2003;45(3):160–167.
84. Valavanidis A, Vlachogianni T, Fiotakis C. 8-hydroxy-2' -deoxyguanosine (8-OHdG): A critical biomarker of oxidative stress and carcinogenesis. *J Environ Sci Health C Environ Carcinog Ecotoxicol Rev.* 2009;27(2):120–139.
85. Chen HI, Liou SH, Ho SF, et al. Oxidative DNA damage estimated by plasma 8-hydroxydeoxyguanosine (8-OHdG): influence of 4, 4'-methylenebis (2-chloroaniline) exposure and smoking. *J Occup Health.* 2007;49(5):389–398.
86. Zhang TT, Zhao G, Li X, Xie FW, Liu HM, Xie JP. Genotoxic and oxidative stress effects of 2-amino-9H-pyrido[2,3-b] indole in human hepatoma G2 (HepG2) and human lung alveolar epithelial (A549) cells. *Toxicol Mech Methods.* 2015;25(3):212–222.
87. Ohnishi S, Murata M, Kawanishi S. Oxidative DNA damage induced by a metabolite of 2-naphthylamine, a smoking-related bladder carcinogen. *Jpn J Cancer Res.* 2002;93(7):736–743.
88. Tafazoli S and O'Brien P J. Accelerated Cytotoxic Mechanism Screening of Hydralazine Using an in Vitro Hepatocyte Inflammatory Cell Peroxidase Model. *Chem. Res. Toxicol.* 2008; 21*,* 904-910.
89. Flückiger-Isler S, Baumeister M, Braun K, et al. Assessment of the performance of the Ames II assay: a collaborative study with 19 coded compounds. *Mutat Res.* 2004;558(1-2):181–197.
90. Turesky RJ, Bendaly J, Yasa I, Doll MA, Hein DW. The impact of NAT2 acetylator genotype on mutagenesis and DNA adducts from 2-amino-9H-pyrido[2,3-b] indole. *Chem Res Toxicol*. 2009;22(4):726–733.
91. Baldauf KJ, Salazar-González RA, Doll MA, Pierce WM Jr, States JC, Hein DW. Role of Human N-Acetyltransferase 2 Genetic Polymorphism on

Aromatic Amine Carcinogen-Induced DNA Damage and Mutagenicity in a Chinese Hamster Ovary Cell Mutation Assay. *Environ Mol Mutagen*. 2020;61(2):235–245.

92. Huang YS, Chern HD, Su WJ, Wu JC, Lai SL, et al. (2002) Polymorphism of the N-acetyltransferase 2 gene as a susceptibility risk factor for antituberculosis drug-induced hepatitis. *Hepatology* 35: 883–889.

93. Ruiz JD, Martínez C, Anderson K, et al. The differential effect of NAT2 variant alleles permits refinement in phenotype inference and identifies a very slow acetylation genotype. *PLoS One*. 2012;7(9): e44629.

94. McQueen CA, Maslansky CJ, Williams GM. Role of the acetylation polymorphism in determining susceptibility of cultured rabbit hepatocytes to DNA damage by aromatic amines. *Cancer Res*. 1983;43(7):3120–3123.

95. Orzechowski A, Schrenk D, Bock KW. Metabolism of 1- and 2-naphthylamine in isolated rat hepatocytes. *Carcinogenesis*. 1992;13(12):2227–2232.

96. Weber CA, Salazar EP, Stewart SA, Thompson LH. Molecular cloning and biological characterizationof a human gene, ERCC2, that corrects the nucleotide excision repair defect in CHO UV5 cells. *Mol Cell Biol*. 1988; 8:1137–1146.

97. Cascorbi I, Roots I, Brockmöller J. Association of NAT1 and NAT2 polymorphisms to urinary bladder cancer: significantly reduced risk in subjects with NAT1*10. *Cancer Res*. 2001;61(13):5051–5056.

98. Sanderson S, Salanti G, Higgins J. Joint effects of the N-acetyltransferase 1 and 2 (NAT1 and NAT2) genes and smoking on bladder carcinogenesis: a literature-based systematic HuGE review and evidence synthesis. *Am J Epidemiol*. 2007;166(7):741–751.

99. Doaei S, Hajiesmaeil M, Aminifard A, Mosavi-Jarrahi SA, Akbari ME, Gholamalizadeh M. Effects of gene polymorphisms of metabolic enzymes on the association between red and processed meat consumption and the development of colon cancer; a literature review. *J Nutr Sci*. 2018;7: e26

100. Doll MA, Hein DW. Comprehensive human NAT2 genotype method using single nucleotide polymorphism-specific polymerase chain reaction primers and fluorogenic probes. *Anal Biochem*. 2001;288(1):106–108.

101. Leff MA, Epstein PN, Doll MA, et al. Prostate-specific human N-acetyltransferase 2 (NAT2) expression in the mouse. *J Pharmacol Exp Ther*. 1999;290(1):182–187.

102. Millner LM, Doll MA, Cai J, States JC, Hein DW. NATb/NAT1*4 promotes greater arylamine N-acetyltransferase 1 mediated DNA adducts and mutations than NATa/NAT1*4 following exposure to 4-aminobiphenyl. *Mol Carcinog*. 2012;51(8):636–646.

103. Metry KJ, Neale JR, Doll MA, et al. Effect of rapid human N-acetyltransferase 2 haplotype on DNA damage and mutagenesis induced by 2-amino-3-methylimidazo-[4,5-f]quinoline (IQ) and 2-amino-3,8-dimethylimidazo-[4,5-f]quinoxaline (MeIQx). *Mutat Res*. 2010;684(1-2):66–73.

104. Metry KJ, Zhao S, Neale JR, et al. 2-amino-1-methyl-6-phenylimidazo [4,5-b] pyridine-induced DNA adducts and genotoxicity in Chinese hamster ovary

(CHO) cells expressing human CYP1A2 and rapid or slow acetylator N-acetyltransferase 2. *Mol Carcinog*. 2007;46(7):553–563.

105. Bonnier F, Keating ME, Wróbel TP, et al. Cell viability assessment using the Alamar blue assay: a comparison of 2D and 3D cell culture models. *Toxicol In Vitro*. 2015;29(1):124–131.

106. Bendaly J, Doll MA, Millner LM, et al. Differences between human slow N-acetyltransferase 2 alleles in levels of 4-aminobiphenyl-induced DNA adducts and mutations. *Mutat Res.* 2009;671(1-2):13–19.

107. Sim E, Lack N, Wang CJ, et al. Arylamine N-acetyltransferases: structural and functional implications of polymorphisms. *Toxicology*. 2008;254(3):170-183.

108. Hein DW. Molecular genetics and function of NAT1 and NAT2: role in aromatic amine metabolism and carcinogenesis. *Mutat Res*. 2002;506-507:65–77.

109. Walraven JM, Zang Y, Trent JO, Hein DW. Structure/function evaluations of single nucleotide polymorphisms in human N-acetyltransferase 2. *Curr Drug Metab*. 2008;9(6):471–486.

110. Doll MA, Hein DW. Genetic heterogeneity among slow acetylator N-acetyltransferase 2 phenotypes in cryopreserved human hepatocytes. *Arch Toxicol*. 2017;91(7):2655–2661.

111. Chapron DJ, Kramer PA, Mercik SA. Kinetic discrimination of three sulfamethazine acetylation phenotypes. *Clin Pharmacol Ther*. 1980;27(1):104–113.

112. Chen B, Zhang WX, Cai WM. The influence of various genotypes on the metabolic activity of NAT2 in a Chinese population. *Eur J Clin Pharmacol*. 2006;62(5):355–359.

113. Hein DW, Doll MA, Rustan TD, Gray K, Ferguson RJ, Feng Y. Construction of Syrian hamster lines congenic at the polymorphic acetyltransferase locus (NAT2): acetylator genotype-dependent N- and O-acetylation of arylamine carcinogens. *Toxicol Appl Pharmacol*. 1994;124(1):16–24.

114. Hein DW, Doll MA, Xiao GH, Feng Y. Prostate expression of N-acetyltransferase 1 (NAT1) and 2 (NAT2) in rapid and slow acetylator congenic Syrian hamster. *Pharmacogenetics*. 2003;13(3):159–167.

115. Hein DW, Doll MA. Role of the N-acetylation polymorphism in solithromycin metabolism. *Pharmacogenomics*. 2017;18(8):765–772.

116. Hein DW, Smolen TN, Fox RR, Weber WW. Identification of genetically homozygous rapid and slow acetylators of drugs and environmental carcinogens among established inbred rabbit strains. *J Pharmacol Exp Ther*. 1982;223(1):40–44.

117. Hein DW, Doll MA. Rabbit N-acetyltransferase 2 genotyping method to investigate role of acetylation polymorphism on N- and O-acetylation of aromatic and heterocyclic amine carcinogens. *Arch Toxicol*. 2017;91(9):3185–3188.

118. Oda Y. Analysis of the involvement of human N-acetyltransferase 1 in the genotoxic activation of bladder carcinogenic arylamines using a SOS/umu assay system. *Mutat Res*. 2004;554(1-2):399-406.

119. Hickman D, Palamanda JR, Unadkat JD, Sim E. Enzyme kinetic properties of human recombinant arylamine N-acetyltransferase 2 allotypic variants expressed in Escherichia coli. *Biochem Pharmacol*. 1995;50(5):697-703.

120. Hein DW, Fretland AJ, Doll MA. Effects of single nucleotide polymorphisms in human N-acetyltransferase 2 on metabolic activation (O-acetylation) of heterocyclic amine carcinogens. *Int J Cancer*. 2006;119(5):1208-1211.

121. Zang Y, Doll MA, Zhao S, States JC, Hein DW. Functional characterization of single-nucleotide polymorphisms and haplotypes of human N-acetyltransferase 2. *Carcinogenesis*. 2007;28(8):1665-1671.

122. Xu WJ, Wen LP, Jiang XX, et al. Association between N-Acetyltransferase 2 Polymorphism and Bladder Cancer Risk: a Meta-Analysis in a Single Ethnic Group. *Clin Lab*. 2017;63(2):287–293.

123. Stojanovic J, Milovanovic S, Pastorino R, Iavicoli I, Boccia S. Occupational exposures, and genetic susceptibility to urinary tract cancers: a systematic review and meta-analysis. *Eur J Cancer Prev*. 2018;27(5):468–476.

124. Saginala K, Barsouk A, Aluru JS, Rawla P, Padala SA, Barsouk A. Epidemiology of Bladder Cancer. *Med Sci (Basel)*. 2020;8(1): E15. Published 2020 Mar 13.

ABBREVIATIONS

8-OHdG	8-hydroxy-2' -deoxyguanosine
ABP	4-Aminobiphenyl
Acetyl-CoA	Acetyl coenzyme A
AF	2-Aminofluorene
ANOVA	Analysis of variance
AαC	2-amino-9H-pyrido[2,3-b] indole
BNA	β-Naphthylamine
CHO	Chinese hamster ovary
EDTA	Ethylenediaminetetraacetic acid
EROD	Ethoxyresorufin O-deethylation
HPLC	High performance liquid chromatography
IARC	International Agency for Research on Cancer
INH	Isoniazid
MOCA	4, 4’-methylene bis (2-chloroaniline)

MTP	3-methyl-s-triazolo [3,4a]-phthalazine
NAT1	Arylamine N-acetyltransferase 1
NAT2	Arylamine N-acetyltransferase 2
NER	Nucleotide excision repair
PBS	Phosphate buffer saline
PCR	Polymerase chain reaction
PhIP	2-amino-1-methyl-6-phenylimidazo[4,5-b] pyridine
ROS	Reactive oxygen species
SMZ	Sulfamethazine
SNP	Single Nucleotide Polymorphism

CURRICULUM VITAE

Mariam Refaat Zaky Habil, MBChB, M.S.
University of Louisville School of Medicine
Department of Pharmacology and Toxicology
Louisville, KY 40202
m0refa01@louisville.edu
dr_mariam_refaat@yahoo.com
502-852-6284

EDUCATION:

Ph.D. Student (2017-present)
Pharmacology and Toxicology Department,
School of Medicine, University of Louisville, USA.

Master's Degree of Medical Pharmacology (2012-2016)
Medical Pharmacology Department,
Faculty of Medicine, Cairo University, Egypt.

MBChB (2003-2009)
Faculty of Medicine, Cairo University, Egypt.

PROFESSIONAL EXPERIENCE:

Graduate Research Assistant of Pharmacology and Toxicology Department, School of Medicine, University of Louisville, USA (**2017-present**).

Assistant Lecturer of Medical Pharmacology, Faculty of Medicine, Cairo University, Giza, Egypt (**2016-2017**).

Teaching Assistant (Demonstrator) of Medical Pharmacology,
Faculty of Medicine, Cairo University, Giza, Egypt **(2012-2016).**

General Practitioner, Child Health Care unit of Giza,
Ministry of Health & Population, Giza, Egypt **(2011-2012).**

House Officer (Internship), Ministry of Health and Population hospitals, Cairo and Sohag, Egypt **(2010 -2011).**

AWARDS:

- SE Regional IDeA Meeting November 2019-travel award.

ABSTRACTS:

- **Mariam R. Habil**, Mark A. Doll, David W. Hein, *"N-acetyltransferase 2 acetylator genotype-dependent N-acetylation of beta-naphthylamine and 4,4'-Methylenebis(2-chloroaniline) in Chinese hamster ovary (CHO) cells*", OVSOT virtual Summer meeting, July 2020. Louisville, KY.

- **Mariam R. Habil,** Raúl A. Salazar-González, Mark A. Doll, David W. Hein. *"N-acetyltransferase 2 acetylator genotype-dependent N-acetylation of beta-naphthylamine in Chinese Hamster Ovary cells",* Graduate Student Regional Research Conference; February 2020. Louisville, KY.

- **Mariam R. Habil,** Mark a. Doll, David W. Hein. *"N-acetyltransferase 2 acetylator genotype-dependent N-acetylation of the arylamine carcinogens 4-aminobiphenyl and beta-naphthylamine in cryopreserved human hepatocytes".* OVSOT Fall annual meeting, November 2018. Louisville, KY.

- **Mariam R. Habil,** Mark A. Doll, David W. Hein*. "N-acetyltransferase 2 acetylator genotype-dependent N-acetylation of the arylamine carcinogens 4-aminobiphenyl and beta-naphthylamine in cryopreserved human hepatocytes"*, Research Louisville; September 2018. Louisville, KY.

PUBLICATIONS:

- **Habil MR,** Doll MA, Hein DW. N-acetyltransferase 2 acetylator genotype-dependent N-acetylation of 4-aminobiphenyl in cryopreserved human hepatocytes. *Pharmacogenet Genomics*. 2020;30(3):61-65.

- Soliman G, Khattab A, **Habil MR**. Experimental Comparative Study of potential anxiolytic effect of Vitamin C and Buspirone in rats. *Funct. food health dis.* 2017; 8(2): 91-10.

CONFERENCE PRESENTATIONS:

Oral Presentations:

- **Mariam R. Habil**, Mark a. Doll, David W. Hein. *"N-acetyltransferase 2 acetylator genotype-dependent N-acetylation of the arylamine carcinogens 4-aminobiphenyl and beta-naphthylamine in cryopreserved human hepatocytes".* OVSOT Fall annual meeting, November 2018. Louisville, KY.

Poster Presentations:

- **Mariam R. Habil,** Raúl A. Salazar-González, Mark A. Doll, David W. Hein. *"N-acetyltransferase 2 acetylator genotype-dependent N-acetylation of beta-naphthylamine in Chinese Hamster Ovary cells"*, Graduate Student Regional Research Conference; February 2020. Louisville, KY.

- **Mariam R. Habil,** Mark A. Doll, David W. Hein. *"N-acetyltransferase 2 acetylator genotype-dependent N-acetylation of the arylamine carcinogens 4-aminobiphenyl and beta-naphthylamine in cryopreserved human hepatocytes",* Research Louisville; September 2018. Louisville, KY.